Outer membrane proteins of *Anabaena* sp. strain PCC 7120

Dissertation der Fakultät für Biologie
der Ludwig-Maximilians-Universität München

vorgelegt von
Sunčana Moslavac

München, 2007

Dissertation eingereicht am: 18. 06. 2007

Datum der mündlichen Prüfung: 20. 07. 2007

Erstgutachter: PD Dr. Enrico Schleiff
Zweitgutachter: Prof. Dr. Jörg Nickelsen

Ehrenwörtliche Versicherung

Die vorliegende Dissertation wurde von Sunčana Moslavac selbständig und ohne unerlaubte Hilfe angefertigt. Die Verfasserin hat zuvor nicht versucht, anderweitig eine Dissertation einzureichen oder sich einer Doktorprüfung zu unterziehen. Die Dissertation wurde keiner weiteren Prüfungskommission weder in Teilen noch als Ganzes vorgelegt.

München, 15.06.2007

_____

Sunčana Moslavac

Table of Contents

List of Abbreviations

ABC transporter	ATP-binding cassette transporter
Acc.	accession number
Anabaena sp.	*Anabena* sp. PCC 7120
A. thaliana	*Arabidopsis thaliana*
ATP	adenosin triphosphate
A.U.	arbitrary units
Avar	*Anabaena variabilis*
BN-PAGE	blue-native PAGE
bp	base pare
Ct	C-terminus
DNA	deoxyribonucleic acid
DNase	deoxyribonuclease
DoMa	dodecyl maltoside
E. coli	*Escherichia coli*
EDTA	ethylenediamine tetraacetic acid
Exp.	experiment
HEP	heterocyst specific polysaccharide
GFP	green fluorescent protein
HEPES	4-(2-hydroxyethyl)-1-piperazineethanesulfonic acid
HGL	heterocyst specific glycolipid
IM	inner membrane
INT	internal
LTP	lipid transfer proteins
MF	mass fingerprint
MS	mass spectrometry
MW	molecular weight
No.	number
Npun	*Nostoc punctiforme*
OG	octylglucoside
OM	outer membrane
ORF	open reading frame
OX	over-expression

PAGE	polyacrylamide gel electrophoresis
PCR	polymerase chain reaction
pI	isoelectric point
PM	plasma membrane
PMSF	phenylmethylsulfonylfluorid
PS	peptide sequencing
PSI	photosystem I
PSII	photosystem II
RNA	ribonucleic acid
RT	reverse transcriptase
SDS	sodium dodecyl sulphate
Selo	*Synechococcus elongatus*
Synechocystis sp.	*Synechocystis* sp. PCC 6803
TBDT	TonB-dependent transporter / receptor
Teri	*Trichodesmium erythraeum*
TLC	thin layer chromatography
TM	thylakoid membrane
VRC	vanadyl ribonucleoside complex solution
v/v	volume per volume
w/v	mass per volume
WT	wild type
Δ	deletion

1. Abstract

The filamentous cyanobacterium *Anabaena* sp. PCC 7120 (further referred to as *Anabaena* sp.) is a model system to study nitrogen fixation, cell differentiation, cell pattern formation and evolution of plastids. It is a multicellular photosynthetic microorganism consisting of two cell types, vegetative cells and nitrogen fixing heterocysts. This study focuses on the function and dynamics of the proteome of the Gram-negative outer membrane in *Anabaena* sp. with emphasis on cell differentiation and iron limitation. The newly developed methods for the membrane fractionation are presented, followed by analysis and comparison of the outer membrane proteomes of vegetative cells and heterocysts. The absence of major proteomic alterations in the outer membrane between two cell types, together with the presented data on GFP activity in mutant strains, experimentally support the previously proposed continuum of the outer membrane and the periplasm in *Anabaena* sp. filament. Also, somewhat different properties of the *Anabaena* sp. periplasm than in unicellular cyanobacteria are suggested. Furthermore, two common classes of the outer membrane β-barrel proteins are analyzed closer. First, Alr2887 protein, as shown here, is a TolC homologue present in both cell types. Protein secretion through Alr2887 / TolC channel-tunnel is essential for the heterocysts maturation and the glycolipid layer formation. Furthermore, the inner membrane ABC transporter encoded by *devBCA* operon is proposed as component of the TolC efflux system in *Anabaena* sp. heterocysts. Second, phylogenetic analysis of the surprisingly abundant protein family of 24 TonB-dependent iron transporters in *Anabaena* sp. is presented. Five members of this family are detected in the outer membrane of vegetative cells under iron-repletion and two of them, All4026 and Alr0397, are explored closer. It is demonstrated that the function of these iron transporters is required for maintaining iron homeostasis of the filaments under iron-replete conditions. Consequently, their gene expression is constant and not enhanced by iron limitation. All4026 and Alr0397 have different specificity for siderophore substrates and in addition to iron transport, All4026 protein is capable of copper uptake and influence on copper homeostasis in *Anabaena* sp. as well.

2. Zusammenfassung

Das filamentöse Cyanobakterium *Anabaena* sp. PCC 7120 (in Folgenden *Anabaena* sp. bezeichnet) ist ein Modellsystem für Studien der Stickstofffixierung, Zell-Differenzierung, Zell-Musterbildung und Evolution der Plastiden. Es handelt sich um einen multizellulären photosynthetischen Organismus, der aus zwei Zelltypen besteht – den vegetativen Zellen und den Stickstoff fixierenden Heterozysten. Die vorliegende Arbeit befasst sich mit der Funktion und Dynamik des Proteoms der Gram-negativen äußeren Membran von *Anabaena* sp. unter besonderer Berücksichtigung der Zelldifferenzierung und Anpassung an Eisenmangel. Hierfür wurden neue Methoden zur Membranfraktionierung entwickelt, welche eine Analyse und Vergleich des Proteoms der vegetativen Zellen und Heterozysten ermöglichten. Das Fehlen signifikanter Unterschiede im Proteom der äußeren Membran beider Zelltypen, zusammen mit den Ergebnissen der GFP-Mutantenanalyse, stützen experimentell die zuvor vorgeschlagene Existenz eines Kontinuums der äußeren Membran und des Periplasmas. Es werden außerdem unterschiedliche Eigenschaften des Periplasmas von *Anabaena* sp. im Vergleich zu einzelligen Cyanobakterien angenommen. Darüber hinaus wurden zwei Klassen der β-Barrel Proteine aus der äußeren Membran näher charakterisiert. Zunächst Alr2887, wie es hier betrachtet wird, ist ein Homolog von TolC, das in beiden Zelltypen vorhanden ist. Die Proteinsekretion durch den Alr2887 / TolC Kanal ist essenziell für die Heterozystenreifung und Bildung der Glykolipidschicht. Der vom *devBCA* Operon kodierte ABC Transporter in der inneren Membran wird als Komponente des TolC Exportsystems in *Anabaena* sp. vorgeschlagen. Weiterhin wird die phylogenetische Analyse der überraschend zahlreichen Proteinfamilie der 24 TonB abhängigen Eisentransporter in *Anabaena* sp. präsentiert. Fünf Mitglieder dieser Familie sind in der äußeren Membran der vegetativen Zellen unter Eisensättigungsbedingungen lokalisiert, von denen zwei, All4026 und Alr0397, näher untersucht wurden. Die Funktion dieser Proteine ist für die Aufrechterhaltung der Eisen-Homöostase der Filamente unter Eisensättigungsbedingungen erforderlich und ihre Expression ist dementsprechend nicht erhöht unter Eisenmangelbedingungen. All4026 and Alr0397 haben unterschiedliche Spezifitäten für Siderophor-Substrate und All4026 ist, zusätzlich zum Eisentransport, zur Kupferaufnahme fähig und beeinflusst ebenso die Homöostase dieses Metalls in *Anabaena* sp.

3. Introduction

3.1. Filamentous nitrogen fixing cyanobacterium *Anabaena* sp. PCC 7120

Anabaena sp. strain PCC 7120 (also known as *Nostoc* sp. PCC 7120; further in text referred to as *Anabaena* sp.) is a representative of cyanobacteria, an ancient and diverse class of Gram-negative bacteria capable of performing oxygenic photosynthesis. The most prominent morphological feature of *Anabaena* sp. is its multicellularity (Figure 1; Flores *et al*., 2006). In the presence of a combined nitrogen source in the medium, being either ammonium or nitrate compounds, *Anabaena* sp. forms long filaments of 100 and more identical vegetative cells (Figure 1; Wolk, 1996; Golden and Yoon, 2003).

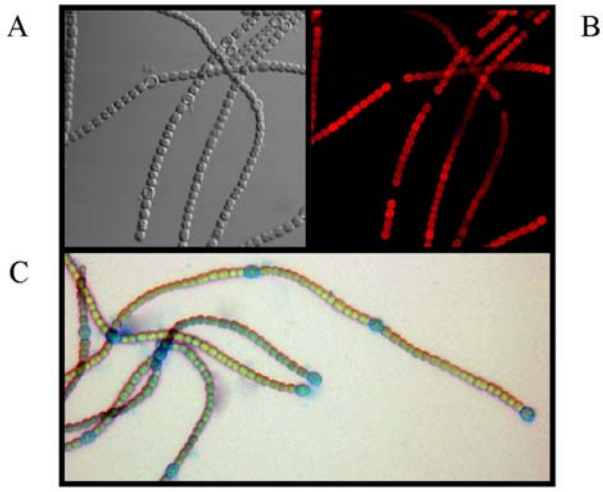

Figure 1. (A) *Anabaena* sp. PCC 7120 wild type filaments in the bright field; heterocysts are visible as bigger morphologically different cells in the filament. (B) Autofluorescence of the same *Anabaena* sp. wild type filaments. Black spots in the autofluorescence are places of non-photosynthetic heterocysts. (C) Long filament of vegetative cells with the semi-regular pattern of Alcian Blue stained heterocysts

As in every Gram-negative cell, the *Anabaena* sp. membrane system consists of an inner (or plasma) membrane and an outer membrane separated by the periplasm. However, in *Anabaena* sp. the size of periplasmic space ranges between 30 - 40 nm in comparison to 7 - 25 nm separating the inner and the outer membrane in most classical Gram-negative bacteria. Furthermore, in *Anabaena* sp. only the inner membrane belongs exclusively to each cell, while the outer membrane encompasses the entire filament and does not enter the septa between neighboring cells (Flores *et al*., 2006). In that way the outer membrane and the periplasmic space are rather common and continuous for the whole filament, then structures belonging to just one cell in the filament (Flores *et al*., 2006). Which role plays the outer membrane continuum and the periplasmic continuum in the intercellular metabolite exchange and signal transfer of the filament is just starting to be elucidated.

Next to the outer and the inner membrane surrounding the cells, well developed thylakoid membrane system, bearing the photosynthetic apparatus, is also present inside of vegetative cells (Wolk, 1996).

Anabaena sp. and some other cyanobacteria belong to unique microorganisms able to perform not only oxygenic photosynthesis but also nitrogen fixation (Wolk, 1996). Nitrogen fixation takes place when no other source of nitrogen but atmospheric dinitrogen is available. In that process relatively inert atmospheric dinitrogen is reduced to ammonium, and ammonium is assimilated further to glutamine, using 2-oxoglutarat as a carbon skeleton (Ikeda *et al*., 1996; Laurent *et al*., 2005). The only known enzyme able to catalyze breaking of the triple bond between two nitrogen atoms in the nitrogen molecule (N_2), being an essential predisposition for nitrogen fixation, is nitrogenase (Golden and Yoon, 2003). However, nitrogenase is highly oxygen sensitive and becomes completely inactivated already by minute concentrations of oxygen. For that reason photosynthesis and nitrogen fixation represent two intrinsically incompatible processes which have to be spatially separated (Fay, 1992; Gallon, 1992). To accomplish the separation, *Anabaena* sp. differentiates the second type of cells called heterocysts when deprived of combined nitrogen source (Figure 1; Fay *et al*., 1968; Wolk *et al*., 1994). Heterocysts develop from preexisting vegetative cells and are evenly spaced along the filament in a semi-regular pattern with approximately every tenth to twentieth cell becoming a heterocyst (Figure 1). Under continuous light and laboratory growth conditions the process of heterocyst differentiation takes about one generation time or approximately 20 hours (Fay, 1992; Wolk *et al*., 1994; Adams and Duggan, 1999). Vegetative cells and heterocysts are interdependent relying on mutual metabolite exchange (Wolk, 1996, Herrero *et al*., 2004). Heterocysts supply vegetative cells with products of nitrogen fixation in the form of amino acids glutamine or arginine (Wolk *et al*., 1976; Thomas *et al*., 1977). In return heterocysts receive reduced carbon products in the form of sucrose from vegetative cells (Wolk *et al*., 1994; Curatti *et al*., 2002).

Heterocysts are terminally differentiated cells, morphologically and functionally very much different from vegetative cells (Figure 1). Being a place of nitrogen fixation, they must provide oxygen-free (microoxic) environment crucial for nitrogenase activity (Fay, 1992). In order to accomplish that, heterocysts must remove all traces of preexisting oxygen, prevent its further release through photosynthesis and prevent oxygen leaking from the surroundings into the cell. Therefore, oxygen-producing photosystem II (PSII) is inactivated in heterocysts (Wolk *et al*., 1994), although ATP continues to be generated by

cyclic photophosphorylation around photosystem I (Ernst *et al*., 1983). Furthermore, two additional heterocyst specific layers are deposited outside the outer heterocyst membrane. The outermost homogenous layer consists of polysaccharides (HEP layer) and provides mechanical protection for the second laminated layer, deposited between the polysaccharide layer and the outer membrane (Murry and Wolk, 1989). The laminated layer consists of the heterocyst-specific glycolipids and represents, in fact, a barrier that limits the entry of oxygen (Murry and Wolk, 1989). Oxygen that still passes the glycolipid barrier together with dinitrogen is removed by increased respiratory activity or scavenged by oxygenases (Murry and Wolk, 1989; Valadares *et al*., 2003). The heterocyst-specific glycolipids (HGLs) forming the laminated layer are identified as polyhydroxy alcohols with 26 to 28 carbon atoms glycosidically linked to glucose at C-1 (Winkenbach *et al*., 1972). *Anabaena* sp. has two HGLs: HGL1 or 1-(O-α-D-glucopyranosyl)-3,25-hexacosanediol and HGL2 or 1-(O-α-D-glucopyranosyl)-3-keto-25-hexacosanol (Gambacorta *et al*., 1996). In the synthesis of the HGLs, fatty acid synthases, polyketide synthases, ketoreductases, dehydrases, acyl transferases or thioesterases are probably involved (Hopwood and Sherman, 1990; Fan *et al.*, 2005). How deposition and transport of the HGLs outside the outer membrane occur, remains to be elucidated in the future.

The genes involved in heterocysts differentiation or function are numerous in *Anabaena* sp. genome and a huge progress has been made in their identification and characterization over the last decades. The expression of *ntcA* gene is the earliest response of *Anabaena* sp. to nitrogen deprivation. NtcA protein is a transcriptional regulator regulating genes responsible for heterocyst differentiation and nitrogen metabolism (Wei *et al*., 1994; Frias *et al*., 1994). Further, *hetR* gene is a key regulator of heterocyst development in *Anabaena* sp. (Buikema and Haselkorn, 1991). Its expression is under control of NtcA protein and is detectable already 30 min after nitrogen step-down. HetR autoregulates its own expression as well as *ntcA* gene expression. In this way *ntcA* and *hetR* form very efficient regulatory loop and enable *Anabaena* sp. to respond fast to nitrogen starvation (Black *et al*., 1995; Herrero *et al*., 2004). Two genes play the most prominent role in the heterocyst pattern formation. The first gene is *patS*, which encodes a small PatS peptide acting as inhibitor of heterocyst differentiation. PatS peptide is produced by proheterocysts in the first 12 hours after nitrogen step-down. It spreads along the filament in unknown way and creates probably a gradient of inhibitory signal which results in early heterocyst pattern of the filament (Yoon and Golden, 1998, 2001). The second gene is *hetN* whose product is involved in maintenance of the heterocyst pattern as

vegetative cells continue to divide and new heterocysts insert in the growing filament. It is expressed after 12 hours of nitrogen step-down (Callahan and Buikema, 2001).

The genes responsible for the formation of the heterocyst-specific layers have also been identified. So called *hep* genes are involved in heterocyst polysaccharide layer synthesis. Their mutations result in immature heterocysts unable to fix nitrogen under aerobic conditions. *hepA*, *hepB* and *hepC* genes encode proteins with similarity to ABC-type transporter, glycosyltransferase and UDP-galactose-lipid carrier transferase, respectively (Wolk, 2000; Maldener *et al.*, 2003). Furthermore, genes *alr2825*, *alr2827*, *alr2831*, *alr2833*, *alr2837*, *alr2839* and *alr2841* are localized on a well-defined specific "HEP-island" in the *Anabaena* sp. chromosome. They all encode enzymes with putative function in the synthesis of the HEP layer (Huang *et al.*, 2005). *devBCA* operon, regulated by NtcA regulator, encodes components of an inner membrane ABC transporter essential for glycolipid layer deposition (Fiedler *et al.*, 1998; Herrero *et al.*, 2001). Moreover, *hglB*, *hglC*, *hglD* and *hglE* genes encode enzymes for the synthesis of the heterocyst specific glycolipids (Bauer *et al.*, 1997; Campbell *et al.*, 1997). The protein product of *hglK* gene is also needed for the glycolipid layer formation (Black *et al.*, 1995). Recently several other genes involved in glycolipid layer formation, including *devB/devC* homologues, have been identified (Fan *et al.,* 2005). Soon after All5341 glycosyl transferase was shown to be necessary for glycosylation of the glycolipid aglycone (Awai and Wolk, 2006). Furthermore, in their microarray analysis Ehira *et al.* (2003) reported that several genes with function related to polysaccharide layer and glycolipid layer formation were up-regulated after nitrogen step-down.

3.2. *Anabaena* sp. PCC 7120 – a model organism for plastid evolution

Given that the tools for genetic manipulation of *Anabaena* sp. PCC 7120 are well established and that its genome has been fully sequenced (Kaneko *et al*., 2001), this cyanobacterium is generally accepted as a model microorganism for biological and biochemical studies of nitrogen fixation, pattern formation and cell differentiation. Recently a new aspect related to the endosymbiotic theory of eukaryotic evolution has been added to the studies on *Anabaena* sp. According to this theory plastids of higher eukaryotes originate from a single primary endosymbiotic event during which an oxygenic photosynthetic cyanobacterium-like prokaryote was engulfed by a eukaryotic host (Martin *et al*., 1998; Ishida, 2005). Over time, the majority of genes of the endosymbiont were

transferred to the nuclear genome of the host, thereby reducing the gene content of the endosymbiont to approximately the size of a plasmid (Martin *et al*., 1998; Timmis *et al.*, 2004). Over time many of the transferred genes became functionally competent nuclear copies and a protein machinery for targeting and re-import of their protein products back to the endosymbiont was created (Heins and Soll, 1998). In that way endosymbiont evolved to a semi-autonomous cell organelle - the plastid.

Martin *et al*. (2002) performed a wide phylogenetic analyses of *Arabidopsis thaliana*, cyanobacterial, bacterial and yeast proteins. Their results demonstrate that overall gene complement of the genus *Nostoc* (comprising *Anabaena* sp.) is far more similar to that which the ancestor of plastids possessed than is the gene complement of any other cyanobacterium. This notion identifies members of the *Nostoc* genus as the closest known evolutionary relatives of plastids and places *Anabaena* sp. in the focus of evolutionary studies, making it one of the major players of the endosymbiotic theory.

3.3. β-barrel proteins of the outer membrane

Gram-negative bacteria, including *Anabaena* sp., are surrounded by the outer and the inner membrane, separated by peptidoglycan containing periplasm. The inner membrane of classical Gram-negatives is a symmetrical bilayer composed of the three major phospholipids (phosphatidylethanolamine, phosphatidylglycerol and cardiolipin; Kanemasa *et al*., 1967; Kadner, 1996) and proteins. Proteins are either integral transmembrane proteins or lipoproteins anchored to the outer leaflet (Tokuda and Matsuyama, 2004). The transmembrane proteins are generally α-helical, hydrophobic and involved in transport of nutrients, protein translocation and lipid biosynthesis or provide energy for the cell processes by oxidative phosphorylation (Ruiz *et al.*, 2005). The outer membrane is an asymmetrical bilayer with an inner leaflet composed of the same phospholipids as the inner membrane and an outer leaflet composed of lipopolysaccharides (Smit *et al*., 1975; Kamio and Niakido 1976) chelated by divalent cations (Nikaido, 2003). In the outer membrane two types of proteins are found: to the inner leaflet anchored lipoproteins and integral transmembrane β-barrel proteins (Ruiz *et al*., 2005). Since β-barrel proteins appear exclusively in the outer membrane of Gram-negative bacteria and in the outer membrane of the endosymbiotically derived organelles, plastids and mitochondria, they represent an evolutionary marker that supports the endosymbiotic

theory (Keegstra *et al*., 1984; Tamm *et al*., 2004; Paschen *et al*., 2005). However, beside β-barrels some proteins with transmembrane α-helical regions are also targeted to the outer membrane of these organelles (Pfanner and Wiedemann, 2002; Wimley 2003). Recently Dong *et al*. (2006) have described a novel α-barrel transmembrane domain of the Wza translocon for the capsular polysaccharides located in the outer membrane of *E. coli*.

The β-barrel proteins contain from 8 to 22 β-strands, usually with tight turns on the periplasmic side and large quite flexible loops on the extracellular side of the outer membrane. The smallest 8-stranded β-barrels (e.g. structural outer membrane protein OmpA) have tightly packed residues closing the barrel lumen (Arora *et al*., 2001). On the other hand, 16, 18 and 22-stranded β-barrels serve as the outer membrane transporters with large water filled pores. In the case of 22-stranded transporters the pores are occluded with the "plug" domain.

The outer membrane β-barrel transporters are divided into four groups (Buchanan, 2001; Tamm *et al*., 2004). The first group are general porins (e.g. OmpF, OmpC and PhoE), which are 16 stranded β-barrels structured as homotrimers with three barrels and three pores (Weis *et al*., 1991; Cowan *et al*., 1992.). Surprisingly, until now this classical bacterial porins have not been found in cyanobacteria (Flores *et al*., 2006). The second group comprises specific porins with 18-stranded homotrimeric structures, importing sugars like maltose or sucrose. Their pores are partially constricted by three extracellular loops folding into each β-barrel (Schirmer *et al*., 1995; Forst *et al.,* 1998). In both cases substrates of limited size up to approximately 600 Da diffuse passively through the pores into the periplasm. In the periplasm they are bound by the substrate-specific binding proteins and shuttled further to the inner membrane ATP-binding cassette (ABC) transporter. ABC transporters utilize energy generated by ATP hydrolysis to perform an active transport across the inner membrane into the cytoplasm (Buchanan, 2001).

However, many compounds crossing the outer membrane are much bigger than 600 Da and their transport requires energy at both steps: for the active transfer over the inner membrane and for the active transfer over the outer membrane. These big substrates are transported across the outer membrane with a help of the third and the fourth group of the outer membrane transporters. The third group of the transporters mediate an active import of larger substrates into the periplasm and include TonB-dependent iron or vitamin B_{12} transporters (Faraldo-Gomez and Samson, 2003), described later in details. The fourth group of the transporters, presented by TolC protein (Koronakis *et al.*, 2004), mediate the transport in reverse direction: an active secretion of compounds out of the cell. However,

because of the porous structure of the outer membrane, membrane potential cannot be established across this membrane and energy rich compounds such as ATP, GTP, NADPH are not present in the periplasm (Postle, 1990). To solve this problem, transporters of TonB-dependent group and TolC-like proteins establish physical contact with the inner membrane components, which provide them with energy from the cytoplasmic sources to drive the active transport across the outer membrane.

3.3.1 TolC-dependent protein secretion

The fourth group of the outer membrane transportes will be described first. Among four known secretion systems of Gram-negative bacteria (type I-IV), type I is the simplest. This system requires only three proteins: (1) the substrate-specific inner membrane component (ABC transporter or proton antiporter), (2) the TolC channel-tunnel as an outer membrane component and (3) the so-called membrane fusion (MFP) or adaptor protein (Figure 2; Delepelaire, 2004). Type I secretion system exports many large proteins, including some bacterial toxins such as 110 kDa *E. coli* hemolysin (Koronakis and Hughes, 1993), 170 kDa *Bordatella pertussis* cyclolysin (Glaser *et al*., 1988) and different enzymes like proteases, lipases, nucleases, phospahateses, and glucanases (Paulsen *et al*., 1997; Delepelaire, 2004).

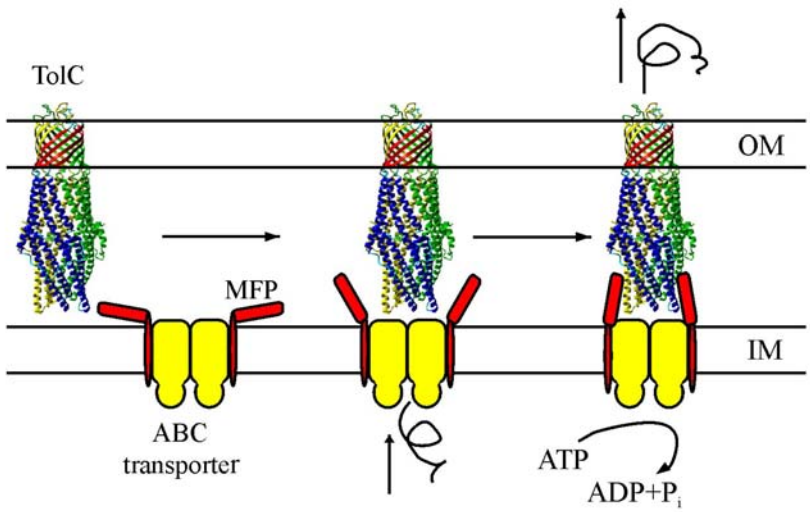

Figure 2. Protein secretion through the TolC channel-tunnel. The contact between TolC (protein model, see also later Figure 34A) and the inner membrane ABC transporter (yellow subunits) is established transiently with a help of the adaptor or membrane fusion protein (MFP, red subunits) when the protein substrate (curly line) binds to the substrate specific ABC transporter (according to Koronakis *et al.*, 2004).

Energy for the transport is provided by the cytoplasmic ATP hydrolysis performed by ABC transporter in the inner membrane. Furthermore, type I secretion governs efflux of small noxious compounds out of the bacterial cell, such as detergents, organic solvents, antibacterial drugs (e.g. nalidixic acid) and antibiotics (tetracycline, chloramphenicol, erythromycin). In that case energy is provided by the inner membrane complex utilizing the proton motive force (Zgurskaya and Nikaido, 2000).

TolC is a rather promiscuous protein, coupling with different inner membrane complexes in order to transport a variety of substrates. The substrate specificity is determined by the periplasmic and the inner membrane component. The contact between TolC and the inner membrane complex is established in the periplasm with a help of the MFP or adaptor protein (Figure 2). The adaptor protein has a small cytoplasmic domain, a single transmembrane segment and a large periplasmic domain (Thanabalu *et al.*, 1998; Delepelaire, 2004). This complex is transient and once the substrate secretion has been completed, the complex disengages and reverts to the resting state (Thanabalu *et al*., 1998). TolC family is widespread among Gram-negative bacteria and has evolved by gene duplication, as reflected in similarity of N- and C-terminal halves of the TolC-like proteins (Johnson and Church, 1999).

The most distinctive feature of the type I secretion is that the export happens from the cytoplasm into the extracellular medium in a single step bypassing the periplasm and without involvement of any periplasmic intermediates. This is due to an exquisite TolC channel-tunnel structure (Koronakis *et al*., 2000). TolC is a homotrimer building a single 140 Å long channel-tunnel. It comprises the 40 Å long, 12-stranded β-barrel (the channel domain) embedded in the outer membrane and the 100 Å long, 12-stranded α-helical "barrel" (the tunnel domain) traversing the periplasm (see Figure 2 and later Figure 34A). Each of three monomers contributes four antiparallel α/β mixed strands to the TolC structure. TolC channel-tunnel interior is 35 Å wide and water filled, large enough to accommodate secondary structure elements or even small folded polypeptides (Sharff *et al*., 2001). On the extracellular side TolC duct is wide open, while α-helices close the structure to an opening that measures only 3.5 Å on the periplasmic end (Koronakis *et al.*, 2000). An iris-like unwinding of α-helices by as much as 30 Å on the periplasmic end has been proposed as a mechanism of the channel-tunnel opening (Sharff *et al*., 2001).

3.3.2 TonB-dependent transporters and iron uptake

The third group of the outer membrane transporters comprises TonB-dependent transporters (also known as TonB-dependent receptors). These proteins play a crucial role in iron uptake and iron regulation in the Gram-negative bacterial cell (Clarke *et al.*, 2001; Faraldo-Gomez and Samson, 2003). In biological systems iron is one of the most important elements acting as a major redox mediator. Either alone or incorporated into iron-sulfur clusters, iron is a part of catalytic centers of enzymes catalyzing redox reactions. These enzymes are essential for the cellular processes such as electron transport, photosynthesis, amino acid or nucleoside synthesis, DNA syntheses, activation of oxygen, etc. However, under aerobic conditions and biological pH iron bioavailability is poor because of rapid oxidation of ferrous ion (Fe^{2+}) into ferric iron (Fe^{3+}) followed by the formation of insoluble hydroxides. Fe^{2+} reacts with hydrogen peroxide in a so-called Fenton reaction leading to the production of hydroxyl radicals (Arroyo *et al*., 1994). Free radicals are very reactive species and, as such, deleterious for most biological macromolecules. For this reason iron uptake and metabolism have to be very tightly regulated inside of every living cell. Beside having a number of enzymes for detoxification of free radicals, microorganisms also prevent radical formation by sensing the intracellular iron level, regulating precisely iron uptake and storing the intracellular iron excess into the iron-binding proteins ferritins, bacterioferritins and smaller Dps protein (Clarke *et al*., 2001; Andrews *et al*., 2003). Altogether makes iron acquisition and homeostasis a great challenge for microorganisms.

As a representative of cyanobacteria, *Anabaena* sp. is a Gram-negative microorganism capable of oxygenic photosynthesis (Ting *et al*., 2002). In that purpose it contains intracellular thylakoid membrane system where photosynthetic apparatus is placed (Gantt, 1994). Iron is important for the photosynthetic electron transfer (Keren *et al*., 2004) as an essential metal of photosystem I, cytochrome b_6f complex and photosystem II (Kamiya and Shen, 2003; Stroebel *et al*., 2003; Jordan *et al*., 2001). Because of that cyanobacteria generally have exceptional requirements for iron, but also for copper and manganese in comparison to other nonphotosynthetic bacteria (Waldron *et al*., 2006).

In order to circumvent minute bioavailability of iron, bacteria have developed a range of mechanisms for its uptake. The sources of iron are diverse. Many pathogens obtain iron from iron-containing molecules of the host such as transferrin, lactoferrin and ferritins, or heme, hemoglobin and other hemoproteins (Dyer *et al*., 1987; Cornelissen and Sparling, 1994; Genco and Desai, 1994; Gray-Owen and Schryvers, 1996; Wandersman and Delepelaire, 2004). Some others utilize the fact that in anaerobic and reducing

conditions of mammalian intestine and stomach Fe^{2+} is soluble and can freely defuse through the outer membrane porins (Kammler *et al.*, 1993; Coulanges *et al*., 1997). Alternatively, bacteria (Gram-positive and Gram-negative) and fungi have well developed iron uptake pathway relying on secretion of siderophores ("iron carriers"). Siderophores are low-molecular weight compounds that chelate Fe^{3+} with high affinity. More than 500 siderophores have been described, most of them with a peptide backbone (Drechsel and Jung, 1998; Crosa, 2002). Depending on the iron-ligation groups siderophores classify into three major types (Winkelman, 1991 and 2002): hydroxamate (e.g. aerobactin, schizokinen, ferrichrome, rhizobactin or coprogen; Clarke *et al*., 2000), catecholate (e.g. enterobactin, yersiniabactin, vibriobactin; Cohen *et al.*, 1998) and α-hydroxycarboxylates (e.g. pyochelin). Ferric citrate is a simple compound not belonging to any of these groups that functions as siderophore and is transported into the cell as diferric-dicitrate (Yue *et al*., 2003). In addition, citrate is a common structural base of some siderophores like aerobactin, schizokinen and rhizobactin (Fadeev *et al*., 2005). Microorganisms usually secrete only one or two siderophores, but can utilize exogenous siderophores secreted by other bacteria and fungi found into the medium (Braun *et al*., 2003). For example, the only siderophore secreted by *E. coli* is a catecholate enterobactin, while the only known siderophore secreted by *Anabaena* sp. is a citrate based hydroxamate schizokinen (Goldman *et al*., 1983). The mechanisms of siderophore secretion across two cell membranes into the surrounding medium, where they bind iron, are still not well understood, in contrast to the systems for the uptake of Fe^{3+}-loaded siderophores (Furrer *et al*., 2002).

Siderophores, heme, heme- and iron-binding proteins (lactoferin, transferrin) and vitamin B_{12} are too big to diffuse through the outer membrane porins. The pathways for their transport share common properties. They all comprise the outer membrane TonB-dependent transporter / receptor (TBDT). TBDT is energized after establishing a physical contact with the inner membrane TonB complex (Figure 3). This complex exploits a cytoplasmic energy source to activate the conformational changes in TBDT and siderophore transport (Andrews *et al*., 2003; Wiener, 2005). Each TBDT is specific for a certain Fe^{3+}-loaded siderophore. Therefore, ferric citrate transporters, ferrichrome transporters, enterobactin transporters, schizokinen transporters, etc., can be distinguished. After the active transport of Fe^{3+}-loaded siderophore across the outer membrane through TBDT is completed, siderophore is bound to the substrate-specific binding protein in the periplasm. The binding protein shuttles siderophore further to the inner membrane ABC

transporter, which hydrolyzes ATP and transfers the Fe^{3+}-siderophore in cytoplasm (Figure 3). There Fe^{3+} is reduced to Fe^{2+}, released from siderophore and either incorporated immediately into enzymes or stored inside of iron storage proteins (Andrews *et al*., 2003; Almoron *et al*., 1992).

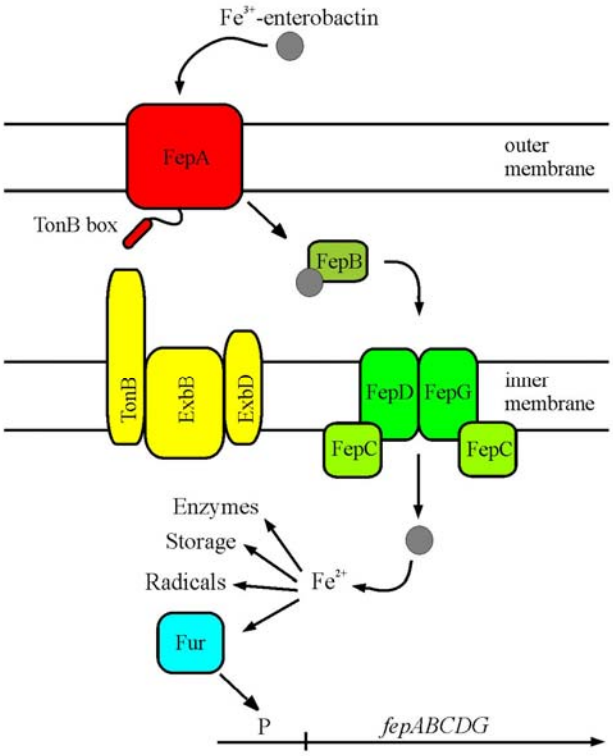

Figure 3. The system for the ferric-enterobactin uptake in *E. coli*. FepA (red) is the outer membrane TonB-dependent transporter energized by the contact of its "TonB box" with the TonB protein of the TonB complex in the inner membrane (yellow). Energized FepA transports ferric-enterobactin (grey circle) into the periplasm. There ferric-enterobactin is bound to the FepB binding protein (dark green) and shuttled further to the inner membrane ABC transporter consisting of FepD, FepG and FepC subunits (green). ABC transporter transports ferric-enterobactin in the cytoplasm where ferri-iron is reduced to ferro-iron and released from eneterobactin. Now free intracellular Fe^{2+} ions bind to the Fur protein (blue). Fe^{2+}-loaded Fur associates with promoters of the iron transport genes preventing their expression (according to Buchanan, 2005).

Currently, the three-dimensional structures of five outer membrane TBDT have been solved. Four of them are from *E. coli*: FhuA (specific for the hydroxymate type siderophore ferrichrome; Ferguson *et al*., 1998; Locher *et al*., 1998), FepA (specific for the catecholate type siderophore enterobactin; Buchanan *et al*., 1999) and FecA (ferric citrate transporter; Ferguson *et al*., 2002; Yue *et al*., 2003) and vitamin B12 transporter BtuB (Kadner, 1990; Chimento *et al*., 2003), and one, FpvA, is from *Pseudomonas aeruginosa* (transporting pyoverdin; Cobessi *et al*., 2005). TBDT are the largest described β-barrel proteins consisting of 22 β-strands with long extracellular loops and short periplasmic

turns (Ferguson and Deisenhoffer, 2004). Their β-barrel channel is occluded by a globular domain, called the "plug", consisting of 150 N-terminal amino acids (Klebb and Newton, 1998; Buchanan *et al*., 1999). When the substrate is bound and transported, the "plug" undergoes through the conformational changes, but it does not "unplug" the channel (Yue *et al*., 2003). Energy for this is secured from the inner membrane TonB complex, consisting of three proteins: TonB, ExbB and ExbD (Higgs *et al*., 1998 and 2002). TonB is a periplasmic protein with an N-terminal inner membrane anchor. When the substrate is bound to TBDT, interaction between TonB and the TBDT is established through a conserved heptapeptide region, the "TonB box", placed at the C-terminal border of the N-terminus (Figures 3 and 4; Lundrigan and Kadner, 1986; Schramm *et al*., 1987). With this interaction energy of ATP hydrolysis is transferred to TBDT to support the conformational changes and active transport.

The majority of TBDT are expressed only in times of iron deficiency (Figure 3, Braun *et al*., 2003). When the intracellular iron supply is sufficient, a global regulator of iron metabolism genes, Fur protein, is loaded with Fe^{2+} ion (Figure 3; Bagg and Neilands, 1987; Escolar *et al*., 1999; Andrews *et al*., 2003). Fur-Fe^{2+} binds to promoter regions of the operons encoding parts of iron transporting systems (the outer membrane and the inner membrane components and the binding protein). When the intracellular Fe^{2+} level is low, Fe^{2+} dissociates from Fur protein, Fur separates from the promoters and transcription of the downstream genes follows (Le Cam *et al*., 1994; Escolar *et al*., 1998 and 2000). This type of regulation is presented at an example of the FepA transporter and the ferric-enterobactin transporting Fep system of *E. coli* (Figure 3).

The minority of TonB-dependent transporters function also as signal transducers. TonB-dependent transducers participate in the transcriptional regulation of the iron transport genes encoding the components of their own iron transport system (Figure 4; Koebnik, 2005). Their expression is influenced not only by iron deficiency but also by availability of the appropriate siderophore in the medium. Among seven iron receptors in *E. coli* only FecA transporter of a ferric citrate transport system is also a signal transducer (Figure 4). In comparison to the standard TBDT, transducers have a unique N-terminal extension or the N-domain upstream from the TonB box (Kim *et al*., 1997; Schalk *et al*., 2004; Koebnik, 2005). Induction of the ferric citrate transport genes is a result of a signal cascade. The signal starts at the cell surface when ferric citrate binds to the minimal number of FecA receptors present under iron repletion in the outer membrane (Braun *et al*.,

2003). If at the same time iron becomes limited inside of the cell, the inner membrane spanning FecR anti-sigma factor is being synthesized (Enz *et al*., 2003; Braun *et al*., 2003).

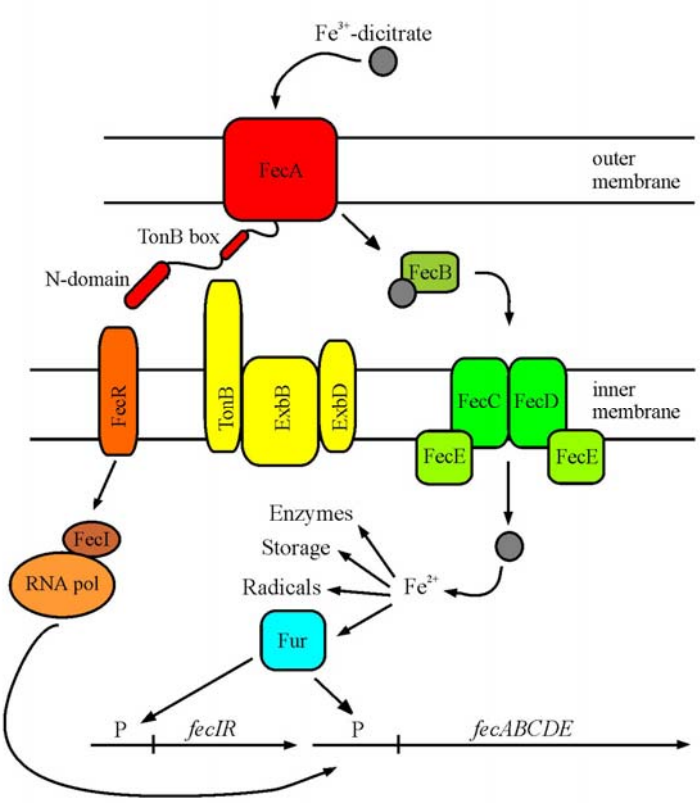

Figure 4. Ferric citrate uptake system in *E. coli*. Intracellular Fe^{2+} ions bind to the Fur protein (blue). Fe^{2+}-loaded Fur associates with promoters of the iron regulating operons preventing their expression. When intracellular Fe^{2+} is scarce it dissociates from Fur and Fur is released from the promoter of *fecRI* operon. As a result a cytoplasmic sigma factor FecI and an inner membrane anti-sigma factor FecR are synthesized. When ferric citrate is present in the surrounding medium, it binds to FecA but without being transported into the cell. The N-domain of FecA interacts then with FecR anti-sigma factor. FecR interacts with FecI sigma factor which then binds to RNA polymerase resulting in transcription of *fecABCDE* genes. After the outer, the inner and the periplasmic components of the ferric citrate uptake system have been synthesized, ferric-dicitrate uptake starts. FecA (red) as an outer membrane TonB-dependent transporter is energized by the contact of its "TonB box" with the TonB protein of the TonB complex in the inner membrane (yellow). Energized FecA transports ferric-dicitrate (grey circle) into the periplasm. There it is bound to the FecB binding protein (dark green) and shuttled further to the inner membrane ABC transporter consisting of FecC, FecD and FecE subunits (green). ABC transporter transports ferric-enterobactin in the cytoplasm where ferri-iron is reduced to ferro-iron and released. Now free intracellular Fe^{2+} can bind again to Fur (blue) in the cytoplasm and prevent further iron uptake to avoid the iron overloading of the cell (according to Buchanan, 2005).

FecR expression is also regulated by Fur protein, being repressed when iron is present and de-repressed when iron is limited. FecR interacts in the periplasm with the N-domain of FecA receiving a signal that ferric citrate siderophore is present in the medium and bound to FecA. The signal is transferred from FecR anti-sigma factor to FecI, an extracytoplasmic function (FEC) σ-factor (Lonetto *et al*., 1994). *fecI* gene is co-transcribed in the same Fur-

regulated operon with *fecR* under iron limitation (Braun, 1997). FecI σ-factor binds to RNA polymerase which than transcribes *fecABCDE* operon encoding the outer and the inner membrane components and the periplasmic binding protein of the ferric citrate transport system (Luck *et al*., 2001). In this way both signals, iron limitation and presence of an adequate siderophore, regulate iron transport together (Enz *et al*., 2000; Buchanan, 2005). Therefore, the function of the *E. coli* FecA transducer is dual: an induction of *fec* operon and a ferric citrate transport (Braun *et al.,* 2003).

3.4. An objective

The significance of the outer membrane for the function of the Gram-negative bacterial cell is huge. The outer membrane provides additional protection against osmotic stress, antibiotics, detergents and other factors that may pose a danger for a bacterial cell. However, besides being a barrier, the outer membrane offers a number of mechanisms to ensure an adequate compound exchange with the surrounding medium and to sense and react to the outside conditions. The protein machineries, pores and channels involved in these processes are numerous and their investigation is essential for understanding of the Gram-negative cell functionality and endosymbiotic relations. Cyanobacterium *Anabaena* sp. PCC 7120 as a model system offers possibility to explore not only the features of a classical Gram-negative microorganism, but also photosynthesis, nitrogen fixation and one of the simplest known cell differentiation process - all of it co-existing and functioning in the same cell. But how are the outer membrane proteome composition and its functions adapted to the multicellularity of this cynobacterium? Do known outer membrane protein machineries of Gram-negative bacteria adopt new characteristics and functions in order to support the multicellularity and cell differentiation? What is the importance of the outer membrane continuum and the periplasmic continuum along the *Anabaena* sp. filament? Attempts to answer these questions, first, by analyzing the outer membrane proteomes of both cell types (heterocysts and vegetative cells) and second, by closer insight in the two outer membrane protein families (TolC protein and TonB-dependent transporters) and their specificities in *Anabaena* sp., have been presented and discussed.

4. Materials

4.1. Chemicals

Chemicals used in this study were purchased from Carl Roth (Karlsruhe, Germany), Sigma-Aldrich (München, Germany) and Merck (Darmstadt, Germany). Special chemicals were purchased as follows: Vanadyl Ribonucleoside Complexes Solution, (±) Propylen Oxide and Alcian Blue 8GX from Sigma-Aldrich (München, Germany), SeaKem LE Agarose from Biozyme Scientific (Hess. Oldendorf, Germany), Bacto™ Agar from Otto Nord Wald (Hamburg, Germany) and digitonin from Serva (Heidelberg, Germany). L-U-^{14}C- labeled amino acids and radio-labeled ^{35}P nucleotides originate from GE-Healthcare (Buckinghamshire, UK).

4.2. Enzymes and kits

Enzymes and kits used for the cloning procedures were purchased as follows: TrippleMaster PCR System kit, Taq-polymerase and T4-DNA ligase from Eppendorf (Hamburg, Germany) and restriction enzymes from Fermentas (St. Leon-Rot, Germany). DNase I, RNase free was obtained from Roche (Manheim, Germany), RNase from GE-Healthcare (Freiburg, Germany), lysozyme and trypsin from Sigma-Aldrich (Steinheim, Germany). SuperScript™ III First Strand Synthesis System for RT-PCR was purchased from Invitrogen (Karlsruhe, Germany). Plasmid isolation in a small scale was performed with FastPlasmid Mini Kit from Eppendorf (Hamburg, Germany) and for higher plasmid yields NucleoBond PC100 Midi Kit from Machinery-Nagel (Düren, Germany) was used. DNA extraction from agarose gels were performed with NucleoSpin® Extract II Kit from Machinery-Nagel (Düren, Germany) and QIAEX II Gel Extraction Kit from Qiagen (Hilden, Germany).

The embedding for electron microscopy was performed with assistance of Epoxy Embedding Medium (Sigma-Aldrich, München, Germany). Probes for Southern blotting were labeled with a help of Ready-To-Go DNA Labeling Beads from GE-Healthcare (Buckinghamshire, UK). ELC™ Western Blotting Analyses System obtained also from GE-Healthcare (Freiburg, Germany) was used for visualization following Western blotting on BioMax MR Films (Kodak).

4.3. Primers

All primers were purchased from Invitrogen (Karlsruhe, Geramany).

Table 1a. List of primers used in this study. The primer names begin with a name of the gene from *Anabaena* sp. PCC 7120. F stands for the forward and R for the reverse primer.

Primer name	Sequence
Generation of deletion strains	
alr2887-INT-F	5'-ATCGGGATCCCCAGCAGATACTCAGTCACCAA-3'
alr2887-INT-R	5'-ATCGGGATCCAGCAATACGGACTTGTTCATCTGC-3'
alr0397-INT-F	5'-ATCGGGATCCAGCACTAACCTACAGCATTTTATCTC-3'
alr0397-INT-R	5'-ATCGGGATCCGGTATCTTCCTGGGAGTAATCTAC-3'
all4026-INT-F	5'-ATCGGGATCCGTAATCAGCCAGAGATGCGAATTA-3'
all4026-INT-R	5'-ATCGGGATCCAGAACATTAAAATTCCGTGACTCGTAA-3'
Generation of over-expression strains	
alr0397-OX-F	5'-ATCGCCATGGAAATGGATTGTGTCACTAGCCATAATC-3'
alr0397-OX-R	5'-ATCGGAATTCGGAATCTTGAGCTACTTCAGTAG-3'
all4026-OX-F	5'-ATCGCCATGGAAGTGGTTTTTGTGGAGTGTGGG-3'
all4026-OX-R	5'-ATCGGAATTCCGTTAAACCATTAGATTGATTTACTACCTG-3'
Generation of GFP-promoter fusion strains	
alr2887-pGFP-F	5'-ATCGATCGATACAGGTACAGGTAAAACCCTGTTA-3'
alr2887-pGFP-R	5'-ATCGGATATCATAGAATAAGTGTTGTCCTTTCACCG-3'
alr0397-pGFP-F	5'-ATCGATCGATGCATCGCTTCTATTGCTACTGG-3'
alr0397-pGFP-R	5'-ATCGGATATCATTATGGCTAGTGACACAATCCATC-3'
all4026-pGFP-F	5'-ATCGTTCGAAGCGCGCCTTTACGTTTAAATGTC-3'
all4026-pGFP-R	5'-ATCGGATATCCCCACACTCCACAAAAACCAC-3'
Generation of GFP-protein fusion strains	
alr2887-Ct-GFP-F	5'-ATCGATCGATTTAGCAGGGCTGTGGAACCAAT -3'
alr2887-Ct-GFP-R	5'-ATCGGATATCCTGACTACTAATTAATGCTCTAGAAGT -3'
alr0397-Ct-GFP-F	5'-ATCGATCGATGAACCGCAAAAAGTAGATAACTATGAA -3'
alr0397-Ct-GFP-R	5'-ATCGGATATCCCAATCAAAAGAATACTTAATACTCAAAGTC -3'
all4026-Ct-GFP-F	5'-ATCGATCGATACCTGGACTTACGAAGCAGGTT-3'
all4026-Ct-GFP-R	5'-ATCGGATATCAAAACTCGCACTTACTCGCACAC-3'
alr2269-Ct-GFP-F	5'-ATCGATCGATACGGGAGAAGATGACTTATTACTAG-3'
alr2269-Ct-GFP-R	5'-ATCGGATATCAAACCTTTCTCCAATACCGAAATTGAT-3'

Table 1b. List of primers used in this study. The primer names start with a name of the gene from *Anabaena* sp. PCC 7120. F stands for the forward and R for the reverse primer.

Primer name	Sequence
GFP primers for sequencing	
GFPseq.1	5'-CCTCTCCACTGACAGAGAATTTTT-3'
GFPseq.2	5'-GGGTAAGTTTTCCGTATGTTGCAT-3'
RT-PCR primers	
isiA-F	5'-GCCCGCTTCGCCAATCTCTC-3'
isiA-R	5'-CCTGAGTTGTTGCGTCGTAT-3'
rnpB-F	5'-AGGGAGAGAGTAGGCGTTGG-3'
rnpB-R	5'-GGTTTACCGAGCCAGTACCTCT-3'

4.4. Vectors

All vectors used in the cloning purpose or for conjugations into wild type *Anabaena* sp. PCC 7120 are a gift from the laboratory of Dr. Enrique Flores (CSIC, Seville, Spain).

Table 2. List of vectors used in this study.

Vector	Resistance	Origin	Purpose	Source
pCSEL21	Ap^R	pIC20R	*gfp*	Olmedo-Verd *et al.*, 2006
pCSEL24	Sp^RSm^R (C.S3 cassette)	pBR322	cargo vector	Olmedo-Verd *et al.*, 2006
pCSV3	SpRSmR (C.S3 cassette)	pRL500	cargo vector	E. Flores, unpublished
pCSM1	Sp^RSm^R (C.S3 cassette)	pTrc99A	cargo vector	Olmedo-Verd *et al.*, 2005
pREP4	Km^R	/	LacI repressor	Olmedo-Verd *et al.*, 2005
pRL623	Cm^R	/	helper vector	Elhai & Wolk, 1988a
pRL443	Ap^R	/	conjugal vector	Elhai & Wolk, 1988a

4.4.1 Cyanobacterial and bacterial strains

***Anabaena* sp. PCC 7120 strains:**

WT	• gift from Dr. Enrique Flores (Seville, Spain)
hetR	• gift from Dr. Enrique Flores (Seville, Spain)
DR181	• gift from Dr. Iris Maldener (Tübingen, Germany)

***Escherichia coli* strains:**

DH5α	• Invitrogen (Karlsruhe, Germany)
BL21 (DE3)	• Novagen (Madison, USA)
XL1Blue	• Invitrogen (Karlsruhe, Germany)
ED8654	• gift from Dr. Enrique Flores (Elhai & Wolk, 1988b)
HB101	• gift from Dr. Enrique Flores (Elhai & Wolk, 1988b)

4.5. Antibodies

Primary antibodies were raised against heterologously expressed full-length proteins of *Anabaena* sp. PCC 7120 or *Synechocystis* sp. PCC 6803. NrtA, OxaA and synToc75 antibodies were a kind gift from Prof. Dr. J. Soll. Commercial primary antibody against GFP from *Aquorea victoria* (rabbit fraction) was purchased from Invitrogen (Karlsruhe, Germany). Secondary antibodies against rabbit and chicken IgG and risen in a goat were purchased from Sigma-Aldrich (München, Germany). Commercial D1 antibody (AgriSera, Vänäs, Sweeden) was a kind gift from Dr. Jörg Meurer.

4.6. Glass beads, TLC plates and membranes

Glass beads, acid washed come from Sigma Aldrich (München, Germany) and TLC Silica gel 60 F_{254} aluminum sheets 20 cm x 20 cm are from Merck (Darmstadt. Germany). Nitrocellulose Protran BA-S83 membranes were purchased from Schleichter & Schüll (Dassel, Germany) and positively charged Hybond-N+ nylon membranes were purchased from Amersham Pharmacia Biothec (Buckinghamshire, England). Conjugations were performed on white surfactant-free Millipore filters (Schawalbach, Germany).

4.7. System for the growth of *Anabaena* sp. PCC 7120 cultures

An improvised system for the growth of cyanobacterial air/CO_2 bubbled cultures (Figure 5A) consists of the 50 cm x 30 cm x 30 cm glass water tanks with water heathers (Julabo Labortechnik, Seelbach, Germany) and a regulatory panel (Figure 5B, big circle). The regulatory panel comprises an air pressure control device (Knf Neuberger, Balterswil, Switzerland), CO_2 pressure control device (Aalborg, Monsey, Germany) and Grässlin light switch with an inbuilt timer and power doses (Löbbe GmbH, Kamen, Germany). Light tubes originate from Norka (Hamburg, Germany) while Labport air pump is purchased from Knf Neuberger (Balterswil, Switzerland; Figure 5B).

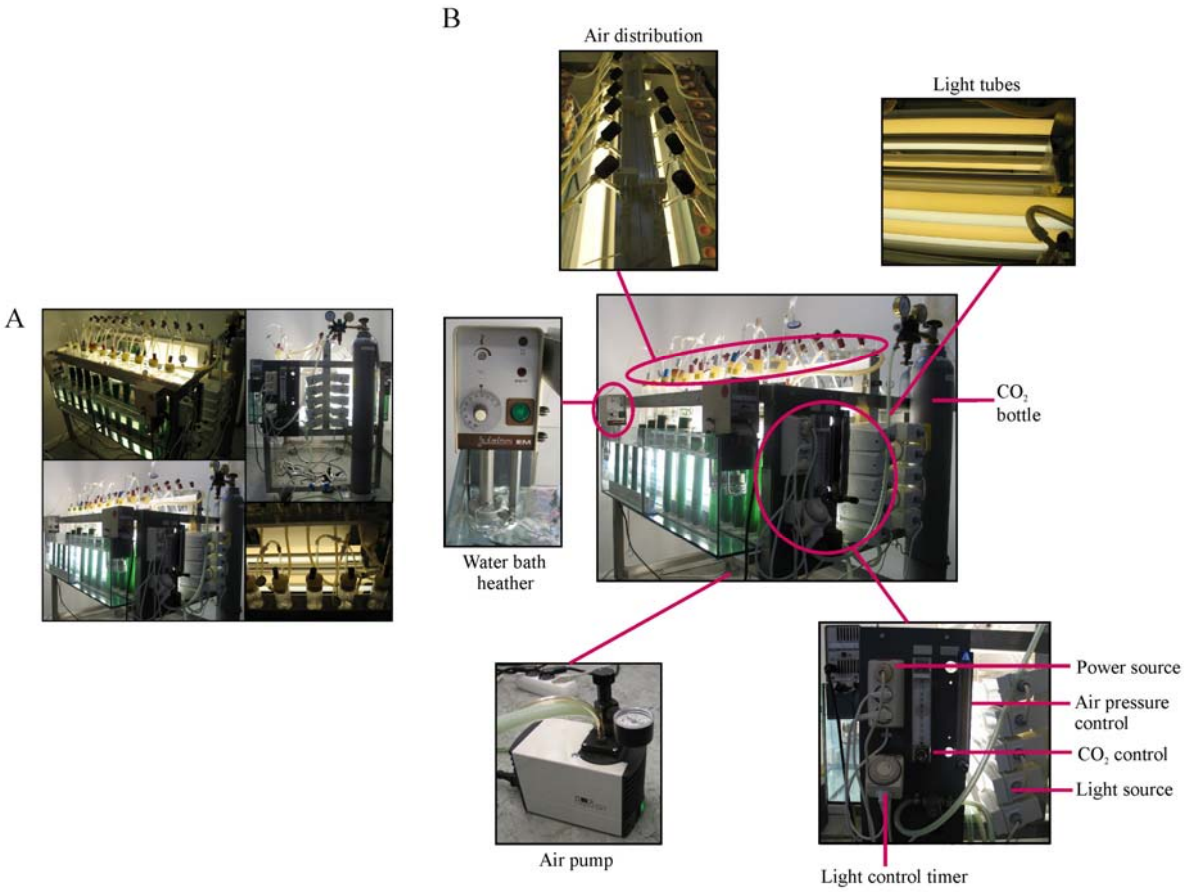

Figure 5. System used for the growth of air/CO_2 bubbled cultures of *Anabaena* sp. PCC 7120; (A) presents the complete system and (B) presents the more important parts separately.

5. Methods

5.1. Molecular biological methods

5.1.1 General molecular biological methods

The growth conditions of the *E. coli* cultures, phenol/chlorophorm extraction or isopropanol/ethanol precipitation of DNA, agarose electrophoresis and transformation were performed as described in Sambrook *et al*. (1989). Competent *E. coli* cells were prepared according to Hanahan *et al.* (1985). Restriction, ligation, purification and extraction from agarose gels of PCR products, plasmid DNA and DNA fragments were performed according to the recommendation of the manufacturer of the corresponding kit (see "Materials"). For the lager DNA fragments *Eco*RI/*Hin*dIII restricted λ-phage DNA was used as a molecular weight standard and for the smaller fragments the molecular weight standard used was the *Pst*I restricted λ-phage DNA.

5.1.2 Polymerase chain reaction (PCR)

DNA fragments for cloning into the plasmid vectors were obtained by multiplying the DNA regions on the genomic DNA template with PCR (Saiki *et al*., 1988). Reactions were performed according to recommendations provided by manufacturer of the DNA polymerase containing kit (TripleMaster PCR System, Eppendorf, Hamburg, Germany). The appropriate restriction sites were incorporated in the primers used in PCR reactions (Table 1).

5.1.3 Cloning strategies

5.1.3.1 Generation of deletion strains

In order to generate the *Anabaena* sp. deletion strains NMΔ-*alr2887*, NMΔ-*all4026* and NMΔ-*alr0397*, internal 600 bp of the corresponding gene coding regions were amplified by PCR on the genomic DNA template, using primers containing *Bam*HI restriction sites (Table 1). The restricted PCR products were cloned directly into the cargo pCSV3 vector containing Sm^R/Sm^R C.S3 gene cassette (Elhai & Wolk, 1988a). In this way plasmids pNMΔ-*alr2887*, pNMΔ-*al4026* and pNMΔ-*alr0397* were produced (Table 3).

The plasmids were multiplied by transformation into the *E. coli* DH5α competent cells and their sequence was confirmed by conventional sequencing. The transformation of *Anabaena* sp. wild type by conjugal transfer of pNMΔ-*alr2887*, pNMΔ-*all4026* and pNMΔ-*alr0397* was performed as previously described (Elhai and Wolk, 1988b) resulting in single recombination mutants (Table 4).

5.1.3.2 Generation of over-expression strains

In order to generate the over-expression strains of *Anabaena* sp., named NMOX-*all4026* and NMOX-*alr0397*, 500 bp of *all4026* and *alr0397*open reading frames (ORF) encoding N-terminus of the proteins were amplified by PCR on genomic DNA using primers with *Nco*I/*Eco*RI restriction sites (Table 1). Restricted PCR products were cloned directly into the pCSM1 cargo plasmid where they were placed under control of the strong artificial *trc* promoter. The plasmids were multiplied by electroporation into *E. coli* XL1Blue strain expressing LacI repressor and the sequence was confirmed by conventional sequencing. The generated plasmids pNMOX-*alr2887*-GFP, pNMOX-*all4026*-GFP, pNMOX-*alr0397*-GFP were transferred by conjugation into *Anabaena* sp. wild type (Elhai and Wolk, 1988b) resulting in single recombination mutants (Table 4).

5.1.3.3 Generation of GFP-protein fusion strains

In order to generate NMP-*alr2887*-GFP, NMP-*all4026*-GFP, NMP-*alr0397*-GFP and NMP-*alr2269*-GFP strains with GFP fused to a C-terminus of the protein, 500 bp of the *alr2887*, *all4026, alr0397* and *alr2269* open reading frames encoding the C-terminus of the corresponding proteins were amplified by PCR on genomic DNA using primers with *Cla*I/*Eco*RV restriction sites (Table 1). The restricted PCR products were cloned into pCSEL21 to generate an in-frame product with the *gfp* ORF. The plasmids were amplified by transformation into the *E. coli* DH5α and the sequences were confirmed by conventional sequencing. Subsequently, the GFP fusion constructs were excised by restricting with *Eco*RI. The fragments were precloned into pCSV3 cargo plasmid generating constructs named pNMP-*alr2887*-GFP, pNMP-*all4026*-GFP, pNMP-*alr0397*-GFP and pNMP-*alr2269*-GFP (Table 3). Transformation of *Anabaena* sp. wild type was performed as previously described (Elhai and Wolk, 1988b) resulting in single recombination mutants (Table 4).

5.1.3.4 Generation of GFP-promoter fusion strains

In order to generate NME-*alr2887*-GFP, NME-*all4026*-GFP and NME-*alr0397*-GFP GFP-promoter fusion strains, 800 bp of the promoter region of the corresponding genes including the first 24 bp of the gene coding region were amplified by PCR on the genomic DNA using primers with *Cla*I/*Eco*RV restriction sites in the case of *alr2887* and *alr0397* and *Bst*BI/*Eco*RV in the case of *all4026* (Table 1). Restricted PCR products were further cloned into pCSEL21 in front of the *gfp* ORF. The fusion fragments were excised by digestion with *Pst*I/*Eco*RI and ligated into cargo vector pCSEL24. The resulting plasmids were named pNME-*alr2887*-GFP, pNME-*all4026*-GFP and pNME-*alr0397*-GFP (Table 3). Their conjugation into *Anabaena* sp. wild type was performed as described (Elhai and Wolk, 1988b) resulting in single recombination mutants (Table 4).

Table 3. List of constructs generated in this study. INT stands for internal 600 bp of the gene, P for promoter, Ct for the C-terminus of the protein and Nt for the N-terminus of the protein.

Construct	Plasmid	Resistance	Purpose
INT*alr2887*	pCSV3	Sp^RSm^R	cargo vector, deletion of *alr2887*
INT*all4026*	pCSV3	Sp^RSm^R	cargo vector, deletion of *all4026*
INT*alr0397*	pCSV3	Sp^RSm^R	cargo vector, deletion of *alr0397*
$P_{alr2887}$	pCSEL21	Ap^R	insertion of $P_{alr2887}$ in front of *gfp*
$P_{all4026}$	pCSEL21	Ap^R	insertion of $P_{all4026}$ in front of *gfp*
$P_{alr0397}$	pCSEL21	Ap^R	insertion of $P_{alr0397}$ in front of *gfp*
Ct-*alr2887*	pCSEL21	Ap^R	*gfp* fusion to 3' end of *alr2887*
Ct-*all4026*	pCSEL21	Ap^R	*gfp* fusion to 3' end of *all4026*
Ct-*alr0397*	pCSEL21	Ap^R	*gfp* fusion to 3' end of *alr0397*
Ct-*alr2269*	pCSEL21	Ap^R	*gfp* fusion to 3' end of *alr2269*
Nt-*all4026*	pCSM1	Sp^RSm^R	cargo vector, over-expression from P_{trc}
Nt-*alr0397*	pCSM1	Sp^RSm^R	cargo vector, over-expression from P_{trc}
$P_{alr2887}$-*gfp*	pCSV3	Sp^RSm^R	cargo vector, promoter-*gfp* fusion
$P_{all4026}$-*gfp*	pCSV3	Sp^RSm^R	cargo vector, promoter-*gfp* fusion
$P_{alr0397}$-*gfp*	pCSV3	Sp^RSm^R	cargo vector, promoter-*gfp* fusion
Ct-*alr2887-gfp*	pCSV3	Sp^RSm^R	cargo vector, protein-GFP fusion
Ct-*all4026-gfp*	pCSV3	Sp^RSm^R	cargo vector, protein-GFP fusion
Ct-*alr0397-gfp*	pCSV3	Sp^RSm^R	cargo vector, protein-GFP fusion

Table 4. Mutant strains of *Anabaena* sp. PCC 7120 generated in this study.

***Anabaena* strain**	**Resistance**	**Relevant genotype**	**Purpose**
NMΔ-*alr2887*	Sp^RSm^R (C.S3 cassette)	*alr2887* :: pCSV3	deletion *alr2887*
NMΔ-*all4026*	Sp^RSm^R (C.S3 cassette)	*all4026* :: pCSV3	deletion *all4026*
NMΔ-*alr0397*	Sp^RSm^R (C.S3 cassette)	*alr0397* :: pCSV3	deletion *alr0397*
NMOX-*all4026*	Sp^RSm^R (C.S3 cassette)	*trc* promoter :: *all4026*	over-expression *all4026*
NMOX-*alr0397*	Sp^RSm^R (C.S3 cassette)	*trc* promoter :: *alr0397*	over-expression *alr0397*
NMP-*alr2887*-GFP	Sp^RSm^R (C.S3 cassette)	*alr2887* :: *gfp*	C-terminal GFP fusion to Alr2887
NMP-*all4026*-GFP	Sp^RSm^R (C.S3 cassette)	*all4026* :: *gfp*	C-terminal GFP fusion to All4026
NMP-*alr0397*-GFP	Sp^RSm^R (C.S3 cassette)	*alr0397* :: *gfp*	C-terminal GFP fusion to Alr0397
NMP-*alr2269*-GFP	Sp^RSm^R (C.S3 cassette)	*Alr2269* :: *gfp*	C-terminal GFP fusion to Alr2269
NME-*alr2887*-GFP	Sp^RSm^R (C.S3 cassette)	$P_{alr2887}$-*gfp* in *nucA* region	*alr2887*-promoter GFP fusion
NME-*all4026*-GFP	Sp^RSm^R (C.S3 cassette)	$P_{all4026}$-*gfp* in *nucA* region	*all4026*-promoter GFP fusion
NME-*alr0397*-GFP	Sp^RSm^R (C.S3 cassette)	$P_{alr0397}$-*gfp* in *nucA* region	*alr0397*-promoter GFP fusion

5.1.4 RT-PCR

SuperScript™ III First Strand Synthesis System for RT-PCR (Invitrogen, Freiburg, Germany) was used to generate DNA on *Anabaena* sp. RNA template. 1-2 μg of the isolated total *Anabaena* sp. RNA were used in reactions with random hexamers. The reactions were performed according to the protocol provided by manufacturer. Every reaction was performed two times: once in the presence of reverse transcriptase enzyme (RT) in reaction and once without RT, as control for the presence of the genomic DNA contaminations in the RNA isolates. 2 μl of the synthesized DNA was used further for PCR with gene specific primers. The results were considered positive only when a clear difference in intensity of the PCR bands was obtained for reactions with and without addition of RT.

5.1.5 Southern blotting

Southern blotting of the enzyme restricted genomic DNA from the deletion mutants NMΔ-*alr2887*, NMΔ-*all4026* and NMΔ-*alr0397* was performed according to the standard procedure (Sambrook *et al*., 1989) using ^{35}P-radioactively labeled DNA as a probe. The DNA probes were produced by PCR and were radioactively labeled with a help of Ready-To-Go DNA Labeling Beads from GE-Healthcare (Buckinghamshire, UK). The genomic DNA of the NMΔ-*alr2887* mutants was digested with *Dra*I enzyme, of the NMΔ-*all4026* mutants with *Ase*I and of the NMΔ-*alr0397* mutants with *Hin*dIII.

5.2. Biochemical methods

5.2.1 Determination of protein concentration

Total protein content of the isolated membrane fractions or of *Anabaena* sp. cells previously lysed in a buffer containing 50 mM Tris/HCl pH 8.0, 2% SDS, 5 mM EDTA, 10 mM β-mercaptoethanol, 100 mM NaCl was determined by Bio-Rad Protein Assay Kit (Bio-Rad Laboratories, München, Germany).

5.2.2 SDS-Polyacrylamid Gel Electrophoresis (SDS-PAGE) and Blue-Native electrophoresis (BN-PAGE)

Proteins were separated in SDS-polyacrylamide gels with acrylamide concentrations 10% or 12.5% depending on the protein size and the purpose according to Laemmli (1970). Prior to applying on the gel, samples were solubilized in a sample buffer (Laemmli buffer) and incubated at 96°C for 2 min. The gels were stained with Coomassie Brillant Blue (R 250 for normal or G for colloidal Coomassie) or by silver staining according to the methods published in Sambrook *et al*. (1989).

For BN-PAGE 150 µl of an isolated outer membrane fraction of *Anabaena* sp. was solubilized by addition of 1% dodecylmaltoside, 100 mM octylglucoside or 100 mM FOS-Choline. The protein complexes were separated by BN-PAGE (4% - 12.5%) as described in Schägger *et al*., 1994. Proteins were subsequently separated by SDS-PAGE (12.5%). The bands of interest were extracted and subjected to the mass spectrometric analysis in collaboration with the laboratory of Dr. Lutz A. Eichacker.

5.2.3 Western blotting

Western blotting was performed according to the "semi-dry-blot" method (Towbin *et al*., 1979). Proteins were transferred to the nitrocellulose membranes which were incubated three times for 10 min in a blocking buffer (100 mM Tris/HCl pH 7.5, 150 mM NaCl, 0.3% skim milk powder, 0.03% BSA) followed by an overnight incubation at 4°C in primary antibody diluted in the blocking buffer (dilutions varied from 1:500 to 1:2 000 depending on the choice of primary antibody). The nitrocellulose membranes were washed again three times 10 minutes in the blocking buffer, incubated for 1 hour in a secondary antibody (against rabbit or chicken IgG, dilution 1: 10 000 in blocking buffer) and washed again three times in the blocking buffer.

For the protein visualisation with colorimetric reaction with alkaline phosphatase the blotting membranes were incubated in 100 mM Tris/HCl pH 9.5, 100 mM NaCl, 5 mM $MgCl_2$, 0.035% NBT (w/v), 0.0175% BCIP (w/v). For the chemiluminescent visualisation ELC™ Western Blotting Analyses System (GE-Healthcare, Freiburg, Germany) was applied according to the manufacturer's recommendation.

5.2.4 Protein extraction

60 µl of isolated outer membrane fractions were pelleted at 80 000 rpm, 10 min, 4°C. Pellet was resuspended in 100 ml of 8 M urea, 0.1 M Na_2CO_3 and 1 M NaCl, and it was subsequently kept on ice for 30 min. The control sample was resuspended in a phosphate buffer pH 8.0. The samples were pelleted again at 80 000 rpm, 10 min, 4°C. The pellet and 60 µl of the resulting supernatant were resuspended in Laemmli sample buffer and separated on SDS-polyacrylamide gels.

5.2.5 Digestion of *Anabaena* sp. outer membrane proteins and mass spectrometry

An outer membrane fraction of *Anabaena* sp. was centrifuged at 80 000 rpm, 10 min, 4°C. The pellet was resuspended in 80% acetone, 5% formic acid and 0.1% deoxycholic acid and incubated on ice for 10 min. After centrifugation at 80 000 rpm, 15 min, 4°C, the pellet was washed with 20 µl of 80% acetone and repelleted by 10 min centrifugation. The resulting pellet was submitted to the tryptic digestion by resuspension in 100 mM Tris/HCl pH 8.5, 1 mM $CaCl_2$ and 10 µg/µl Trypsin, with an enzyme to

substrate ratio of approximately 1:100. For digestion, probes were transferred into LoBind tubes (Eppendorf, Hamburg, Germany) and digested for 16 hours at 37°C with gentle shaking. Digestion was stopped by addition of 40% formic acid to a final concentration of 5%. After proteolysis, preparations were directly subjected to the mass spectrometric analysis.

Mass spectrometric analysis and protein identification was performed with Q-TOF Ultima API (fractionation in the presence of digitonin) and LCQ Deca XP (fractionation without usage of digitonin) in cooperation with the laboratory of Dr. Lutz A. Eichacker (Eichacker *et al.*, 2004).

5.3. Chromatography methods

5.3.1 Thin Layer Chromatography (TLC) of lipids

Lipid analysis was performed as described in Fiedler *et al.* (1998a). Lipids were extracted from *Anabaena* sp. filaments, isolated heterocysts and cell wall/outer membrane fractions by addition of methanol/chloroform (1:2). Organic solvent was evaporated in a stream of nitrogen. Lipids were dissolved in 200 µl of chloroform and spotted on the thin-layer aluminum sheets covered with a silica gel layer (Kieselgel 60 $F_{254,}$ Merck, Germany). The sheets were developed in a glass chamber with a running phase comprising 170 ml chloroform, 30 ml methanol, 20 ml acetic acid and 7.4 ml distilled water. Lipids were visualized by sprinkling with 25% sulfuric acid, and exposing the plate to 220°C, 30 sec to 1 min.

5.4. Methods related to *Anabaena* sp. PCC 7120

5.4.1 Media and growth conditions

Anabaena sp. wild type and mutants strains were grown photoautotrophically at 30°C in liquid BG11 medium (Rippka *et al*., 1979) supplied with 17.6 mM of $NaNO_3$ as a source of bound nitrogen and under constant illumination from incandescent lamps at 70 mol photons $m^{-2}s^{-1}$. For the "bubbling" cultures aeration by air containing 1% CO_2 was applied. The same medium without source of bound nitrogen was $BG11_0$. The cultures of deletion, over-expression strains, GFP-protein and GFP-promoter fusion strains (Table 4)

were grown in the presence of 2 μg ml^{-1} streptomycin and 2 μg ml^{-1} spectinomycin, except DR181 cultures which contained 50 μg ml^{-1} of neomycin. Heterocyst formation was induced in liquid cultures by washing the cells three times in $BG11_0$ medium without bound nitrogen and reinoculating them in the same medium for the next 48 hours. Experiments with the metal transporter mutants NMΔ-*all4026*, NMΔ-*alr0397*, NMOX-*all4026*-GFP and NMOX-*alr0397*-GFP were performed in the $BG11_{-Fe}$ medium without source of iron (no ferric ammonium citrate added) or in the medium $BG11_{-Fe-Cu}$ without sources of iron and copper (no ferric ammonium citrate and no $CuSO_4$ x $5H_20$ added). All glassware used in experiments under iron-limited conditions was soaked with 6 M HCl and 1 mM EDTA to remove residual iron, and rinsed thoroughly with MiliQ water.

Agar plates were prepared with 1.5 % Bacto™ Agar (Otto Nord Wald, Hamburg, Germany). In order to test the ability of the mutant strains to grow without bound nitrogen source, cells were spotted on agar medium without antibiotics, being either standard BG11 agar medium or $BG11_0$. To test ability for growth of the metal transporter mutants medium $BG11_{-Fe-Cu}$ was supplemented with increasing concentrations of $CuSO_4$ x $5H_20$ as a copper source and $FeCl_3$ x $6H_20$ as an iron source, 1.5% agar plates with and without antibiotic were prepared and cells were spotted on the plates.

5.4.2 Determination of the chlorophyll a concentration

In order to determine the chlorophyll a concentration, 50 μL of *Anabaena* sp. wild type culture or the deletion, over-expression or GFP- promoter mutant culture (Table 4) were mixed with 1 ml of methanol and vortexed vigorously for 1 min. Cell debris were pelleted down in a table centrifuge at maximum speed and optical density of clear supernatant was measured at 665 nm. Chlorophyll a concentration was calculated according to a formula:

$$\mu g\ Chl\ a/ml = 13.43 \times OD_{665nm} \times \text{dilution factor}$$

5.4.3 Growth curve

Wild type and mutant cultures NMD-*alr0397*, NMD-*all4026* and NMOX-*alr0397*, NMOX-*all4026* were grown in the standard BG11 medium for a week. The cells were washed three times in the medium without iron source and amount of cell co corresponding

to 0.4 μg/μl of chlorophyll a was reinoculated in the same iron depleted medium. 200 μl samples were taken immediately after the reinoculation and afterwards regularly every morning and every evening for 5-6 days. The cultures were thoroughly resuspended with a help of syringe and 0.8 mm needle by pulling the filaments 6-8 times through the needle every time before 200 μl samples were taken. Collected samples were frozen and stored at -20°C and the protein content was determined spectrophotometrically.

5.4.4 DNA isolation out of *Anabaena* sp. PCC 7120

Total DNA of *Anabaena* sp. was isolated according to Cai and Wolk (1990) from 50 ml of the two week old cultures. Cells were collected by centrifugation at 3 000 x g, 5 min, room temperature, resuspended in 10 mM Tris/HCl pH 8.0 and 0.1 mM EDTA pH 8.0 up to 400 μl final volume. 150 μl of the glass beads, 20 μl of 10% SDS and 450 μl of phenol: chlorophorm = 1:1 (v/v) was added. Mixture was vigorously vortexed four times for 1 min, while keeping the cells 1 min on ice between every vortexing period, and subsequently centrifuged 15 min, 13 000 rpm, 4°C. The clean upper phase was extracted twice with phenol/chlorophorm and twice with chlorophorm. DNA was precipitated out of the water phase with two volumes of ethanol absolute and 0.1 volume of 3 M sodium acetate pH 5.2, overnight at -20°C, and then it was washed with 70% ethanol, air dried and dissolved in a sterile water.

5.4.5 RNA isolation out of *Anabaena* sp. PCC 7120

Total *Anabaena* sp. RNA was isolated as published in Valladares *et al.* (1999). Filaments were collected by centrifugation at 3 000 x g, 5 min and resuspended in 50 mM Tris/HCl pH 8.0 and 100 mM EDTA pH 8.0. While keeping the samples on ice 200 mM of VRC (Vanadyl Ribonucleoside Complexes) solution was added together with 150 μl of acid washed glass beads, 400 μl of STET buffer (8% sucrose, 5% Triton X-100, 50 mM EDTA pH 8.0, 50 mM Tris/HCl pH 8.0), 200 μl of phenol and 200 μl of chlorophorm. The mixture was vortexed vigorously four times for 1 min, with 1 min breaks while still keeping the cells on ice, and subsequently centrifuged at 13 000 rpm, 15 min, 4°C. Supernatant was transferred to a fresh tube and nucleic acids were precipitated with 0.1 volumes of 3 M sodium acetate pH 5.2 and two volumes of ethanol absolute and followed

by 30 min at -80°C. The precipitate was centrifuged for 15 min at 4°C and 13 000 rpm, pellet was resuspended in 300 µl of water and extracted twice with phenol/chlorophorm and twice with chlorophorm and then keept overnight at -20°C. The next day precipitate was washed with 70% ethanol, pellet was air dried and resuspended in 200 µl of water. To the each sample 10 µl of 3 M sodium acetate pH 5.2, 5 mM of $MgSO_4$, 90 µl of water and 1 µl of DNase, RNase-free from Roche (Manheim, Germany) were added to remove the co-isolated DNA. Samples were incubated for 1 hour at 30°C and RNA was extracted twice with phenol/chlorophorm and twice with chlorophorm, precipitated with two volumes of ethanol absolute (1 hour, -80°C), washed with 70% ethanol, air dried and resuspended in the RNase-free water. After testing on the gel, DNase treatment of the samples was repeated when necessary.

5.4.6 Conjugation

Anabaena sp. wild type strain was transformed with plasmids according to the method of three-parental mating (Elhai and Wolk, 1988b). The cargo strain HB101 was created by pre-transformation with helper plasmid pRL623 and subsequent transformation with the cargo plasmids bearing cloned constructs (pCSV3 or pCSM1). The cargo strain was mixed gently with the conjugal strain ED8654, carrying conjugal plasmid pRL443, and with wild type *Anabaena* sp cells (three parents). The mixture was spread onto nitrocellulose filter placed on BG11 agar medium supplemented with 5% LB medium. After 24 hours of incubation in the growth chamber the filter was first transferred to fresh BG11 plates without antibiotics for the next 24 hours and then every second day on the fresh BG11 plates with antibiotics for at least two weeks. After the thick green background of *Anabaena* sp. cells had died out, the single colonies of exconjugants appeared on the filters. Some of the exconjugant colonies were singled out from the filters and during few following weeks regularly re-streaked with a help of a magnifying lens to the new selective BG11 plates in order to clean obtained *Anabaena* sp. mutants from *Escherichia coli* cells. In this way single recombination mutants were obtained. Their segregation and genetic structure were confirmed by Southern blotting in the case of the deletion mutants or by PCR in the case of the GFP-promoter fusions, the GFP-C-terminal protein fusions and the over-expression mutants.

5.4.7 Heterocyst isolation

To induce heterocyst differentiation wild type cells were grown in 3 l of BG11 medium up to the late exponential phase under conditions mentioned above. Filaments were collected by centrifugation at 3000 x g, 10 min, room temperature, washed twice in $BG11_0$ medium and grown further for 48 hours in 1.5 l of the same nitrate-free medium.

Heterocyst isolation was performed according to the slightly modified protocol of Golden *et al.* (1991). Wild type cells were collected by centrifugation after 48 hours induction in $BG11_0$ medium. Filaments were checked under the microscope for the presence of mature heterocysts. The pellet was resuspended in 15 ml of an ice-cold STET buffer (8% sucrose, 5% Triton X-100, 50 mM EDTA pH 8.0, 50 mM Tris/HCl pH 8.0) containing 1 mg/ml of lysozyme and vortexed vigorously 2-3 minutes at room temperature. To reduce viscosity and break vegetative cells the solution was subjected to a mild sonication (Bandeln Sonopuls Sonifier, MS73 tip) for around 3 min and on ice. Heterocysts were collected by centrifugation at 3000 x g, 5 min, 4°C, and washed three to four times (if necessary even more) in SET buffer (8% sucrose, 50 mM EDTA pH 8.0, 50 mM Tris/HCl pH 8.0) and either immediately processed further or frozen in liquid nitrogen and stored at -20°C.

5.4.8 Membrane fractionation of vegetative cells

After harvesting, filaments were washed once in 5 mM HEPES pH 8.0 and 1 mM PMSF (4,000 x g, 10 min, room temperature), resuspended in 30 ml of the same buffer and broken by one time French pressing at 1100 Psi (SLM instruments, Inc). Prior to breaking, protease cocktail inhibitor tablets (Roche, Manheim, Germany) were added to the cell suspension to prevent protein degradation. All the following steps were performed on ice. The broken cells were centrifuged at 48 000 x g, 45 min, 4°C. The dark green pellet was carefully resuspended in 55% sucrose solution containing 20 mM HEPES pH 8.0 and 0.2 mM PMSF. 0.2% digitonin (w/v) was added to this cell-sucrose mixture when indicated. The floating sucrose density gradients were prepared by adjusting the sucrose concentration of the cell suspension to 55% and overlaying the mixture with 40%, 30% and 10% sucrose solutions (all containing 20 mM HEPES pH 8.0 and 0.2 mM PMSF). The cell fractions were separated by centrifugation at 130 000 x g, 16 hours, 4°C. An orange pigment layer from the very top of the gradients was discarded. The plasma membrane band and the green thylakoid membrane layer were collected and diluted with washing

buffer containing 20 mM HEPES pH 8.0 and 1 mM PMSF. The outer membrane pellet was washed and diluted in the same buffer. The plasma membranes and the outer membranes were collected by centrifugation at 380 000 x g, 1 hour, 4°C, whereas thylakoid membranes were collected at 130 000 x g, 1 hour, 4°C. Membranes were resuspended and stored in 20 mM HEPES pH 8.0 and 1 mM PMSF buffer at –20°C.

5.4.9 Membrane fractionation of isolated heterocysts

Membrane fractionation (specifically outer membrane isolation) was performed out of isolated heterocysts of wild type or NMΔ-*alr2887* mutant of *Anabaena* sp. PCC 7120. After staining with 0.5% Alcian Blue (50% ethanol solution) followed by visualisation under microscope, as well as after Coomassie stained PAGE gel and after Western blotting with D1 antibody, isolated heterocysts show minimal contamination with vegetative cells. Immediately after the isolation heterocyst pellet was resuspended in 30 ml of 5 mM HEPES/NaOH buffer (pH 8.0) with addition of 1 mM PMSF (phenylmethylsulfonyl fluoride). The heterocyst suspension was strongly sonicated on Branson Sonifier 450 (macro-tip, output 5) five times 2 min, while keeping the cells on ice and making regularly breaks between the cycles to prevent the overheating. The sonication was followed by four cycles of French Pressure cell press (SLM instruments, Inc) at 1100 Psi. Only after this harsh treatment most of heterocysts appear to be broken, as viewed under the microscope. The suspension of the broken heterocysts was mixed with protease inhibitor ("Complete" - Protease Inhibitor Cocktail Tablets; Roche, Germany) and subsequently centrifuged at 15 000 x g, 4°C for 1 hour. The pellet was resuspended in 15 ml of 55% sucrose solution and loaded at the bottom of the sucrose gradient, followed by 8 ml of 40% sucrose, 3 ml of 30% sucrose and 7 ml of 10% sucrose solution (all sucrose solutions contained 20 mM HEPES pH 8.0 and 0.2 mM PMSF). The prepared gradients were centrifuged for 16 hours at 130 000 x g and 4°C. On the next day an orange outer membrane pellet was collected from the bottom of the gradient and washed one to two times in a buffer containing 20 mM HEPES/NaOH pH 8.0 and 1 mM PMSF (130 000 x g, 1 hour, 4°C). The outer membrane pellet was resuspended in a small volume of the same buffer, frozen in liquid nitrogen and stored at -20°C.

5.4.10 Thermoluminescence measurements

Thermoluminescence measurements were performed in the temperature range of 40°C to 100°C and wave length range of 350 nm to750 nm on a Luminescence Spectrometer LS55 (Perkin Elmer, Germany). WT, NMΔ-*all4026*, NMΔ-*alr0397*, NMOX-*all4026*-GFP, NMOX-*alr0397*-GFP cultures were washed three times in $BG11_{-Fe-Cu}$ medium prior to reinoculation to $BG11_{-Fe-Cu}$ or $BG11_{-Fe}$ medium (supplied with antibiotics in the case of mutants). Measurements with wild type *Anabaena* sp. and all mutants were performed also in the standard BG11 medium for control. Measurements started 48 hours after the reinoculation to iron limited medium. Samples were taken every hour in a period of 12 hours and thermoluminescence was monitored every 5°C in the range of 40°C to 100°C. All glassware used in experiments was carefully washed with 6 M HCl and miliQ water to diminish the traces of metals as much as possible.

5.4.11 Determination of metal uptake

Metal uptake of copper, iron and as control of magnesium was measured for wild type and NMΔ-*all4026*, NMΔ-*alr0397*, NMOX-*all4026*-GFP and NMOX-*alr0397*-GFP mutants. *Anabaena* sp. filaments were grown for two weeks in BG11 cultures (supplied with adequate antibiotics in the case of mutants), washed three times in $BG11_{-Fe-Cu}$ and reinoculated to grow for the next three days in $BG11_{-Fe-Cu}$ or $BG11_{-Fe}$ with an addition of antibiotics where necessary. BG11 grown cultures were used as control. Filaments were collected by centrifugation, 3 000 x g, 5 min, washed in fresh medium and lyophilized. Filament metal content for iron, copper and magnesium was quantified in g/kg or mg/kg of the dry cell weight by atom absorption spectroscopy performed by Dr. Bernhard Mischalke on inductively coupled plasma atomic emission spectrometer (ICP-AES) „Spectro Ciros Vision“ system (SPECTRO Analytical Instruments GmbH & Co. KG, Kleve, Germany).

5.4.12 Amino acid transport assay

Transport of the radio-labelled L-[U-^{14}C] amino acids: L-arginine, L-aspartic acid, L-glutamic acid, L-glutamine, L-phenylalanine was performed as described in Montesinos *et al.* (1995) in co-operation with laboratory of Dr. Enrique Flores. Wild type and NMΔ-*alr2887* mutants were grown in BG11 medium for one week. Chlorophyll a concentration

of the previously carefully homogenized cultures was determined. Cells were collected by centrifuging at 3 000 x g, 5 min, washed with tricine buffer (25 mM N-tris(hydroxymethyl)-methylglycine (Tricine)-NaOH, pH 8.1) and resuspended in the same buffer. Transport assays were performed by mixing 1 ml of the culture with 0.1 ml of the tricine buffer solution of the amino acid to be tested (1 ml of cold amino acid plus 40 µl of radio-labelled L-[U-^{14}C] amino acid). 1 ml of boiled cells was used as control. Final concentration of the measured amino acid in the assay was 10 µM. The mixture of cells and amino acid was incubated for 10 min at 30°C under the white light of incandescent lamp (100 Wm^{-2}). 1 ml of the assayed cell solution was filtrated over Milipore HA filters (0.45 µm pore size) and washed with 10 ml of tricine buffer. Filters together with the cells on them were immersed in scintillation solution and radioactivity (β-emission) was measured. Results were recalculated according to the chlorophyll a concentration used in each assay (Montesinos *et al*., 1995).

5.4.13 Spectrometric GFP fluorescence measurement

Anabaena sp. wild type and the GFP-promoter strains, NME-*alr2887*, NME-*all4026*, NME-*alr0397*, were grown for a week in a standard BG11 medium. After a week all strains were washed three times with an induction medium (nitrogen depleted or iron depleted medium) and GFP fluorescence was measured in periods of two hours. GFP fluorescence from GFP-promoter fusion strains was measured in comparison to wild type *Anabaena* sp. by excitation at 480 nm and recording the emission in a window of 400-570 nm (Luminescence Spectrometer LS55, Perkin Elmer, Germany). An integral of each spectrum was determined and corrected for background fluorescence obtained by the wild type strain and adjusted according to the chlorophyll a concentrations for each sample taken.

5.4.14 Measurements of the chlorophyll fluorescence by PAM

Measurements of the chlorophyll fluorescence utilizing pulse amplitude technique (PAM) were performed with Maxi-Imaging-PAM chlorophyll fluorimeter (Heinz Walz GmbH, Effeltrich, Germany) according to Ivanov *et al*., 2006. Intensity of actinic (photosynthetically active) light used for saturation pulses was 185 µmol/m^2s. Pulses were 2 sec long in intervals of 20 sec. The result was express as a ration between maximum PSII

fluorescence in the light adapted state and maximum PSII fluorescence in the dark adapted state.

5.4.15 Measurements of nitrogenase activity

Nitrogenase activity of wild typa and the mutant strain NMΔ-*alr2887* was measured in co-operation with the laboratory of Prof. Dr. Enrique Flores (Rafael Pernil) according to established method described in Valladares *et al*. (2003).

5.4.16 Analysis of in the medium secreted *Anabaena* sp. proteins

Anabaena sp. wild type and NMΔ-*alr2887* filaments were grown in 1 l of BG11 medium up to the late logarithmic phase, washed three times in $BG11_0$ medium and reinoculated into 0.5 l of $BG11_0$ medium. Every three hours during the period of 12 hours cells were collected by centrifugation at 4 000 x g, 5 min, room temperature and reinoculated into fresh $BG11_0$ medium. Collected supernatant was kept on ice and immediately following its collection one protease inhibitor cocktail tablet and 1 mM PMSF were added. The supernatant was additionally centrifuged at 9 000 x g, 10 min, 4°C two times to clean it from remaining cells. $(NH_4)_2SO_4$ was added into the cleaned supernatant to the concentration of 60 % in a cold room at 4°C and the solution was stirred until the salt dissolved completely. Precipitated proteins were collected by centrifugation at 20 000 rpm, 10 min, 4°C in the volume of around 1-2 ml and subsequently dialysed overnight against the solution containing 3 M urea and 20 mM Tris/HCl pH 7.5. Maximal possible amount of the samples was subjected to SDS-PAGE and stained in parallel with Coomassie and with silver staining. On the basis of comparison between Coomassie and Silver stained gel, protein bands of difference were cut out of the Coomassie stained gel and subjected to protein sequencing.

5.5. Microscopy

5.5.1 Light microscopy

Anabaena sp. filaments were visualized with a use of the standard reverse light microscope (DM1000, Leica, Germany). Heterocyst containing cultures were stained with 0.5% Alcian Blue dye in 50% ethanol solution for 2 min prior to microscopy.

Fluorescence imaging of the strains expressing protein-GFP and promoter-GFP fusions was performed on TCS SP2 or TCS SP5 Leica confocal microscope (Wetzlar, Germany; HCX PLAN-APO 63x 1.4 NA oil immersion objective). All images of wild type and mutants were taken using the same microscope settings in order to compare intensities. GFP was excited at 488 nm line supplied by an argon ion laser and GFP fluorescence was analyzed by collection through the window of 500-570 nm while *Anabaena* sp. autofluorescence was monitored by collection through the window of 630-700 nm (Muro-Pastor *et al.*, 2006).

5.5.2 Electron microscopy

Preparation of the samples for the transmission electron microscopy was performed as described in Fiedler *et al.* (1998a). Small amount of collected filaments was fixed immediately in 2.5% glutaraldehyde in a fixing buffer (2% paraformaldehyde, 50 mM sodium cacodylate, 3 mM $CaCl_2$, pH 7.4) and post-fixated overnight in $KMnO_4$ at 4°C. The filaments were washed thoroughly in water and pre-embedded in 1% SeaKem agarose blocks. The agarose blocks were cut to small cubes (1-2 mm^3) and dehydrated with increasing concentrations of ethanol (2 x 10 min in 70%, 80%, 90%, 95% and 3 x 20 min in 100%). Prior to embedding cells were incubated 2 x 30 min in 1 ml of propylene oxide and then overnight in 1:1 (v/v) mixture of EPON and propylene oxide. The embedding in EPON resin was performed according to description provided by supplier (Epoxy Embedding Medium, Sigma-Aldrich, München, Germany). The post-staining was performed with uranyl acetate and lead citrate. The samples were examined with Zeiss EM10C microscope at 80 kV.

5.6. Protein modelling and bioinformatic analyses

The TolC protein modeling (Figure 34A) and β-barrel score calculations (Table 5-10) was performed in cooperation with Oliver Mirus and phylogenetic analysis (Figures 20, 34B) was performed in cooperation with Thomas Schlegel and Oliver Mirus. The signal peptides were analysed by SignalP 3.0 (http://www.cbs.dtu.dk/services/SignalP) and LipoP 1.0 program (http://www.cbs.dtu.dk/services/LipoP), helical transmembrane regions were predicted by TMHMM (http://www.cbs.dtu.dk/services/TMHMM). The transmembrane β-barrel regions were analysed by calculating β-barrel score (BBS) and MCMBB score (Schleiff *et al*., 2003; Mirus and Schleiff, 2005; http://athina.biol.uoa.gr/bioinformatics/mcmbb). Subcellular localisations were predicted with a help of PSORTb tool (http://www.psort.org/psortb) and putative domain prediction was performed by Pfam tool (http://www.sanger.ac.uk/Software/Pfam/search.shtml). Protein sequences were analysed by BLAST search at the NCBI website. Predictions of the three-dimensional protein structure on the basis of their amino acid sequence were performed with a help of PHYRE server (http://www.sbg.bio.ic.ac.uk/~phyre). The source of the gene sequences and information on cyanobacterial genes was CyanoBase – The Genome Database for Cyanobacterai of Kazusa DNA Research Institute (http://bacteria.kazusa.or.jp/cyanobase).

6. Results

6.1. Proteomic analysis of the outer membrane of *Anabaena* sp. PCC 7120

The outer membrane is a border of a Gram-negative cell, such as *Anabaena* sp., toward the surrounding medium. For this reason the structure and the function of the outer membrane are essential for establishing the contact and compound exchange with the surroundings, sensing the outside conditions and reacting to them. Since the outer membrane proteins are crucial in all these processes, revealing the protein composition of the *Anabaena* sp. outer membrane supports successfull utilisation of this cyanobacterium as a model system in cell differentiation, nitrogen fixation and plastid evolution studies. It is also the first step toward elucidating how the multicellularity and differentiation in *Anabaena* sp. reflect on the proteome composition and functions of the outer membrane.

6.1.1 New method for the membrane fractionation of vegetative cells of *Anabaena* sp. PCC 7120

An application of the previously developed method for membrane fractionation of *Synechocystis* sp. PCC 6803 (Murata & Omata, 1988; Bölter *et al.* 1998) did not achieve satisfying results in *Anabaena* sp. PCC 7120. Repeated unsuccessful trials led to conclusion that filamentous *Anabaena* sp. cannot be fractionated as unicellular *Synechocystis* sp. Therefore, a new method for *Anabaena* sp. fractionation had to be established to enable the proteome analysis.

Similar to *Synechocystis* sp., *Anabaena* sp. membrane fractions can be separated by centrifugation on a sucrose density gradient (see "Methods", section 5.4.8.). The fractionation was performed in the absence (Figure 6, lanes 1, 3, 5) or in the presence of digitionin (Figure 6, lanes 2, 4, 6). The purity of the fractions was determined by immunodecoration with antibodies against proteins specific for each of the membrane fractions. Generally, better results were achieved when digitonin was applied in the course of isolation procedure.

In the absence of digitonin, blotting with anti-Oxa antibody, a protein involved in protein translocation into the thylakoids (Luirink *et al*., 2001; Robinson *et al.*, 2001), revealed only minor contamination of the outer membrane fraction with the thylakoid

membranes (Figure 6, lane 5). This contamination was further reduced in the presence of digitonin (Figure 6, lane 6). The same was found for contaminations with the inner membrane proteins, detected on the basis of presence of NrtA (Omata, 1995), the inner membrane nitrate/nitrite binding lipoprotein (Figure 6, lanes 5, 6). Furthermore, the Omp85 homologue of *Anabaena* sp. Alr2269 (Ertel *et al*., 2005), expected in the outer membrane, was only weakly detected in the thylakoid and the inner membrane fractions (Figure 6, lanes 1-4). The purity of the thylakoid fraction again improved when the membranes when digitonin was present (Figure 6, lane 2). Effect of digitonin on the isolation procedure and fraction purity can be explained either by disruption of the membrane aggregations or by partial solubilisation of the membrane sheets. The volume-normalised amounts of all membrane fractions visualized by Coomassie stained SDS-PAGE reveal that this procedure allowed efficient production of the thylakoid and the outer membrane fractions. The inner membrane fraction was obtained, although with a lower yield.

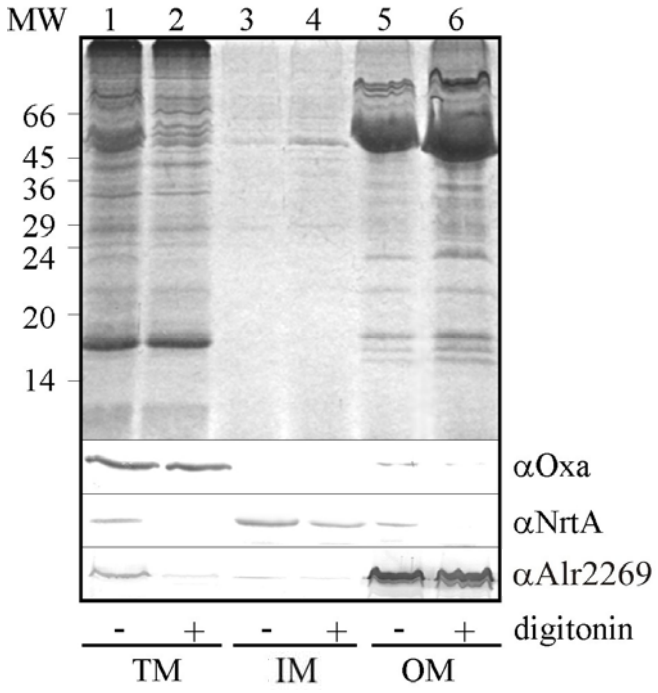

Figure 6. Membrane fractionation of *Anabaena* sp. PCC 7120. Wild type filaments grown in BG11 medium were fractionated into the thylakoid membranes (TM; lane 1, 2), the inner membrane (IM; lane 3, 4) and the outer membrane (OM; lane 5, 6) in the absence (lane 1, 3, 5) or in the presence of digitonin (lane 2, 4, 6). Equal volumes of fractions were visualized on Coomassie Blue stained SDS-PAGE (upper part). The purity of the fractions was determined by immunodecoration with antibodies against IM (NrtA), TM (Oxa) or OM (Alr2269) specific proteins, as indicated (lower part).

6.1.2 General characterisation of identified proteins

After the method for membrane fractionation had been established, the protein composition of the outer membrane was investigated. The outer membrane fractions obtained in the absence or presence of digitonin were digested with trypsin and the proteome was analysed by two different mass spectrometry approaches (see "Methods, section 5.2.5.). Altogether 55 proteins were identified by MS analysis (Table 5). About 52% of these proteins had known or proposed functions. To further 37% of the detected proteins, termed as "unknown" or "hypothetical", putative function was ascribed on the basis of their high sequence similarity to the proteins with known functions from other cyanobacteria (Table 6). To 11% of identified proteins no putative or known function could be ascribed.

In order to localize the proteins inside of the cell, the presence of a signal peptide was analysed in each detected protein with a help of Internet available tools SignalP 3.0 (Bendtsen *et al.*, 2004) and LipoP 1.0. (Juncker *et al*., 2003). 73 % or 40 proteins among all identified proteins contained a putative signal peptide (Table 5, column 5). Some of the proteins without a predictable secretion signal were typical outer membrane proteins such as porin (protein 41) or probable N-acetylmuramoyl-L-alanine amidase (protein 14). The protein sequences were further analysed with a usage of bacterial subcellular localisation prediction tool PSORTb (Gardy *et al*., 2003, 2005). In this way the cellular localisation was assigned to 22 among 55 proteins and for 11 of them PSORTb predicted an outer membrane localization (Table 5, column 7).

To find contaminations of the outer membrane fraction with the inner membrane proteins, the presence of the putative helical transmembrane regions in identified proteins was analysed with a help of Internet available TMHMM 2.0 server (Krogh *et al*., 2001). In some of the proteins helical transmembrane regions were identified. However, all predicted transmembrane regions overlapped with identified secretion signals (not shown). Based on this, it can be concluded that contaminations with the inner membrane proteins are very low.

To finalise the protein localisation prediction, the presence of β-barrel structures characteristic for the bacterial outer membrane proteins was investigated in identified proteins (Koebnik *et al*., 2000). β-barrel proteins were identified by calculating the β-barrel score (BBS; Schleiff *et al*., 2003b; Wimley 2002) with a cut off value 0.7 (Oliver Mirus-personal communication; Mirus and Schleiff, 2005).

Table 5. Proteins identified in the outer membrane fraction of *Anabaena* sp. PCC 7120. Sequences are sorted according to the total number of peptides identified by MS. Given are: an accession number of the corresponding gene (column 2), functional name of the protein (column 3), numbers of identified peptides (non-redundant peptides in – digitonin approach / non-redundant peptides in + digitonin approach / total number of peptides; column 4), predicted cleavage site (column 5), Mr of the preprotein and mature protein (column 6), localisation according to PSORTb, β-barrel score (cut of value 0.7; column 8) and MCMBB score (cut off value 0; column 9). Printed in bold are predicted β-barrel proteins.

No.	Acc.	Name	Peptides	Signal P 3.0/ LipoP 1.0	MW (kDa) pre/mat [b]	PSORTb	BBS	MCMBB
1	alr4550	hypothetical protein	15/9/57	AIA-AT(28)	60.5 / 57.8	-	**1.74**	**0.051**
2	alr2269	chloroplastic outer envelope homologue	31/4/56	ANA-QT (18)	89.5 / 87.8	**OM**	**1.21**	**0.033**
3	all4499	hypothetical protein	15/2/44	ALA-VE (28)	58.5 / 55.4	**OM**	**1.94**	**0.054**
4	all1861	hypothetical protein	9/11/26	VIA-NQ (12)	28.4 / 27.1	-	**1.26**	**0.033**
5	alr3608	similar to endoglucanase	10/4/19	VNA-SA (43)	58.2 / 53.7	-	0.10	0.021
6	alr0092	N-acetylmuramoyl-L-alanine amidase	15/1/18	ALA-TR (23)	68.0 / 65.6	**OM**	**0.06**	**0.024**
7	alr1819	hypothetical protein	8/3/17	ITA-NP (24)	58.0 / 54.4	**OM**	**0.63**	**0.040**
8	all4999	N-acetylmuramoyl-L-alanine amidase	9/1/12	ALA-SS (34)	65.2 / 61.6	-	0.33	-0.01
9	all4388	hypothetical protein	8/1/11	AQG-QQ (35)	51.5 / 48.0	-	0.47	0.034
10	alr2887	hypothetical protein	5/2/10	AVA-EA (26)	80.7 / 78.0	**OM**	**0.65**	**0.047**
11	all7598	unknown protein	4/2/9	ASA-NE (35)	18.7 / 15.0	-	0.00	0.00
12	all1455	nitrogenase subunit NifH	3/1/8	-	32.2	Cyt	0.00	-0.07
13	alr0702	serine proteinase	3/2/6	VHD-ES (22)	45.4 / 42.9	PP	0.00	0.032
14	all4294	probable N-acetylmuramoyl-L-alanine amidase	2/2/6	-	55.5	-	0.29	0.052
15	all5036	unknown protein	1/1/6	LLA-SG (38)	51.1 / 46.9	IM	0.00	0.00
16	all3585	hypothetical protein	4/2/5	VLA-QQ (35)	29.4 / 25.7	-	0.56	0.026
17	alr0663	alpha amylase like protein	13/0/20	-	72.4	Cyt	0.19	-0.04
18	alr1666	probable D-alanyl-D-alanine carboxypeptidase	9/0/9	VKA-QT (27)	52.8 / 49.9	-	0.03	0.031
19	all1140	hypothetical protein	5/0/9	-	34.4	-	0.30	0.000
20	all2430	hypothetical protein	5/0/9	GMA-VG (29)	21.6 / 21.3	-	**1.11**	**0.056**
21	all8079	unknown protein	6/0/8	VGA-AV (19)	83.5 / 81.5	-	0.47	0.013
22	all3984	hypothetical protein	4/0/8	ANA-QF (36)	24.7 / 21.0	-	0.28	0.028
23	all0405	hypothetical protein	2/0/8	LIS-GY (37)	77.2 / 73.1	-	0.77	-0.02
24	all3826	unknown protein	2/0/7	TFA-DR (30)	25.4 / 22.3	-	0.17	-0.02
25	alr2588	ferrichrome-iron receptor	1/0/7	VWA-EV (32)	93.8 / 90.2	**OM**	**0.71**	**0.032**
26	all7606	two-component response regulator	5/0/6	-	27.4	-	0.00	-0.04
27	all4575	phosphate ABC transporter	4/0/6	LAA-CG (28)	41.3 / 38.1	PP	0.31	0.023
28	alr0397	similar to ferric aerobactin receptor	2/0/6	VWS-LI (36)	94.2 / 90.2	**OM**	**1.58**	**0.055**
29	alr4740	unknown protein	2/0/6	-	20.8	-	**0.88**	**0.055**
30	all1776	hypothetical protein	4/0/5	-	74.9	-	0.08	0.000
31	all0089	hypothetical protein	3/0/5	-	23.4	PP	0.00	0.049
32	alr1890	phosphoglycerate dehydrogenase	2/0/5	-	55.8	Cyt	0.00	-0.01
33	all2500	carboxyl-terminal protease	1/0/5	GQA-LF (33)	47.3 / 44.0	-	0.00	0.000
34	all1951	ABC transporter	1/0/5	LKA-CA (26)	47.6 / 44.5	PP	0.00	-0.02
35	all0268	hypothetical protein	1/0/5	ADA-QS (30)	27.3 / 24.2	-	0.06	-0.01
36	alr7326	hypothetical protein	2/0/4	ASA-KG (23)	19.6 / 17.2	-	0.79	-0.02
37	all3983	similar to surface layer protein	2/0/4	SFA-QT (21)	42.3 / 40.2	-	0.24	0.020
38	all3310	hypothetical ferrietin outer membrane receptor	2/0/4	ALG-SD (23)	76.8 / 74.1	**OM**	**3.02**	**0.051**
39	alr1834	probable periplasmic branched-chain amino acid binding protein	1/0/4	LLA-AC (22)	44.7 / 42.5	PP	0.19	0.011
40	all7597	hypothetical protein	1/0/4	AWA-KN (23)	16.9 / 14.4	-	0.57	-0.01
41	alr0834	porin	3/0/3	-	54.3	-	**1.84**	**0.048**
42	alr4067	hypothetical protein	3/0/3	LFG-TV (27)	18.3 / 15.2	-	0.00	0.041
43	all5347	membrane fusion protein DevB homolog	3/0/3	TLA-AG (28)	43.2 / 40.0	-	0.13	0.042
44	alr1278	hypothetical protein	2/0/3	-	94.2	**OM**	**1.02**	**0.041**
45	all1101	ferrichrome iron receptor	1/0/3	LIA-PT (31)	98.0 / 94.5	**OM**	**1.09**	**0.034**
46	all2352	WD-repeat containing protein	1/0/3	VSA-AD (40)	38.4 / 34.0	-	0.00	0.000
47	alr1690	cell wall-binding protein	2/0/2	-	46.2	-	0.16	0.041
48	all0868	carbon dioxide concentrating mechanism protein CcmK	2/0/2	-	10.9	-	0.00	-0.01
49	all3144	hypothetical protein	1/0/2	GTA-IV (44)	47.9 / 43.0	IM	0.00	0.029
50	alr3411	hypothetical protein	1/0/2	VIA-GL (36)	21.4 / 17.2	-	0.00	-0.01
51	all2571	hypothetical protein	1/0/2	QEA-PT (23)	15.8 / 13.3	-	0.00	0.026
52	all0865	carbon dioxide concentrating mechanism protein CcmM	1/0/2	-	59.4	-	0.20	-0.02
53	all4026	similar to TonB-dependent receptor	1/0/2	ANA-QE (34)	94.9 / 91.4	**OM**	**1.59**	**0.035**
54	all7611	hypothetical protein	1/0/1	ACS-GG (23)	19.1 / 16.7	-	**0.72**	**0.002**
55	alr0946	hypothetical protein	0/1/1	-	16.0	Cyt	0.55	-0.02

In this way 17 sequences were selected as putative β-barrel proteins (Table 5, column 8). The BBS prediction was further confirmed by the second program searching for the transmembrane β-barrels, Markov Chain Model BB with the cut off value 0 (MCMBB; Bagos *et al*., 2004). With this progam 15 proteins were selected (Table 5, column 9). 13 experimentally identified sequences were selected by both MCMBB and BBS programs and are outer membrane localized, as predicted with PSORTb, suggesting that these proteins are indeed β-barrel proteins.

6.1.3 Classification of identified proteins

With intention to identify the homologues of proteins from the outer membrane fraction, BLAST analysis was performed. That has enabled to ascribe the possible function to 89% of identified proteins. 80% of the sequences were found to have their homologues in *Synechocystis* and 31% in *A. thaliana* (Table 6). Comparing the results to the proteomic data for *Synechocystis* sp. PCC 6803, available for the inner membrane (Huang *et al.*, 2002), the periplasm (Fulda *et al.*, 2000) and the outer membrane (Huang *et al*., 2004), reveales that 35% of identified proteins are close homologues to the proteins previously identified in the proteome of the *Synechocystis* membrane systems.

To finalise the analysis, existence of the conserved domains in identified proteins was investigated with the use of the Pfam database (Bateman *et al*., 2004). In 45 proteins different protein domains were found (Table 7). The comparison of the topology predictions with the protein homology search defined 20 proteins as the outer membrane proteins (Table 6, printed in bold in columns 1 and 4).

In conclusion, according to the β-barrel structure predictions and a homology to the proteins with a known function, 22 proteins altogether can be assigned to the *Anabaena* sp. outer membrane (Table 7, column 3), five to the outer membrane or periplasm fraction, eight to the periplasm fraction, eight to the cytosolic fraction, four to outer membrane or extra-cellular fraction, and only one protein to the inner membrane (Table 7, column 3). Therefore, 46% of all identified proteins are the outer membrane proteins, while in the case of additional 19% an outer membrane localisation is possible. That presents 65% of the detected proteins as either outer membrane inserted or outer membrane associated. For seven sequences localisation to the certain membrane system was not possible (proteins 11, 21, 22, 35, 50, 51, 40, Tables 5-7).

Table 6. List of homologues of identified proteins. Given are: an accession number of the protein (column 2), an accession number and description of the closest homologue with function (columns 3,4, see Abreviations), accession number of the closest homologue in *Synechocystis* sp. and *A. thaliana* (columns 5,7). The numbers of the predicted OM proteins (Table 5) and the functions of three additional putative OM proteins identified on the basis of the closest homologue's function are given in bold. The overlap with the previous analysis of the *Synechocystis* sp. proteome is given; found in: a-periplasm , b-IM, c-OM fraction (column 6).

Identified		The closest homologue with a function		*Synechocystis*		*A.thaliana*
No.	Acc.	Acc.	Function	Acc.	Ident.	Acc.
1	alr4550	slr1841	probable porin	slr1841	b,c	At1g59660
2	alr2269	slr1227	synToc75	slr1227	c	At5g19620
3	all4499	slr1908	probable porin	slr1908	b,c	-
4	all1861	Avar03005977	peptidoglycan-binding protein	-	-	-
5	alr3608	Avar03002018	Nitrous oxidase accessory protein	-	-	-
6	alr0092	slr1744	N-acetylmuramoyl-L-alanine amidase	slr1744	a	-
7	alr1819	Avar03004798	cell surface protein	sll1483	a	At5g03170
8	all4999	slr0891	N-acetylmuramoyl-L-alanine amidase	slr0891	-	-
9	all4388	Avar03001310	involved in polysaccharide export	sll1581	c	-
10	alr2887	Avar03005548	outer membrane protein	slr1270	a, b, c	At5g65390
11	all7598	-	-	-	-	-
12	all1455	slr0749	iron protein subunit ChlL	slr0749	-	At5g24020
13	alr0702	slr1204	protease	slr1204	c	At5g27660
14	all4294	Avar03005813	**peptidoglycan-binding protein**	-	-	-
15	all5036	Avar03004484	TonB	slr1484	-	At5g38560
16	all3585	Npun02000298	DNA segregation ATPase	-	-	-
17	alr0663	-	-	sll0842	-	At4g25000
18	alr1666	Avar03003767	D-alanyl-D-alanine carboxypeptidase	slr0646	-	-
19	all1140	Avar03000254	**N-acetylmuramoyl-L-alanine amidase**	slr1910	-	-
20	all2430	Npun02002132	exoprotein involved in heme utilization or adhesion	sll1586	-	At2g25660
21	all8079	Npun02002027	predicted phosphatase	slr8030	-	-
22	all3984	Npun02001119	predicted ATP-dependent protease	slr1704	-	-
23	all0405	Avar03000695	glycine/D-amino acid oxidases	sll0471	-	-
24	all3826	Avar03003927	peptidoglycan-binding protein	-	-	At5g10430
25	alr2588	slr1490	ferrichrome-iron receptor	slr1490 sll1406	 c	-
26	all7606	sll0789	OmpR homologue	sll0789	-	At5g02810
27	all4575	sll0680	phosphate-binding periplasmic protein	sll0680	-	-
28	alr0397	sll1206	ferric aerobactin receptor FhuA	sll1206	-	-
29	alr4740	-	-	-	-	-
30	all1776	fenI	S-layer protein	sll0736	-	-
31	all0089	Avar03006504	uncharacterized conserved protein	slr0431	b,c	-
32	alr1890	sll1908	D-3-phosphoglycerate dehydrogenase SerA	sll1908	-	At1g17740 At4g34200
33	all2500	slr1751	periplasmic carboxyl-terminal protease	slr1751	a, b, c	At4g17740
34	all1951	slr0447	periplasmic protein, ABC-type urea transport system subunit	slr0447	a, b	-
35	all0268	Avar03000616	predicted Zn-dependent hydrolases	slr2005	a	-
36	alr7326	-	-	-	-	-
37	all3983	Avar03004798	secreted and surface protein	slr1704	-	-
38	all3310	Npun02003515	outer membrane receptor proteins, mostly Fe transport	sll1206	-	-
39	alr1834	Avar03006239	periplasmic ABC-type branched-chain amino acid transport component	slr0559	-	At5g27100
40	all7597	-	-	-	-	-
41	alr0834	sll1550	porin	sll1550 slr1841	b,c	-
42	alr4067	Selo03002066	**organic solvent tolerance protein OstA**	slr4067	-	-
43	all5347	sll1481	ABC transporter membrane fusion protein	sll1481	-	-
44	alr1278	Avar03005080	organic solvent tolerance protein OstA	sll0350	-	At5g53870
45	all1101	slr1490	ferrichrome-iron receptor	slr1490 sll1406	- c	-
46	all2352	sll1491	periplasmic WD-repeat protein	sll1491	a	At3g49660 At5g50230
47	alr1690	-	-	-	-	-
48	all0868	sll1028	CcmK2	sll1028	b	-
49	all3144	sll1053	multidrug efflux transporter	sll1053 sll0180	b c	-
50	alr3411	Tery02001943	chorismate synthase	sll0470	-	-
51	all2571	-	-	-	-	-
52	all0865	sll1031	CcmM	sll1031	c	At1g19580
53	all4026	sll1409	ferrichrome-iron receptor	sll1409	-	-
54	all7611	slr6044	hypothetical protein	slr6044	-	-
55	alr0946	Tery02000700	regulators of stationary/sporulation gene expression	sll0359	-	-

Table 7. List of domains classified by Pfam. Given are: an accession number of the identified sequence (column 2) and the putative localisation (column 3; Ext-extracellular, OM - outer membrane, PP - periplasmic space, IM - inner membrane, Cyt - cytosol, ? - no assignment possible). The description of the closest homologue (column 4, as in Table 6) and the name of the identified Pfam domain (column 5) are also listed. The number or the function of the predicted OM proteins (Table 5, 6) are given in bold (columns 1, 4).

Identified		Loc.	The closest homologue with a function	Pfam domain
No.	Acc.			
1	alr4550	OM	probable porin	S-layer homology domain & OprB family
2	alr2269	OM	synToc75	surface antigen variable number repeat & surface antigen
3	all4499	OM	probable porin	S-layer homology domain
4	all1861	OM	peptidoglycan-binding protein	putative peptidoglycan binding domain
5	alr3608	OM	nitrous oxidase accessory protein	DUF1565 & S-layer homology domain
6	alr0092	OM	N-acetylmuramoyl-L-alanine amidase	N-acetylmuramoyl-L-alanine amidase
7	alr1819	OM	cell surface protein	S-layer homology domain & fasciclin domain
8	all4999	OM/Ext	N-acetylmuramoyl-L-alanine amidase	N-acetylmuramoyl-L-alanine amidase
9	all4388	OM	involved in polysaccharide export	polysaccharide biosynthesis/export protein
10	alr2887	OM	outer membrane protein	outer membrane efflux protein
11	all7598	?	-	-
12	all1455	Cyt	iron protein subunit ChlL	NifH/FrxC family
13	alr0702	OM/PP	protease	Trypsin & PDZ domain
14	all4294	OM	**peptidoglycan-binding protein**	putative peptidoglycan binding domain
15	all5036	PP	TonB	TonB protein of Gram-negative bacteria
16	all3585	Cyt	DNA segregation ATPase	-
17	alr0663	Cyt	-	alpha amylase
18	alr1666	OM/PP	D-alanyl-D-alanine carboxypeptidase	D-Ala-D-Ala carboxypeptidase 3 (S13) family
19	all1140	OM	**N-acetylmuramoyl-L-alanine amidase**	N-acetylmuramoyl-L-alanine amidase & putative peptidoglycan binding domain
20	all2430	OM	exoprotein	DUF490
21	all8079	?	predicted phosphatase	DUF839
22	all3984	?	predicted ATP-dependent protease	-
23	all0405	OM/PP	glycine/D-amino acid oxidases	FAD dependent oxidoreductase & FAD binding domain
24	all3826	PP	peptidoglycan-binding protein	-
25	alr2588	OM	ferrichrome-iron receptor	plug domain & TonB dep. receptor
26	all7606	Cyt	OmpR homologue	response regulator receiver domain & transcriptional regulatory protein, C terminal
27	all4575	PP	phosphate-binding periplasmic protein	bacterial extracellular solute-binding protein
28	alr0397	OM	ferric aerobactin receptor FhuA	plug domain & TonB dep. receptor
29	alr4740	OM	-	-
30	all1776	OM/Ext	S-layer protein	S-layer homology domain
31	all0089	OM/PP	uncharacterized conserved protein	DUF541
32	alr1890	Cyt	D-3-phosphoglycerate dehydrogenase SerA	D-isomer specific 2-hydroxyacid dehydrogenase, catalytic domain & D-isomer specific 2-hydroxyacid dehydrogenase, NAD binding domain & ACT domain
33	all2500	PP	periplasmic carboxyl-terminal protease	PDZ domain & Peptidase family S41
34	all1951	PP	ABC-type urea transport system subunit	receptor family ligand binding region
35	all0268	?	predicted Zn-dependent hydrolases	-
36	alr7326	OM/Ext	-	N-acetylmuramoyl-L-alanine amidase
37	all3983	OM/Ext	secreted and surface protein	S-layer homology domain
38	all3310	OM	outer membrane receptor proteins, mostly Fe transport	plug domain & TonB dep. receptor
39	alr1834	PP	periplasmic ABC-type branched-chain amino acid transport component	receptor family ligand binding region
40	all7597	?	-	-
41	alr0834	OM	porin	S-layer homology domain & OprB family
42	alr4067	OM	**organic solvent tolerance protein OstA**	OstA-like protein
43	all5347	PP	ABC transporter membrane fusion protein	HlyD family secretion protein
44	alr1278	OM	organic solvent tolerance protein OstA	-
45	all1101	OM	ferrichrome-iron receptor	plug domain & TonB dep. receptor
46	all2352	PP	periplasmic WD-repeat protein	WD domain, G-beta repeat
47	alr1690	OM/PP	-	putative peptidoglycan binding domain
48	all0868	Cyt	CcmK2	bacterial microcompartments protein family
49	all3144	IM	multidrug efflux transporter	secretion protein of HlyD family
50	alr3411	?	chorismate synthase	-
51	all2571	?	-	putative phospholipid-binding domain
52	all0865	Cyt	CcmM	small chain, Rubisco
53	all4026	OM	ferrichrome-iron receptor	plug domain & TonB dep. receptor
54	all7611	OM	hypothetical protein	-
55	alr0946	Cyt	regulators of stationary/sporulation gene expression	-

However, the sequences of unknown localisation are all classified as hypothetical or unknown proteins (Table 5). For this reason they cannot be excluded as the possible outer membrane inserted or outer membrane associated proteins.

6.1.4 Cytoplasmic proteins

After completing the analyses presented in Tables 5-7, among all identified proteins eight were assigned to the cytosol (proteins 12, 16, 17, 26, 32, 48, 52, 55; Tables 5-7). These contaminations originate from a soluble cell fraction. For this reason they are hard to avoid in a harsh treatment during membrane fractionation procedure where the cells must be disrupted. Two proteins, CcmK (protein 48) and CcmM (protein 52), involved in the formation of carboxysomes, a proteinaceous micro-compartment of cyanobacteria containing large amounts of RuBisCO (So *et al*., 2004), were identified. CcmM (protein 52) was also found in the analysis of the outer membrane fraction of *Synechocystis* sp. (Huang *et al*., 2004). In addition, some classical cytoplasmic proteins were found as contamination in the outer membrane isolates, such as a nitrogenase subunit (protein 12), an alpha-amylase like protein, as assigned by the Pfam database (protein 17, Table 7) and a phosphoglycerate dehydrogenase (protein 32). The presence of a nitrogenase subunit (protein 14), which is a heterocysts specific protein, may indicate that under used growth conditions certain low level of heterocysts differentiation took place in the culture. That is possible when filaments are grown in dense cultures with nitrate as nitrogen source. Beside these proteins, two gene regulating enzymes were found: an OmpR homologue (protein 26; Jubelin *et al*., 2005) and the protein regulating the expression of the sporulation genes (protein 55). Protein 55 was identified only in the probe treated with digitonin and on the basis of a single matching peptide (Table 5, column 4), which implies that this protein is only a minor contamination of the outer membrane fraction.

6.1.5 Inner membrane and thylakoid membrane proteins

The isolated outer membrane fraction was contaminated with only one hypothetical inner membrane protein (protein 49, Tables 5-7). This protein is homologous to a multidrug efflux transporter (Table 5) and contains by Pfam predicted “HlyD family secretion protein” domain (Table 7). HlyD proteins are adaptor proteins of the TolC-HlyA

system (Figure 2) involved in the export of toxic substances or bacterial protein toxins out of the cell (see, "Introduction"; Levy, 1992; Koronakis *et al*., 2004). However, in addition to a shorter cytosolic domain and a single transmembrane helix, HlyD contains a very big periplasmic domain that interacts with the outer membrane TolC protein (see section 6.1.7)

PSORTb predicted also protein 15 as inner membrane localized. Similarity searches define this protein as TonB, a periplasmic protein with an inner membrane anchor. TonB couples chemiosmotic potential of the inner membrane with siderophore uptake through TBDT across the outer membrane (see "Introduction"; Ferguson *et al*., 2002a). TonB physically associates with iron transporters identified in the outer membrane fraction (Table 5, proteins 25, 28, 38, 45 and 53) in order to enable iron-siderophore transport (Figures 3 and 4).

Physical assiciation of HlyD and TonB proteins with their outer membrane components, TolC and TBDT respectively, as parts of the membrane transport pathways in Gram-negative cell may be an explanation for their presence in the outer membrane fraction. No further inner membrane contaminations could be identified.

No protein sequences originating from the thylakoid membrane fraction were discovered. Therefore, the obtained traces of Oxa detected by immunodecoration (Figure 6) in the outer membrane preparation reflect only a very minor contamination. Together with the data obtained for contaminations with the inner membrane proteins, this confirms the purity of the isolated outer membrane fraction in regard to other cellular membranes (Figure 6).

6.1.6 Periplasmic proteins and exoproteins

For altogether eight among 55 identified proteins the periplasmic localisation was predicted (proteins 15, 24, 27, 33, 34, 39, 43, 46, Tables 5-7). For further five proteins the periplasmic or the outer membrane localisation was possible (proteins 13, 18, 23, 31, 47, Tables 5-7). Only three among these proteins were previously identified in the periplasmic fraction of *Synechocystis* (proteins 33, 34, 46; Fulda *et al*., 2000) and two proteins (protein 13, 31) in the outer membrane fraction (Huang *et al*., 2004). It is interesting that for protein 13, assigned as cytosolic, a secretion signal is predicted (Table 5, column 5). Even more, for both proteins 13 and 31 a significant MCMBB score was obtained (Table 5). Apart from these two proteins and TonB (protein 15, previous section), the pool of proteins assigned to the periplasm contains peptidoglycan binding proteins (proteins 24, 47),

subunits of ABC transporters (proteins 27, 34, 39, 43), a WD-repeat containing protein (protein 46), a periplasmic protease (protein 33) and proteins involved in the peptidoglycan metabolism (proteins 18, 23). Similar to the cytosolic proteins, contamination with the periplasmic proteins is hard to avoid during cell disruption and membrane isolation procedure.

Beside periplasmic proteins, four proteins with a putative extracellular or outer membrane localisation were identified (proteins 8, 30, 36, 37; Tables 5-7). Proteins 8 and 36 were classified as amidases either with homology searches or with Pfam domain prediction. Interestingly, hypothetical protein 30 shares high homology with the S-layer protein FenI (Table 6), while protein 37 also contains a homology region to the S-layer domain (Table 7). This is exceptional since *Anabaena* sp. belongs to the cyanobacterial family *Nostocales* in which S-layer has not been detected and raises the question about the function of these proteins in this cyanobacterium.

6.1.7 Outer membrane proteins

Based on BBS, Pfam domain prediction and homology to the known proteins, most of the proteins, specifically 22 of them, can be assigned to the outer membrane (proteins 1, 2, 3, 4, 5, 6, 7, 9, 10, 14, 19, 20, 25, 28, 29, 38, 41, 42, 44, 45, 53, 54; Tables 5-7). Furthermore, nine additional proteins are probably associated with the outer membrane. Analysis of the proteins identified in both mass spectrometry approaches (proteins 1-16. Table 5) reveales that 12 out of 16 sequences are outer membrane proteins. In addition, two major protein bands obtained in the outer membrane fractions at 55 kDa and 80 kDa (Figure 6) represent three proteins covered by most of the peptides (proteins 1, 2, 3). These proteins were subsequently identified as porins (proteins 1, 3) and an Omp85 homologue (protein 2).

Beside these three proteins, one more porin (protein 41), one peptidoglycan-binding protein (protein 4), proteins involved in the peptidoglycan metabolism (proteins 5, 6, 14, 19), organic solvent tolerance proteins (proteins 42 and 44) and a protein involved in polysaccharide export (protein 9) were identified. What especially draws attention is that even five outer membrane TonB-dependent transporters (see “Introduction”) were identified under iron-replete growth conditions of the cultures used for membrane isolation (proteins 25, 28, 38, 45, 53). Also a protein with homology to the TolC channel-tunnels (protein 10) was identified. The TolC-like proteins form trimeric structures containing the

α-helical periplasmic tunnel domain and the β-barrel outer membrane channel (see "Introduction", Koronakis *et al*., 2000). Furthermore, protein 20 shows high sequence homology to an exoprotein involved in heme utilization or adhesion (Tables 6, 7). However, both the BBS and MCMBB score identify protein 20 as a β-barrel outer membrane protein (Table 5). The same is the case for protein 29, where no function could be assigned. One of most abundant proteins identified in the outer membrane was Alr2269, a member of the Omp85 family (protein 2). This protein contains an N-terminal recognition and complex assembly domain, while the C-terminal domain forms a β-barrel channel in the outer membrane (Ertel *et al*., 2005; Bredemeier *et al*., 2006), which is in line with proteomic results obtained for the outer membrane fraction of *Synechocystis* sp. (Huang *et al*., 2004).

6.1.8 Complex analysis

In plastids, whose closest known evolutionary relative is *Anabaena* sp. (Martin *et al*., 2002), so far only one protein complex of the outer membrane, the Toc complex, has been analysed in more detail (Soll and Schleiff, 2004). For this reason it was interesting to investigate existence of putative protein complexes in the outer membrane of *Anabaena* sp. After the isolated outer membranes had been solubilized by dodecylmaltoside, octylglucoside or FOS-choline (Figure 7), the outer membrane protein complexes were separated by BN-PAGE. The first dimension was transferred to SDS-PAGE and proteins were stained with Coomassie (Figure 7). Bands of interest were further analysed by mass spectrometry to identify the proteins (Table 8; in cooperation with laboratory of Dr. Lutz A. Eichacker).

In the range between 60 kDa and 450 kDa three complexes were identified when the outer membranes were solubilised with dodecylmaltoside (Figure 7, left). The first complex migrates with an approximate molecular weight of 370 kDa (Figure 7, arrows 1, 2, 3), the second complex migrates with 250 kDa (Figure 7, arrow 4) and the third complex has a size between 160 kDa and 200 kDa (Figure 7, arrow 5). In the first complex Alr2887, a protein with homology to the TolC channel-tunnels, was identified. The second identified protein is Alr2269, an Omp85 homologue (Table 8). The third protein could not be identified from this gel. The second complex seems to be a homooligomeric complex formation of Alr2887 and the third complex seems to be a homooligomeric formation of Alr2269. Since the estimated molecular weight of Alr2887 is 78 kDa after processing, a

trimeric formation would fit with the obtained 250 kDa. The third complex would suggest a dimeric assembly of Alr2269. The analysis of the first complex would suggest a hetero-oligomeric complex (Figure 7, Table 8). However, when the complexes were analysed after solubilisation with octylglucoside or FOS-Choline, Alr2269 was less abundant (Figure 7, middle) or not present in the complex of 370 kDa (Figure 7, right). It can be concluded that Alr2269 alone forms the 370 kDa complex, which is not stable when membranes are solubilised by octylglucoside or FOS-Choline. This further suggests a tetrameric conformation, which is in line with the obtained stoichiometry of Omp85 proteins (Schleiff *et al*., 2003a; Schleiff and Soll, 2005).

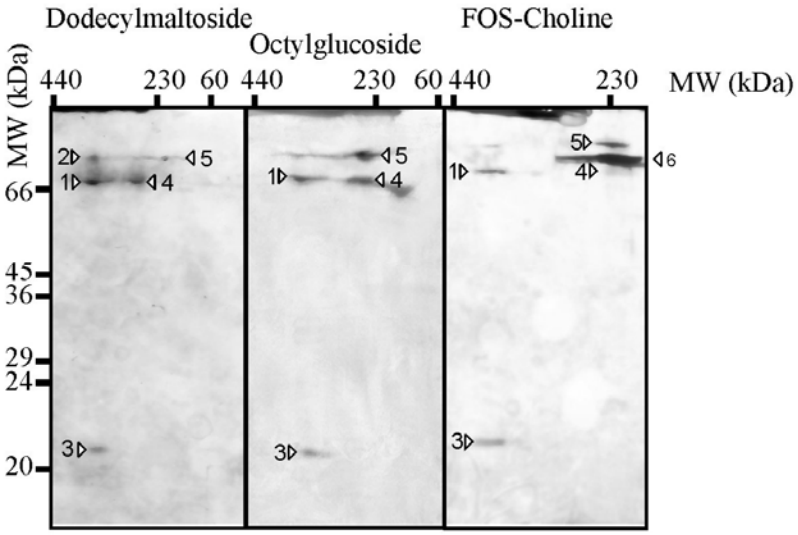

Figure 7. Analysis of protein complexes in the outer membrane fraction of vegetative cells. The OM fraction of *Anabaena* sp. was solubilised with 1% dodecylmaltoside (left), 100 mM octylglucoside (middle) or 100 mM FOS-Choline (right), separated in the first dimension by BN-PAGE and in the second dimension by SDS-PAGE followed by Coomassie staining. Arrows indicate sequenced protein spots and the proteins identified in the gel spots are listed below in Table 8.

Table 8. Proteomic analysis of the complexes present in the outer membrane fraction. Given are the accession number of the identified protein and the number of the gel spot according to Figure 7. The last column gives the identification number of the protein according to Tables 5-7. Here detected catalase protein originates from the protein marker. DoMa - dodecylmaltoside , OG - octylglucoside (middle) or FOS-Choline.

Protein (Acc.)	DoMa	OG	FOS-Choline	Ident. Number
Alr2887	1, 4	1, 4	1, 4	10
Alr2269	2, 5	5	5	2
All2736	?	3	?	-
Catalase	-	-	6	-

In this case, the second complex would contain two proteins. Using the data from the solubilisation by octylglucoside, an assembly of All2736, as the third identified protein (Figure 7, Table 8, see also section 6.3.7.), and Alr2887 could be suggested. However, All2736 was not among proteins identified in the outer membrane proteome. According to the three-dimensional structure predictions by the PHYRE server this protein has similar structure to the plant lipid transporter proteins and might only be associated, with Alr2887, but not inserted into the outer membrane. As a conclusion, two complexes of approximately 370 kDa were identified, one tetrahomomeric complex composed of Alr2269 and one heteromeric complex composed of Alr2887 trimer and associated with All2736 protein (Figure 7, Table 8).

6.2. Proteomic analyses of the heterocyst outer membrane of *Anabaena* sp. PCC 7120

In the first part of this study a few important points were accomplished. A protocol for isolation of the pure outer membrane fractions of *Anabaena* sp. vegetative cells was established, being an essential tool for the following investigations of the outer membrane dynamics and function. The protein composition of the outer membrane fraction was analysed and among 55 identified proteins those truly belonging to the outer membrane were found. In addition, two outer membrane protein complexes were discovered. However, *Anabaena* sp. differentiates the second type of cells, heterocysts, when grown without combined nitrogen source. Being the place of nitrogen fixation, heterocysts must provide an environment for the synthesis and functioning of oxygen sensitive nitrogenase (see "Introduction"; Wolk, 1996; Laurent *et al*., 2005). For this reason heterocysts are morphologically and functionally different from vegetative cells. Given that each heterocyst differentiates from the pre-existing vegetative cell (Wolk, 1996; Herrero *et al*., 2004), it was interesting to investigate how this process effects the outer membrane protein composition and function. For that purpose, proteomic analysis of the outer membrane / cell wall of heterocysts was performed.

6.2.1 Alr2269 protein as an outer membrane / cell wall marker

Anabaena sp. Omp85 homologue Alr2269 protein (Ertel *et al*., 2005; Bredemeier *et al*., 2006) is used as an outer membrane / cell wall marker for both, heterocysts and vegetative cells, since no heterocyst specific outer membrane protein is known to the date. The "outer membrane / cell wall" expression stands here for the heterocyst outer membrane plus co-isolated outer heterocyst specific glycolipid layer (see later Figures 10, 18). Alr2269 is a β-barrel outer membrane protein that forms a homotetrameric complex in vegetative cells (Tables 5-8, Figure 7). Alr2269 is present in both vegetative cells and heterocysts, as shown by Western blotting (Figure 8A), and contains a classical targeting signal for the translocation via the Sec translocon. The gene is expressed independently of nitrogen-source, as shown by the microarray analysis from Ehira *et al*. (2003). To further test the presence of the Alr2269 in both cell types and its membrane localization, *Anabaena* sp. strain NMP-*alr2269*-GFP (Table 4) with GFP attached to the C-terminus of Alr2269 protein was generated. Western blotting of the outer membranes isolated from

wild type and NMP-*alr2269*-GFP mutant with anti-GFP antibody demonstrated the presence of the GFP fusion protein in the the mutant membranes, but not in the wild type outer membranes (Figure 8B). Further analysis of the GFP fluorescence (Figure 8C) showed Alr2269-GFP protein presence in both vegetative cells and heterocysts. The obtained ring-like GFP fluorescent signal (Figure 8C, enlargement) indicates that the protein is present on the periphery of the cell, as expected in the case of the outer membrane localization. However, the GFP signal was relatively weak and only obtained in the focal plane and not out of focus, as found for the cyanobacterial auto-fluorescence (Figure 8C). This observation confirmed the possibility of the use of Alr2269 antibody for the quality control of the heterocyst outer membranes.

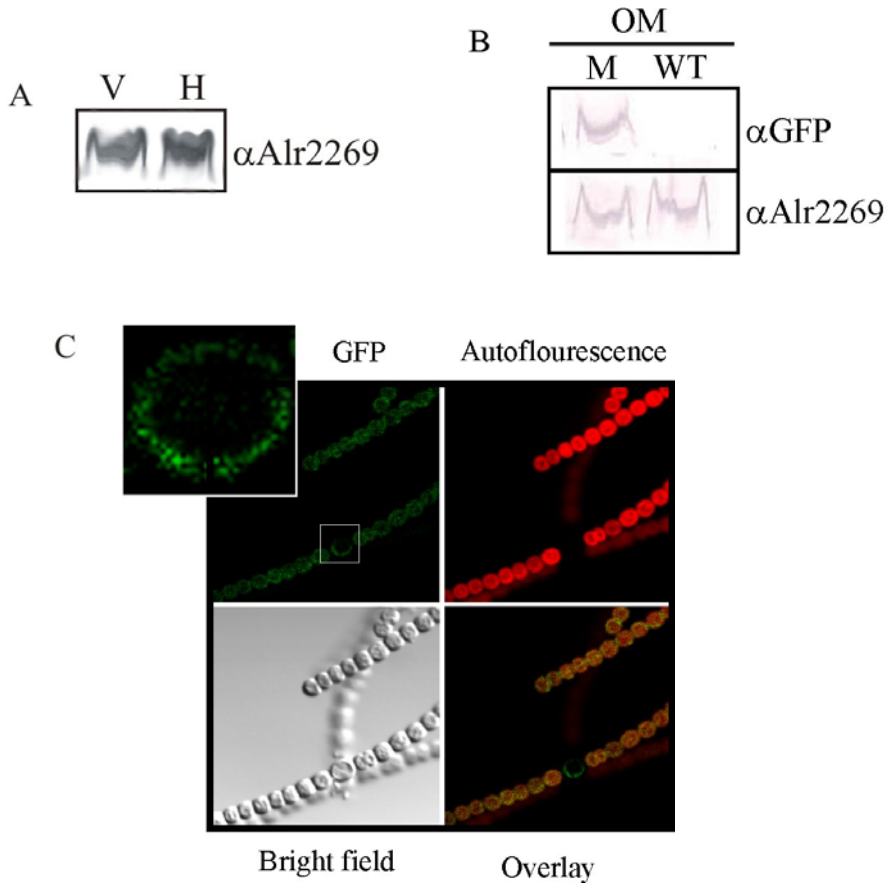

Figure 8. (A) Western blot of vegetative cells (V) and isolated heterocysts (H) with anti-Alr2269 antibody confirms the presence of Alr2269 protein in both cell types of wild type *Anabaena* sp. PCC 7120 (B) Western blot of the outer membranes (OM) isolated from wild type and NMP-*alr2269*-GFP mutant with anti-GFP antibody (αGFP) confirms the presence of Alr2269-GFP fusion protein in the outer membrane of the NMP-*alr2269*-GFP strain (M), but not in the wild type (WT) membranes. Blotting with anti-Alr2269 antibody (αAlr2269) confirms the Alr2269 protein presence in both outer membrane fractions (C) Leica confocal microscopy of the NMP-*alr2269*-GFP strain. Shown are the GFP signal, auto-fluorescence, bright field image and the overlay. One heterocyst signal (white square) is enlarged (left-upper corner). Resulting GFP signal proves Alr2269 presence in both cell types and on the cell periphery, being in line with the protein membrane localization.

6.2.2 New method for the outer membrane / cell wall isolation from heterocyst of *Anabaena* sp. PCC 7120

The predisposition for successful isolation of the clean heterocyst cell wall (the heterocyst outer membrane with additional heterocyst specific layers) was obtaining a clean fraction of isolated heterocysts as free from broken vegetative cells as possible (see "Methods", section 5.4.7.). The purity of the isolated heterocysts was multiple checked by three approaches. In the first approach light microscopy of Alcian Blue stained cells was performed. Alcan Blue stains specifically the outermost heterocyst polysaccharide layer, not present in vegetative cells (Borthakur *et al.*, 2005), and enables to better distinguish isolated heterocysts from vegetative cells (Figure 9A,B). In the second approach Western blotting with antibody against D1 component of the photosystem II was performed. D1 protein is not to present in mature heterocysts (Baier *et al.*, 2004). This enables to detect possible contaminations with remnants of vegetative cells among isolated heterocysts (Figure 9D). And third, an additional conformation of the purity came from a clear difference in the pattern of protein bands (especially at lower molecular weights) between vegetative cells and isolated heterocysts after subjecting them to SDS-PAGE and Coomassie staining (Figure 9C). Only heterocyst isolates of the high purity were used further to isolate the heterocysts cell wall.

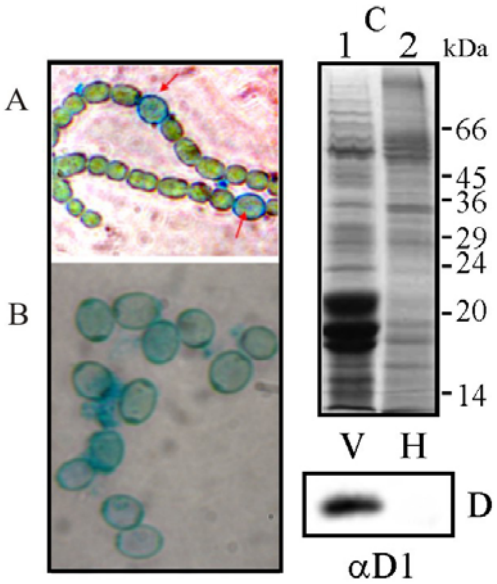

Figure 9. (A) Filaments of *Anabaena* sp. PCC 7120 grown in $BG11_0$ were stained with Alcian Blue and visualized by light microscopy. (B) Isolated and Alcian Blue stained heterocysts were analyzed by light microscopy. (C) Samples (10 µg protein) of vegetative cells (lane 1) and heterocysts (lane 2), were subjected to SDS-PAGE followed by Coomassie Blue staining or (D) immunodecoration with anti-D1 antibodies (lanes 1, 2, bottom). V stands for vegetative cells, H for heterocysts.

Heterocyst cell wall isolation protocol was developed by modifying and adjusting the previously developed protocol for membrane fractionation of *Anabaena* sp. vegetative cells. The crucial step in the procedure was breaking of isolated heterocysts, which are far more resistant to both chemical and mechanical forces in comparison to vegetative cells because of the two additional heterocyst specific layers (see "Introduction"; Murry and Wolk, 1989). The combination of harsh sonication conditions with repeated French Press treatments applied on a diluted heterocyst suspension while keeping the cells cold, finally led to satisfying result (Figure 10; see "Methods" section 5.4.7.). On SDS-PAGE followed by Coomassie staining protein pattern of the cell wall fraction from isolated heterocysts and the outer membrane fraction from *Anabaena* sp. vegetative cells showed a difference (Figure 10A). Additionally, comparison of the lipid pattern of heterocysts to the lipid pattern of the isolated heterocyst cell wall fraction shows enrichment of the heterocysts specific glycolipids in the cell wall fraction (Figure 10B, HGL1 and HGL2). This result also demonstrates that heterocyst specific glycolipids are associated with the outer membrane and can be co-isolated with it (Figure 10B).

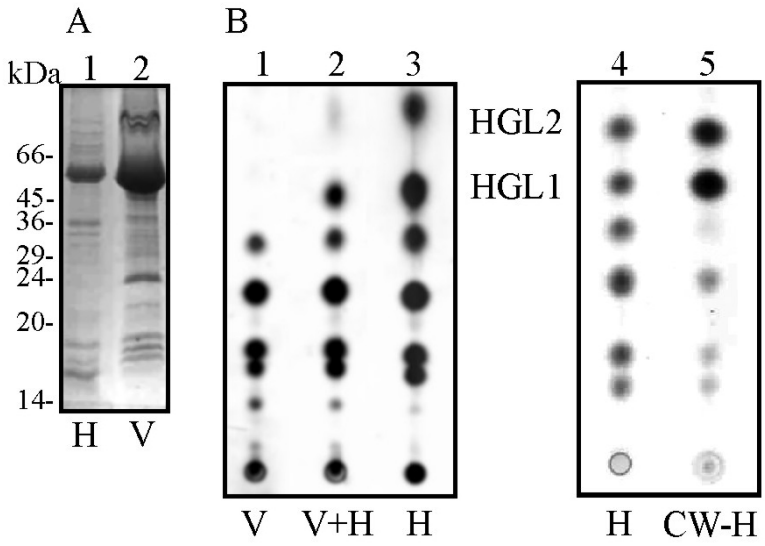

Figure 10. Heterocysts cell wall isolation. (A) Heterocysts cell wall sample (10 µg protein, lane 1) and sample of the outer membrane of vegetative cells (10 µg protein, lane 2) show different protein band pattern on SDS-PAGE followed by Coomassie Blue staining. (B) Lipid content of vegetative cells (BG11 culture, lane 1), filaments with induced heterocysts ($BG11_0$ culture, lane 2), isolated heterocysts (lanes 3, 4) and of heterocyst cell wall fraction (lane 5) was analyzed. Heterocyst specific glycolipids (HGL1 and HGL2) are indicated. H stands for heterocysts, V for vegetative cells, CW-H for heterocyst cell wall. Enrichment in HGLs in isolated heterocysts (lanes 3, 4) and further in isolated heterocyst cell walls (lane 5) is detectable. Lipids spots correspond to one unidentified lipid, sulpholipid, phosphatidyl glycerol and digalactosyl diglyceride (Winkenbach *et al*., 1972).

6.2.3 Proteome analysis of the isolated heterocyst outer membrane / cell wall fraction

The proteome composition of the isolated heterocyst outer membrane / cell wall was analyzed by two strategies: peptide-mass fingerprint analysis and peptide sequencing (Tables 9, 10, in cooperation with laboratory of Dr. Lutz A. Eichacker). For comparison, the outer membrane fractions from vegetative cells were analyzed simultaneously (Table 9). In total 18 proteins were identified in the cell wall fraction isolated from heterocysts. 13 of them have already been identified in the outer membrane fraction of vegetative cells (Table 9 and Tables 5-7) and their function and localization were previously discussed (section 6.1., Tables 5-8, Figure 7).

Table 9. Proteins identified in the outer membrane / cell wall fraction of heterocysts. Given are: an accession number of the identified peptide sequences (column 2), the putative function (column 3), the experiment in which the protein was identified (column 4; MF - mass fingerprint, PS - peptide sequencing), the numbers of detected peptides (column 5) and the detection score for MF. In column 6 listed are: detection in the outer membrane / cell wall fraction of vegetative cells (VC) in the current analysis (denoted with "a") or in previous analysis (denoted with "b"; Tables 5-7). Further given are: protein molecular weight (column 7), isoelectric point for the precursor / mature protein form (column 8) and a significant up-regulation of the gene expression after nitrogen step-down (column 9, according to Ehira *et al.* (2003) + stands for gene up-regulation, - for no gene up-regulation).

No.	Acc.	Name	Exp.	peptides	VC	MW (kDa) pre/mat	pI pre/mat	up-regul.
1	alr4550	probable porin	MF/PS	21 (173) / 12	a/b	60.5/57.8	4.12 / 4.11	-
2	all4499	probable porin	MF/PS	22 (173) / 9	a/b	58.5/55.4	4.14 / 4.12	-
3	alr0834	porin	MF/PS	13 (88) / 5	-/b	54.3	4.42	+
4	alr4392	nitrogen-responsive regulatory protein NtcA	PS	6	-/-	24.9	9.12	+
5	alr2269	nOmp85	PS	8	-/b	89.5/87.8	4.66 / 4.69	-
6	alr0397	similar to ferric aerobactin receptor	PS	7	-/b	94.2/90.2	4.38/ 4.31	-
7	all3984	predicted protein	MF/PS	12 (108) / 4	-/b	24.7/21.0	5.85 / 5.43	+
8	alr5055	hypothetical protein	PS	3	-/-	21.6/19.02	5.86 / 5.45	+
9	alr2887	outer membrane efflux protein	MF/PS	11 (85) / 3	a/b	80.7/78.0	4.88 / 4.80	+
10	all1861	peptidoglycan-binding protein	MF/PS	12 (90) / 4	a/b	28.4/27.1	4.99 / 5.16	+
11	all3585	hypothetical protein	MF/PS	7(69) / 3	a/b	29.4/25.7	4.33 / 4.39	-
12	all0089	hypothetical protein	MF/PS	6 (65) / 3	-/b	55.8	9.56	+
13	all0268	predicted Zn-dependent hydrolases	MF/PS	5 (57) / 2	-/b	27.3/24.2	9.69 / 9.40	-
14	all4388	involved in polysaccharide export	MF/PS	9 (67) / 4	-/b	51.5 / 48.0	4.87 / 4.79	+
15	all1427	hypothetical protein	PS	3	-/-	21.6	6.17	+
16	alr0668	hypothetical protein	PS	4	-/-	23.0	8.77	+
17	alr0874	nitrogenase reductase NifH2	PS	3	-/-	32.6	5.16	+
18	all3826	N-acetylmuramoyl-L-alanine amidase CwlL precursor-like	PS	3	-/b	25.4/22.3	9.86 / 10.06	-

The five remaining proteins were possible heterocyst specific proteins. Indeed, nitrogenase protein NifH2 (Table 9, protein 17) is a heterocyst specific protein just as NifH (Elhai and Wolk, 1990). Also the level of NtcA transcriptional regulator of nitrogen metabolism (Table 9, protein 4) is elevated in heterocysts compared to vegetative cells (Olmedo-Verd *et al*., 2005). However, both proteins 4 and 17 most likely represent cytosolic contaminations. All1427 (Table 9, protein 15) contains two cystathionine-beta synthase domains (CBS), which usually come in tandem repeats and are found in cytosolic and membrane proteins with diverse functions (Ignoul and Eggermont, 2005). Protein 8 or Alr5055 (Table 9) contains a domain found in proteins involved in spore germination. It is speculated that GerM, the homologue of Alr5055 in *Bacillus subtilis*, participates in the peptidoglycan synthesis during sporulation (Slynn *et al*., 1994). For Alr0668 (protein 16), no significant homology to a protein or domain could be identified.

The putative outer membrane localization was further investigated for five "heterocyst specific" proteins with a help of bioinformatical tools (Table 10; Mirus and Schleiff, 2005). No helical transmembrane segments were identified by TMHMM (Krogh *et al*., 2001) in any of these proteins excluding them as the inner membrane localized.

Table 10. Predicted localization of the five proteins identified only in the cell wall fraction of *Anabaena* sp. heterocysts. Given are: an accession number of the sequence (column 2), putative cleavage site of a presequence (column 3), predicted localization (column 4), the β-barrel score according to BBS275 program (column 5), the β-barrel prediction according to dependent/independent approach of BBS275 (column 6) or 0% false-prediction approach of BBS275 program (column 7), where + stands for β-barrel and – for no β-barrel structure. MCMBB score for mature proteins (cut off value > 0; column 8) and a number of transmembrane β-strands predicted by Pred-TMBB (column 9) are also listed. Column 10 shows the final localization prediction (cyt-cytosol; PP – periplasm, (-)-no selection by BBS programs; ? - no secure prediction possible). Results for the β-barrel Alr2269 outer membrane (Figure 8) protein are presented for comparison with other data.

No.	Acc.	Signal P 3.0	Loc.	BBS275	dep/ind.	0%	MCMBB	Pred-TMBB	Final
4	alr4392	-	Cyt	0.00	-	-	-0.044	-.	-
5	**alr2269**	ANA-QT (18)	OM	2.79	+	+	0.033	19	OM
8	alr5055	TVA-GG (26)	OM/PP	0.03	-	-	0.002	2	?
15	all1427	-	Cyt	0.03	-	-	-0.038	-	-
16	alr0668	-	Cyt	1.37	+	-	-0.031	-	?
17	alr0874	-	Cyt	0.05	-	-	-0.065	-.	-

Next, in order to investigate the possible outer membrane localization, the β-barrel structure predictions were performed with Signal P (Bendtsen *et al*., 2004) and P-Sort (Gardy *et al*., 2005) programs, with a program based on the β-barrel score (BBS275; Oliver Mirus, personal communication) developed by Mirus and Schleiff (2005) and with MCMBB (Bagos *et al*., 2004a) and Pred-TMBB (Bagos *et al*., 2004b,c; data summarized in Table 10) tools. For comparison, the results for the outer membrane protein marker Alr2269 present in both cell types (Figure 8) are shown. The collected data confirm the cytosolic localization of NifH2 and NtcA (Tables 9, 10) and suggest the cytosolic localization of CBS domain containing protein All1427. On the other hand, the localization of Alr5055 (protein 8) and Alr0668 (protein 16) was not reliably predictable. The presence of the secretion signal (Table 9) and the selection by the two β-barrel prediction programs (Table 10) favor Alr5055 to be outer membrane localized or attached. For Alr0668 program only one of the two approaches of the BBS275 method suggested a β-barrel fold (Table 10). Accordingly, Alr0688 is also probably a protein from the soluble cell fraction.

Furthermore, according to the microarray data published by Ehira *et al*. (2003), genes encoding 11 proteins among 18 identified are up-regulated upon nitrogen starvation (Table 10, column 9). It is remarkable that the genes encoding classical outer membrane proteins, Alr2269 as an essential Omp85 protein and Alr4550 porin, are down-regulated upon nitrogen step-down (Ehira *et al*., 2003). However, these two proteins belong to the most abundant proteins of the outer membrane of vegetative cells (section 6.1, Tables 5-8). For this reason the down-regulation of their gene expression does not exclude their appearance and function in heterocysts as well, although it could reflect different functional priorities of heterocysts in comparison to vegetative cells. For the β-barrel proteins found in the outer membrane proteome of vegetative cells, but not of heterocysts, microarry data show up-regulation of four genes. Only two of them, *all4026* and *alr2588*, show more significant up-regulation after 24 hours. However, it has to be considered that the microarray analysis by Ehira *et al.* (2003) was performed on whole filaments containing about ten times more vegetative cells than heterocysts (Adams *et al*., 2000). That analysis, therefore, supports the idea of functional modification of the outer membrane proteome after nitrogen step-down but does not exclude that some of the alterations of gene expression occur in vegetative cells rather than in heterocysts. However, in this analysis no significant changes of the heterocysts outer membrane / cell wall proteome are detectable in comparison to the outer membrane proteome of *Anabaena* sp. vegetative cells (Tables 5-7, Tables 9, 10).

6.3. Alr2887 – the TolC-like transporter of *Anabaena* sp. PCC 7120

The proteomic analyses of the outer membrane fractions of *Anabaena* sp. PCC 7120 of vegetative cells and heterocysts (sections 6.1. and 6.2.) revealed few proteins as particularly interesting. As a result of the protein complex analysis of the outer membrane two complexes were detected (Figure 7, Table 8). The first complex comprised Alr2269, an Omp85 homologue of *Anabaena* sp. (Ertel *et al*., 2005; Bredemeier *et al*., 2006). In the second complex, the homologue of the TolC channel-tunnel or Alr2887 protein was identified (Figure 2; Koronakis, 2000). The complex size corresponded to the trimeric structure of TolC proteins and All2736 protein seamed to associate with the Alr2887 complex. Even more, Alr2887 was identified in the outer membrane proteomes of vegetative cells and heterocysts, raising the question about the function of this common outer membrane protein family in both cell types (Tables 5-9). This is especially interesting since until now TolC function has been explored exclusively in classical unicellular Gram-negative bacteria and never in a multicellular differentiating microorganism such as cyanobacterium *Anabaena* sp.

6.3.1 *alr2887* gene expression increases during heterocyst differentiation

Alr2887 protein was detected in both cell types of *Anabaena* sp. PCC 7120. To confirm the *alr2887* gene expression in vegetative cells and in heterocysts *gfp* gene was placed under control of *alr2887* promoter in a mutant strain NME-*alr2887*-GFP (see "Methods", section 5.1.3.4.). The GFP fluorescence of the mutant was examined with Leica confocal microscope after 48 hours of growth in $BG11_0$ medium without combined nitrogen source. As a result, NME-*alr2887*-GFP strain showed GFP signal in vegetative cells as well as in heterocysts. However, the obtained GFP signal was significantly stronger in heterocysts, sometimes found as two heterocysts next to each other, than in vegetative cells (Figure 11). This result demonstrates elevated expression of *alr2887* gene in heterocysts in comparison to the basal level of expression detected in vegetative cells. It appears that Alr2887 function is important in both, vegetative cells and in heterocysts of *Anabaena* sp. However, some special significance could exist in heterocysts.

Since *alr2887* gene expression is elevated in heterocysts in comparison to vegetative cells, the time course of the increase in detected expression level was investigated (Figure 12.).

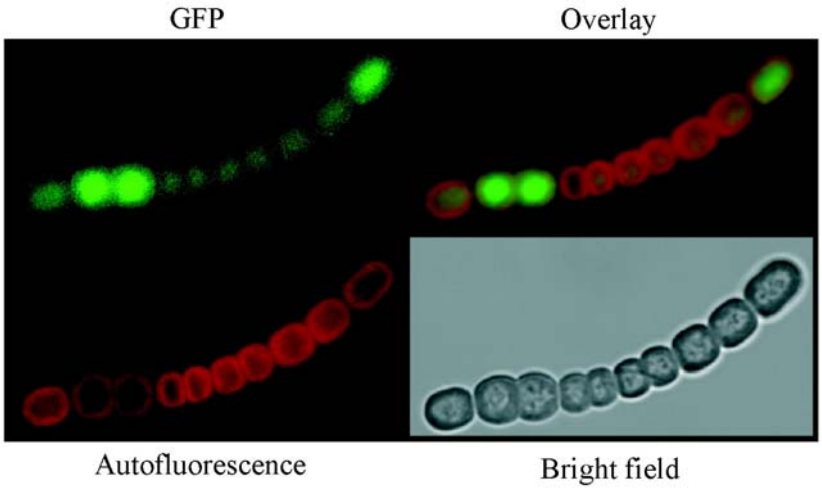

Figure 11. GFP fluorescence in NME-*alr2887*-GFP mutant where *gfp* gene is placed under control of *alr2887* promoter. The mutant was grown 48 hours under nitrogen depletion in $BG11_0$ and examined with confocal Leica PC5 microscope. Shown are autofluorescence, GFP signal, overlay and a bright field image. Vegetative cells show basal level of GFP expression, while heterocysts exhibit high GFP expression (single cell at the end of the filament and double cells, all three showing low level of chlorophyll autofluorescence).

For that purpose the wild type and NME-*alr2887*-GFP filaments were transferred to the heterocysts inducing $BG11_0$ medium and the GFP fluorescence was monitored over a time period of 25 hours with the use of luminescence spectrometer (see "Methods", section 5.4.13.). The resulting curve showes a basal GFP expression level already before nitrogen step-down, confirming the basal activity of the promoter. After nitrogen step-down the GFP fluorescence and *alr2887* promoter activity began to increase to finally obtain the highest intensity sixteen hours after nitrogen step-down (Figure 12A). After that the GFP fluorescence and *alr2887* promoter activity decreased back to the basal level after 24 hours, exactly corresponding to the time necessary for the heterocyst maturation (Figure 12A).

This result supports the microarray data from Ehira *et al.* (2003), where genome-wide expression of *Anabaena* sp. was analyzed in response to nitrogen-deprivation. According to their data *alr2887* expression increases significantly after nitrogen step-down, reaching the highest point eight to nine hours after the filament were exposed to nitrogen deprivation (Figure 12B). The expression finally falls back to the basal level during next 16 hours (all together 25 hours of nitrogen deprivation). Interestingly, expression of *all2736* gene, encoding the protein co-isolated with Alr2887 complex, follows exactly the same curve (Figure 12B, see also Table 8).

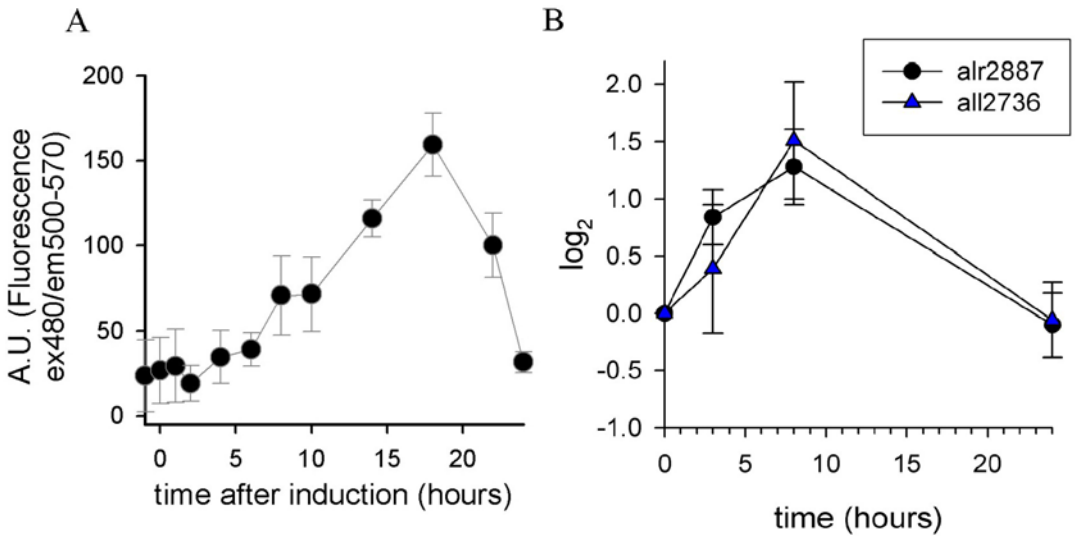

Figure 12. (A) The time curve of the GFP fluorescence level in the NME-*alr2887*-GFP mutant where GFP is expressed from the *alr2887* promoter was measured by luminescent spectrometer. The GFP fluorescence increase appears during first 16 hours after nitrogen step-down and falls back to the basal level during following hours. (B) For comparison, graph based on Ehira *et al.* (2003) microarray data on the genome-wide expression after nitrogen step-down obtained in the case of *alr2887* and *all2736* genes.

The data based on investigation of NME-*alr2887*-GFP mutant (Figure 12) imply a role of Alr2887 in the first phase after nitrogen step-down, possibly connected to heterocyst maturation. The discrepancy in time necessary to obtain the highest level of gene expression in the curve based on Ehira *et al.* (2003) microarray data and to obtain the highest level of GFP fluorescence in NME-*alr2887*-GFP mutant (Figure 12A) could be explained by a time period necessary to accumulate sufficient amount of GFP inside the cell sufficient to detect the fluorescence, which causes the delay. These results demonstrate that *alr2887* gene function is most needed during the middle stage of heterocyst development.

Furthermore, the Northern blot data performed on *alr2887* region in *Anabaena* sp. wild type obtained by Dr. Iris Maldener (personal communication), proved that *alr2887* does not form an operon structure with the neighboring genes and that *alr2887* expression is *ntcA* dependent but *hetR* independent.

6.3.2 Alr2887 is an integral outer membrane protein whose amount of is elevated in developing proheterocysts

In order to experimentally confirm the outer membrane localization and Alr2887 protein presence along the filament (Tables 5-8), GFP protein was fused to the C-terminus of Alr2887 protein in the *Anabaena* sp. mutant strain NMP-*alr2887*-GFP (see "Methods", section 5.1.3.3.). After 48 hours of nitrogen deprivation, wild type and NMP-*alr2887*-GFP filaments were examined with Leica confocal fluorescence microscope. Although the obtained GFP signal did not allow precise localization of the protein inside of the cells, it did revealed clearly elevated amounts of Alr2887-GFP protein inside of developing proheterocysts (Figure 13, detected according to the changed morphology but accompanied with a strong autofluorescence signal) in comparison to the basal amount of the protein inside of vegetative cells and mature heterocysts (Figure 13, detected according to the changed morphology and a complete loss of autofluorescence signal). This result parallels the fluorescent signal distribution of the GFP-promoter mutant filaments (Figure 11) and the gene up-regulation curves, showing an increase in the first hours of nitrogen deprivation (Figure 12).

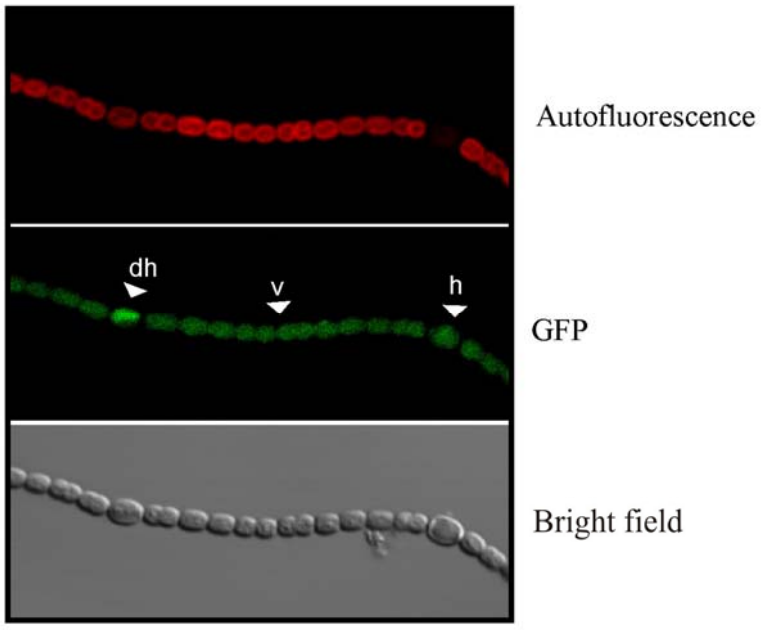

Figure 13. GFP fluorescence in NMP-*alr2887*-GFP strain where GFP is fused to the C-terminus of Alr2887. The filaments were grown 48 hours under nitrogen deprivation in $BG11_0$ and examined with Leica confocal microscope. Shown are autofluorescence, GFP signal and a bright field image. The basal level of the GFP-Alr2887 fusion is present in vegetative cells (v) and mature heterocyst (h) in comparison to the strong GFP signal detected in proheterocysts (developing heterocysts, dh).

As the fluorescence microscopy of NMP-*alr2887*-GFP mutant did not allow ascribing Alr2887 protein to the outer membrane of *Anabaena* sp. (Figure 13), another approach was considered. The outer membranes were isolated from NMP-*alr2887*-GFP filaments grown in nitrate containing medium and the fractions were treated with 8 M urea, 0.1 M Na_2CO_3 and 1 M NaCl (see "Methods", section 5.2.4.). The samples were subjected to SDS-PAGE followed by immunodecoration with commercially available anti-GFP antibody. This antibody did not cross-react with the wild type outer membrane (not shown). The result showed that Alr2887, even when fused with GFP, is present in the outer membrane and cannot be extracted out of it, with exception of a very faint band in the supernatant after the 8 M urea treatment (Figure 14). As control, immunodecoration of the same treated outer membrane fractions was performed with anti-Alr2269 antibody against the outer membrane localized Omp85 homologue (Figure 14). This altogether confirms that Alr2887 is indeed an integral outer membrane protein which presence is significantly elevated in proheterocysts.

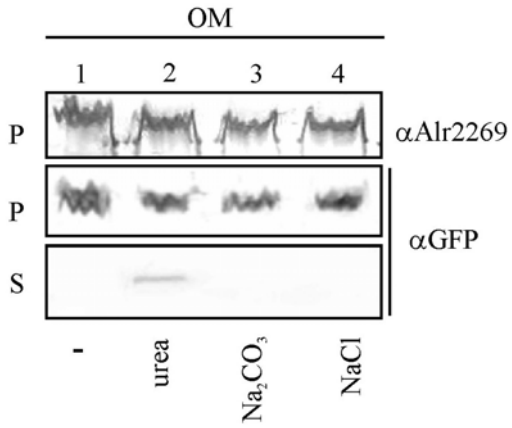

Figure 14. The outer membrane fraction isolated from NMP-*alr2887*-GFP strain grown in BG11 medium was treated with 8 M urea (lane 2), 0.1 M sodium carbonate (lane 3) or 1 M sodium chloride (lane 4). Lane 1 presents a non-treated control. The pelleted membrane fraction (P) or the supernatant (S) were probed with antibodies against the outer membrane protein Alr2269 (αAlr2269) and against GFP (αGFP). The anti-GFP antibody did not cross-react with the wild type membranes (not shown). The GFP-fusion protein was not extracted with any of the treatments except for a faint band in the case of the treatment with urea.

6.3.3 Alr2887 protein function is nonessential

In attempt to investigate the cellular function of Alr2887, the deletion *Anabaena* sp. mutant NMΔ-*alr2887* of the corresponding *alr2887* gene was created (see "Methods", section 5.1.3.1.). The pCSV3 plasmid containing C.S3 cassette was inserted in the centre of the gene and single recombination mutants were selected on the basis of antibiotic

resistance of the filaments (Figure 15A). The mutant genomic DNA was subjected to the Southern blotting analyses to test the level of the chromosomal segregation (Figure 15B). *Anabaena* sp. has multiple copies of the chromosome and deletion mutations of the genes whose functions are essential for the cell do not fully segregate under any selective pressure. In such case, a certain number of the chromosomal copies always keep the wild type version of the gene. The results of Southern blotting on the *alr2887* gene area showed that all four obtained mutants were fully segregated under standard growth conditions, demonstrating that *alr2887* gene encodes a protein with nonessential function for the *Anabaena* sp. cell (Figure 15B).

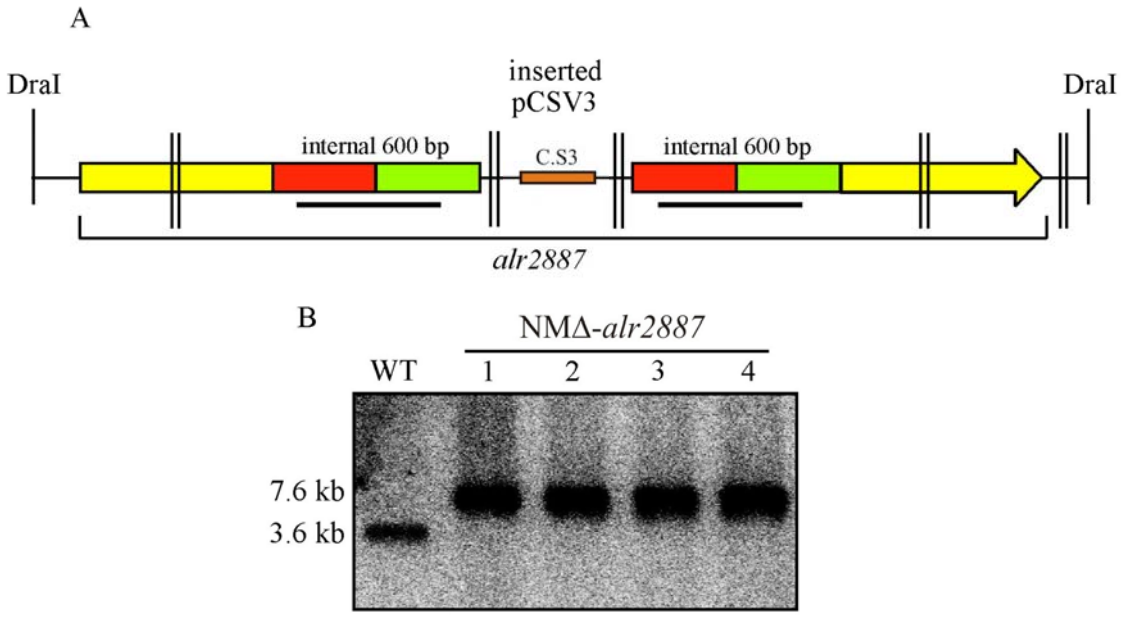

Figure 15. (A) Chromosomal structure of the deletion mutant NMΔ-*alr2887*. The integrity of *alr2887* gene is interrupted by pCSV3plasmid insertion in the centre of the coding sequence. Single vertical lines show *Dra*I restriction sites used to enzymatically digest the genomic DNA while fat horizontal bars under the gene correspond to the places of hybridization of ^{35}P labeled probes. (B) Southern blotting of wild type (WT) and four independent NMΔ-*alr2887* mutants shows complete chromosomal segregation.

6.3.4 Deletion mutant of *alr2887* gene shows *fox*$^-$ phenotype

Heterocysts differentiation is one of the most prominent features of *Anabaena* sp. and a huge number of genes participate directly or indirectly in heterocyst formation and function (Golden and Yoon, 2003; Herrero *et al.*, 2004). Both types of GFP mutants, NME-*alr2887*-GFP and NMP-*alr2887*-GFP, imply function of Alr2887 protein in vegetative cells, in heterocyst and especially in developing proheterocysts (Figures 11-13).

For this reason the growth of the NMΔ-*alr2887* deletion mutant was analyzed in the presence and in the absence of combined nitrogen source. While growing on the nitrate containing BG11 medium, the deletion mutant NMΔ-*alr2887* behaved like wild type. After the transfer of the mutant filaments to the nitrate-free $BG11_0$ medium colonies began to bleach and after a week turned completely yellow (Figure 16E). This so called *fox*$^-$ phenotype (Ernst *et al.*, 1992) signals incapability of the mutant filaments to perform nitrogen fixation under aerobic conditions (Ramirez *et al.*, 2005). That can be a consequence of several factors. First, the deletion mutant does not differentiate heterocysts. Second, the deletion mutant differentiates heterocysts but does not synthesize nitrogenase or nitrogenase is defective and without activity. And third, heterocysts do differentiate but suffer from a structural defect that prevents them from obtaining and/or keeping microoxic environment crucial for the nitrogenase function.

To explore these possibilities, the wild type and NMΔ-*alr2887* cultures were examined by light microscopy (see "Methods", section 5.5.1.). The strains were grown in $BG11_0$ under nitrogen depletion and incubated shortly with Alcian Blue dye, which stains specifically heterocyst polysaccharide layer (Figure 16A, B).

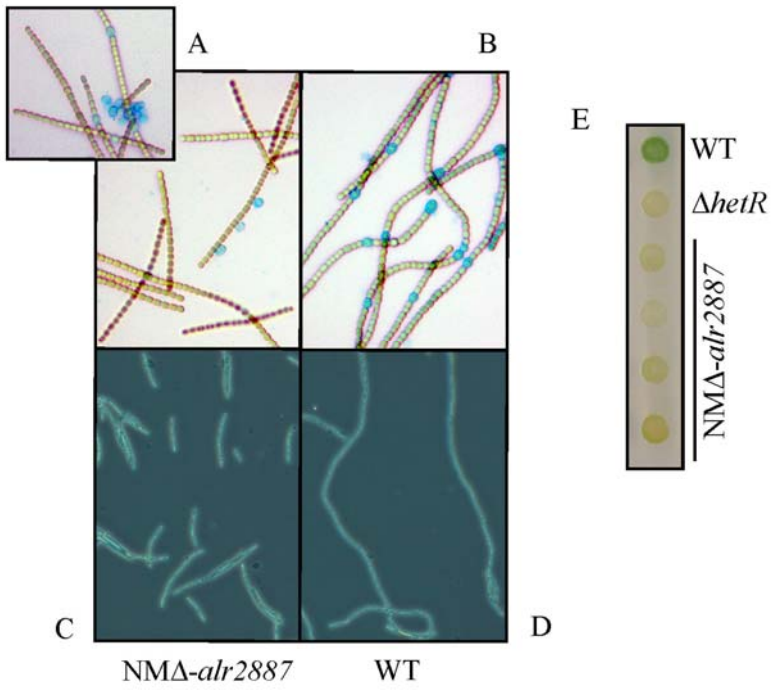

Figure 16. NMΔ-*alr2887* mutant shows *fox*$^-$ phenotype and fragmentation in the $BG11_0$. (A) Shown are short filaments of NMΔ-*alr2887* mutant grown in nitrogen-depleted cultures as a result of fragmentation and Alcian Blue stained heterocysts, many of which are detached and swim free in the medium (small figure). (B) Long filaments with blue stained heterocysts of wild type (WT) grown under the same conditions. Bright field figures showing (C) short NMΔ-*alr2887* filaments and (D) long WT filaments. (E) *fox*$^-$ phenotype of the four independent NMΔ-*alr2887* mutants in comparison to the green WT and *fox*$^-$ HetR (*ΔhetR*) mutant as control, all grown on N_2 as a sole nitrogen source ($BG11_0$).

As a result, mature heterocysts were detected in NMΔ-*alr2887* filaments (*het*$^+$ phenotype), they were stained with Alcian Blue indicating that the outermost heterocysts specific polysaccharide layer existed (Figure 16A, B). On the other hand, filaments of NMΔ-*alr2887* showed significant fragmentation in comparison to the wild type filaments. Their length varied mostly between 10 to 30 cells in comparison to 100 and more cells long wild type filaments (Figure 16C, D). Although blue dyed heterocysts were present in the short mutant filaments, a significant number of heterocysts were detached from the filaments floating free in the surrounding medium. Therefore, the most probable "hot-spots" for the filament breaking in NMΔ-*alr2887* mutant are heterocyst-vegetative cell connections. Heterocysts that remain in the NMΔ-*alr2887* filaments should be enough to support diazotrophic growth of the mutant and a *fox*$^-$ phenotype cannot be simply explained by detachment of heterocysts from the filaments. Therefore, the nitrogenase activity was tested with an acetylene reduction assay (as in Valladares *et al*., 2003) on NMΔ-*alr2887* mutant in cooperation with the laboratory of Dr. Enrique Flores (personal communication). This assay is based on fact that active nitrogenase can reduce not only dinitrogen to ammonium, but also acetylene to ethylene. Under aerobic conditions activity of acetylene reduction of NMΔ-*alr2887* strain was very low in comparison to wild type (0.072 nmoles of ethylene/mg Chl x h for NMΔ-*alr2887* and 5.32 nmoles of ethylene/mg Chl x h for wild type). Under anaerobic atmosphere in the presence of the inhibitor of oxygen evolving photosynthesis DCMO, activity of nitrogenase increased for times in the mutant (0.336 nmoles of ethylene/mg Chl x h for NMΔ-*alr2887* and 6.42 nmoles of ethylene/mg Chl x h for wild type).

The activity of nitrogenase (*fix*$^+$ phenotype) under anaerobic experimental conditions, together with the previously obtained data on the mutant growth and *fox*$^-$ phenotype, suggest that NMΔ-*alr2887* suffers from defect which prevents heterocysts to create and preserve microoxic environment essential for the nitrogenase function.

6.3.5 Heterocysts glycolipid layer is absent in NMΔ-*alr2887* mutant

As shown by acetylene reduction assay, nitrogenase is active under anaerobic conditions in the mutant NMΔ-*alr2887*, proving that its heterocysts are unable to provide microoxic environment. This indicates an existence of the structural defect in NMΔ-*alr2887* heterocysts, probably in heterocyst specific layers. A similar phenotype has

already been described for mutants defective in the heterocyst glycolipid layer (Fiedler *et al*., 1998 a,b). For this reason the cell morphology was examined by electron microscopy (see "Methods, section 5.5.2.). The filaments were grown for 48 hours without bound nitrogen source prior to embedding in Eppon resin. As a result, vegetative cells of the NMΔ-*alr2887* mutant showed no difference in comparison to the wild type filaments (not shown). On the other hand, heterocysts morphology between wild type and NMΔ-*alr2887* strain was significantly different (Figure 17). As previously confirmed by light microscopy and Alcian Blue staining (Figure 16), heterocysts of NMΔ-*alr2887* strain had thick and well developed polysaccharide layer clearly visible in ultra thin sections (Figure 17).

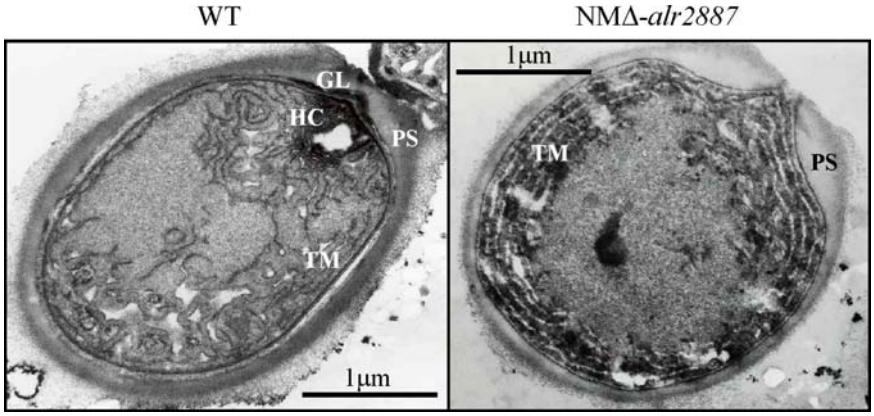

Figure 17. Ultra-thin sections of *Anabaena* sp. wild type (WT) heterocyst and mutant NMΔ-*alr2887* heterocyst 48 hours after nitrogen step-down (representative sample). Electron dense heterocysts glycolipid layer (GL) and "honeycomb" region (HC) are not present in NMΔ-*alr2887* heterocysts, thylakoid membranes (TM) do not rearrange in the mutant heterocysts, while polysaccharide layer (PS) is well developed in both heterocysts.

However, the laminated glycolipid layer, normally visible as a thinner black electron dense layer deposited between the outer membrane and the polysaccharide layer, was completely absent in the mutant. In addition, expected rearrangement of the thylakoid membranes and formation of the so called "honeycomb" region (Giddings and Staehelin, 1979) did not take place in the mutant heterocysts (Figure 17). This ultrastructure explains incapability of the NMΔ-*alr2887* mutant to grow without bound nitrogen. In the absence of the glycolipid layer anaerobic environment of the heterocyst interior, which is essential for the nitrogenase activity, cannot be created and preserved. This indicates that the absence of the Alr2887 protein has impact on the heterocyst glycolipid layer formation.

6.3.6 NMΔ-*alr2887* mutant synthesizes heterocyst specific glycolipids but does not deposit the glycolipid layer

The absence of the heterocyst glycolipid layer in NMΔ-*alr2887* heterocysts implies different putative functions of Alr2887 protein. First, Alr2887 could participate directly in the synthesis of the heterocyst specific glycolipids (HGLs). Second, Alr2887 may participates in the transport of HGLs through the outer membrane to the place of their deposition. And third, Alr2887 may transport proteins / enzymes responsible for the glycolipid layer formation to the place of their action. In attempt to distinguish between these possibilities, the lipid contents of wild type and NMΔ-*alr2887* were analyzed. DR181 mutant, being also an insertion mutant of *alr2887* (obtained from Dr. Iris Maldener), was also used in experiments (Figure 18).

First, lipids were extracted from the whole filaments of the wild type and NMΔ-*alr2887* grown in the presence of combined nitrogen source and subsequently separated by thin layer chromatography (TLC; see "Methods", section 5.3.1.). Both the wild type and NMΔ-*alr2887* lipid samples showed the same lipid pattern (Figure 18, lanes 1, 2). Next, lipids were extracted from the whole cultures of wild type and NMΔ-*alr2887* mutant after 48 hours of growth without combined nitrogen source, therefore, from the filaments containing both cell types. In the wild type lipid pattern HGL1 lipid spot was well detectable, while HGL2 spot was not visible. This is expected for the lipid extracts of the whole cultures where heterocysts comprise around 10-20% of the cells (Figure 18, line 3). On the other hand, in NMΔ-*alr2887* lipid extract both HGLs (HGL1 and HGL2) were not detectable, while other lipid spots showed the same pattern as wild type (Figure 18, line 4).

Whether the absence of HGLs in the NMΔ-*alr2887* lipid extract is a consequence of HGLs absence from the filaments or just reduction of their amount bellow the border of detection in whole cultures was tested further. Heterocysts were isolated from wild type and two deletion mutants, NMΔ-*alr2887* and DR181, after 48 hours of nitrogen starvation and lipids were extracted from isolated heterocysts. When separated by TLC, lipid pattern of isolated wild type heterocyst showed a huge increase in HGL1 and also an appearance of somewhat weaker HGL2 (Figure 18, line 5). Furthermore, HGL1 and HGL2 appeared also in the lipid pattern of heterocysts isolated from deletion mutants NMΔ-*alr2887* and DR181 (Figure 18, lines 6, 7) In both cases, however, HGL1 and HGL2 spots were significantly reduced in comparison to wild type (Figure 18, line 5). This result demonstrates that in the absence of Alr2887 protein, both HGLs still appear in *Anabaena* sp. heterocysts although their amounts are reduced when compared to wild type.

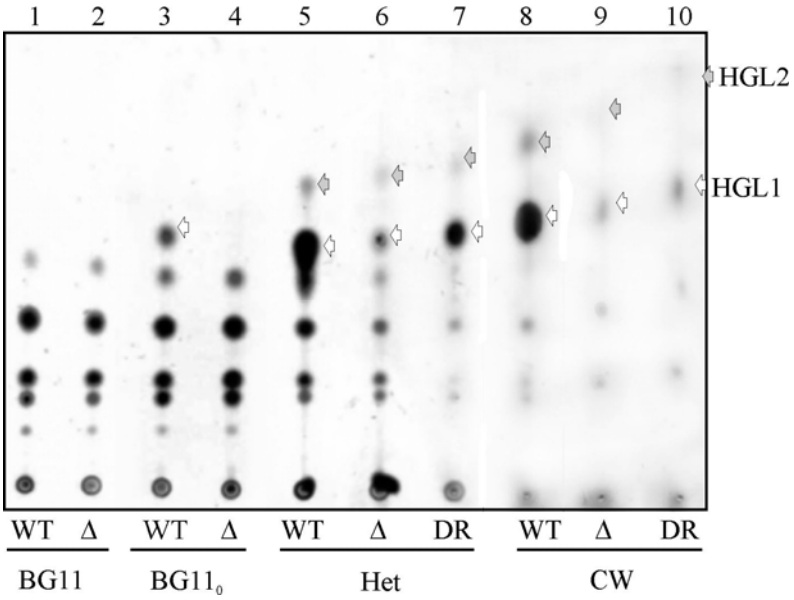

Figure 18. TLC of the lipids extracted from wild type *Anabaena* sp. (lanes 1, 3, 5, 8), mutant NMΔ–*alr2887* (lane 2, 4, 6, 9) and mutant DR181 (7, 10). Lipids were extracted from filaments grown in BG11 (lanes 1, 2), from the filaments 48 hours after the transfer to $BG11_0$ (lanes 3, 4), from isolated heterocysts (lanes 5, 6, 7) and from isolated heterocyst cell walls (lanes 8, 9, 10). Lipids of the cell wall fractions show a slightly altered migration behavior due to the edge effects of the TLC plate. The HGLs are indicated by arrows: grey for HGL1 and black for HGL2. In lanes 9 and 10 the area where HGL2 would be expected is also indicated.

Considering that the cell wall lipids are synthesized at the inner membrane (Doerrler, 2006), the reduction of the glycolipids could be interpreted as a defect in HGL synthesis or in HGL assembly into the heterocyst cell wall. To explore which of the two possible explanations is correct, heterocyst cell wall fractions were purified from heterocyst isolated from the wild type, NMΔ-*alr2887* and DR181 strains, followed by analysis of the lipid content of isolated cell walls. If the deletion mutants are defective in HGL synthesis, the amount of glycolipids detectable in heterocysts and cell walls should be comparable. In case of defect in HGL assembly into the heterocyst glycolipid layer, lipids might accumulate at the place of their synthesis, but not any longer in the cell wall. The analyses showed presence of a high amount of HGL1 and a lower amount of HGL2 in wild type cell wall isolations (Figure 18, lane 8), confirming once again co-isolation and connection between the glycolipid layer and the heterocyst outer membrane (see Figure 10, section 6.2.2.). On the other hand, both HGLs were drastically reduced in lipid extracts from NMΔ-*alr2887* and DR181 cell wall preparations, with HGL2 spot being hardly detectable (Figure 18, lanes 9, 10). It can be concluded that the heterocyst specific glycolipids are still synthesized in deletion strains NMΔ-*alr2887* and DR181, although

they do not assemble into the heterocyst glycolipid layer. Therefore, Alr2887 is involved either in the transport of HGLs to the place of their assembly into the gliycolipid layer or in the transport of proteins / enzymes involved in glycolipid layer formation to the place of their action.

Alr2887 protein seems to participate in the formation of the heterocyst glycolipid layer of *Anabaena* sp. (Figures 17, 18). Since Alr2887 is an outer membrane β-barrel to exclude that the obtained phenotypes are consequence of the influence of the Alr2887 absence on the integritiy or assembly of the outer membrane, the effect of *alr2887* deletion on the general uptake capability of *Anabaena* sp. was tested. In co-operation with laboratory of Dr. Enrique Flores, the transport assays (Picossi *et al.*, 2005) of ^{14}C-radioactively labeled arginine, phenylalanine, glutamine, aspartic acid or glutamic acid were performed on NMΔ-*alr2887* and wild type strains. In this way general uptake capability of the NMΔ-*alr2887* strain was examined through the possible effect of Alr2887 absence on the common membrane amino acid transporters. Wild type and deletion mutant cultures were incubated with ^{14}C-labeled amino acid, washed and retention of radioactivity was measured with β−scintilator (see "Methods", section 5.4.12.). However, significant alterations in the uptake of tested amino acids between the NMΔ-*alr2887* strain and wild type strain could not be detected (Table 11). This finding confirms once again direct influence of Alr2887 on glycolipid layer formation, rather than its influence on general biogenesis of the outer membrane.

Table 11. The transport activity of 10 μM of L-[U-^{14}C]-labeled amino acids of the deletion mutant NMΔ-*alr2887* in comparison to wild type (WT), expressed in nmol/mg Chla in 10 min. Listed are results of two independent experiments (lower part of the cell) and middle value for both experiments (upper part of the cell). Arginine, phenylalanine, glutamine, aspartic acid or glutamic acid were tested in experiment.

Strain	Transport activity (nmol/mg Chla in 10 min)				
	L-Arg 10 μM	L-Asp 10 μM	L-Gln 10 μM	L-Glu 10 μM	L-Phe 10 μM
WT	79.91	30.01	108.73	18.21	133.84
	90.39/69.42	29.40/30.61	72.74/114.71	9.74/26,68	85.85/118.82
NMΔ-*alr2887*	151.83	58.70	132.40	25.27	172.81
	159.03/144.62	51.06/66.34	120.69/144.11	20.58/30.56	155.91/189.172

6.3.7 Alr0267 and All2736 are potential substrates for Alr2887 protein

Previously preformed homology search (Maldener *et al*., 2003), the PHYRE server predictions and protein modeling (Oliver Mirus, personal communication) define Alr2887 as *Anabaena* sp. TolC homologue. Presented experimental data support this notion. Since TolC-like proteins are known to be involved in secretion of substrates from Gram-negative cells into the surrounding medium, possibility that the composition of secreted proteins between wild type and NMΔ-*alr2887* mutant differs was explored. Wild type and NMΔ-*alr2887* cultures were grown in the presence of bound nitrogen in BG11 medium, washed three times with $BG11_0$ medium and transferred to the fresh $BG11_0$ to grow further without the source of combined nitrogen. Every three hours filaments were collected and transferred to the fresh $BG11_0$, while the proteins from the previous medium were precipitated and subjected to SDS-PAGE analyses (see "Methods", section 5.4.15.). Indeed, in the protein collection precipitated from the growth media two bands were clearly absent from the NMΔ-*alr2887* growth medium in comparison to the wild type growth medium in all samples (Figure 19, lanes 1, 3). In the growth medium 9 hours after nitrogen step-down one more band of difference appeared (Figure 19, lane 1, red circle).

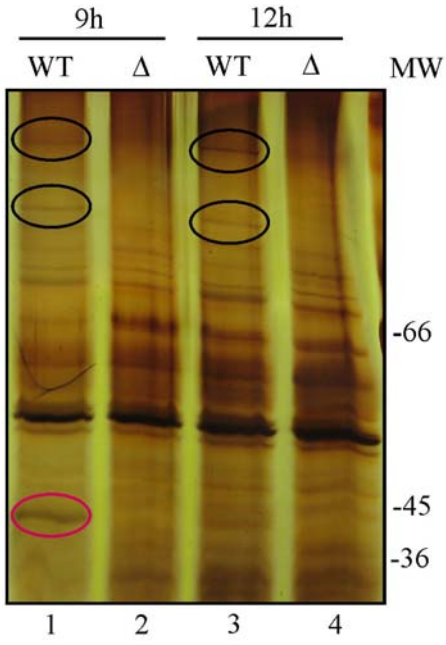

Figure 19. Proteins precipitated from the growth medium of the wild type filaments (WT, lanes 1, 3) and NMΔ-*alr2887* filaments (Δ, lanes 2, 4) 9h and 12h after the nitrogen step-down. Circled are the bands appearing in the wild type but not in the NMΔ-*alr2887* growth medium. Red circled is the band where Alr0267 peptides were found.

All three bands were excised from the gel and analyzed by sequencing. In the most prominent band from the 9-hour fraction Alr0267 protein was identified, annotated as unknown in CyanoBase. According to the PHYRE server prediction this protein corresponds to a 7-bladed β-propeller domain of an N-terminal part of α-integrin and, as

such, is much smaller than α-integrin. Characteristic of the 7-bladed β-propeller is that it forms a micro-surrounding for enzymatic reactions and, as especially interesting, β-propeller domains are found in some enzymes like lipases. TMHMM prediction showed absence of the transmembrane α-helices. SignalP 3.0 predicted existence of a signal peptide with a cleavage site between amino acids 29-30, SSA-YV, while LipoP 1.0 predicted no signal peptide.

However, one more possible substrate of Alr2887 appeared already before during analysis of the outer membrane complexes when small 19 kDa protein All2736 was co-isolated with Alr2887 complex (see Figure 7, Table 8). According to PHYRE server this protein is similar to the plant lipid transfer proteins (LTP, Charvolin *et al.*, 1999). Proteins of this group have eight conserved cystein residues that form disulfide bridges, and contain also α-helices and a signal peptide (Carvalho and Gomes, 2007). In All2736 nine α-helices appear and each of them contains in the center of the primary structure one cystein, as LTP, except for the most N-terminal helix where TMHMM server predicts transmembrane α-helical segment. SignalP and LipoP programs predict existence of a signal peptide with a cleavage site between amino acids 22 and 23 (SVA-VT). PSORTb prediction of protein localization gave no result. All2736 is not identified in the outer membrane fraction and it is easy to imagine it as Alr2887 / TolC substrate caught inside of the long channel-tunnel at the moment of its translocation. Nevertheless, All2736 was not found in the pool of secreted proteins (Figure 19) and, for now, no further experimental data confirm its connection with Alr2887.

6.4. All4026 and Alr0397 – constitutively expressed iron transporters of *Anabaena* sp. PCC 7120

Among 55 proteins identified in the outer membrane proteome of *Anabaena* sp., even five proteins are candidates for the putative TonB dependent receptors (Tables 5-7). Because of strong dependence of the Gram-negative cell on the redox processes mediated by iron-containing enzymes, TonB-dependent iron transport systems are highly diverse and belong to the most tightly regulated protein systems in the membranes of Gram-negative bacteria (see "Introduction"). Yet, until now iron regulation has been poorly described in cyanobacteria and even less in their multicellular representatives such as *Anabaena* sp. Performed phylogenetic analysis reveals a surprisingly large family of iron-transporters appearing in *Anabaena* sp. As the first step toward elucidating the basis of a huge variety of iron-regulating system in this cyanobacterium, the two out of five constitutively present iron transporters, All4026 and Alr0397, were explored closer.

6.4.1 Phylogenetic analysis of the protein family of TonB-dependent transporters

TonB-dependent transporters (TBDT) are known to appear in the Gram-negative outer membrane when bacterial cells are starved for iron (see "Introduction", Figures 3, 4; Braun *et al.*, 2003). It is interesting, therefore, that the outer membrane preparations, in which five putative TBDT were detected, were prepared from the filaments grown in the standard BG11 medium where iron starvation should not appear. This raised a question about the other potential TBDT-family members in *Anabaena* sp. PCC 7120. The subsequent BLAST analyses revealed coding sequences for altogether 24 iron-transporting outer membrane proteins in *Anabaena* sp. genome as follows:

1) Indentified in the proteome of the outer membrane: *all4026*, *alr0397*, *all3310*, *alr2588* and *all1101* (Tables 5-7).

2) Other putative TBDT: *alr2153*, *alr3242*, *all2578*, *alr2179*, *all2148*, *alr2596*, *alr2211*, *all2236*, *alr2175*, *all2158*, *all4924*, *all2674*, *alr2592*, *alr2626*, *all2610*, *alr2185*, *alr2581*, *all2620*, *alr2209.*

On the other hand, extensive BLAST search could not identify more than four outer membrane iron transporters in *Synechocystis* sp. PCC 6803, in line with the report of Katoh *et al.* (2001). Also, in the classical Gram-negative bacterium *Escherichia coli* not more than six TonB-dependent transporters have been described (Buchanan, 2005). In order to

understand the occurrence of such a large TBDT family in *Anabaena* sp., phylogenetic analysis was performed (Figure 20, in co-operation with Oliver Mirus; Vinh and von Haeseler, 2004; Mink *et al*., 2005), using all known and annotated iron transporter families (selected according to Cope *et al*., 1995; LeVier and Guerinot, 1996; Ochsner *et al.*, 2000; Clarke *et al.*, 2001; Pradel and Locht, 2001; Mey and Payne, 2001; Cornelis and Matthijs, 2002*;* Mey *et al*., 2002*;* Mazo*y et al*., 2003; Srikumar *et al.*, 2004; Furano *et al*., 2005, Mourino *et al*., 2005).

The obtained phylogenetic clustering resembles earlier existing classifications (Figure 20). In comparison to the phylogeny reported by Bäumler and Hantke (1992), Koebnik *et al.* (1993) or Rakin *et al.* (1994), the IutA sequences (hydroxamate aerobactin transporter) do not cluster directly together with FecA (ferric citrate transporter) or FyuA (catecholate yersiniabactin transporter) sequences. Instead they form a separate branch slightly more distant from the FecA clade than from the BtuB (vitamin B12 / colicin transporter) and FepA (catecholate enterobactin transporter) clade. A similar result was obtained by LeVier and Guerinot (1996). The hydroxamate transporter class branches as previously reported by LeVier and Guerinot (1996), although in contrast to their phylogeny ViuA (vibriobactin transporter) clearly clusters with FyuA (yersiniabactin transporter) sequences and the lactoferrin / transferring - specific transporters are differently positioned (Figure 20). The discrepancy to the previous reports might result from simultaneous analyses of all annotated iron transporters, including the cyanobacterial sequences, and from improved capacity for such analysis. The only uncertainty in this phylogeny (Figure 20) is the positioning of the BfrA iron receptors of *Bordatella* sp. They are found in a clade with catecholate recognising transporters as well as in a clade with vitamin B_{12} / colicin receptors (Kadner, 1990).

All 24 identified proteins with putative iron transporting function encoded by the genome of *Anabaena* sp. PCC 7120 were included in this phylogeny. A result revealed their distribution in five classes (Figure 20). The first class comprises four sequences, with one of them being Alr0397 protein identified in the outer membrane of iron-replete cultures (Tables 5-7). These four sequences cluster within the phylogenetic clade of transporters specific for the hydroxamate-type citrate-based siderophores, such as the aerobactin transporter IutA (Martinez *et al*., 1994). The only known endogenous siderophore of *Anabaena* sp., schizokinen, is also a citrate-based hydroxamate (Lammers and Sander-Loehr, 1982). For this reason one or more transporters from this clade are candidates for the schizokinen transporter/s in this cyanobacterium.

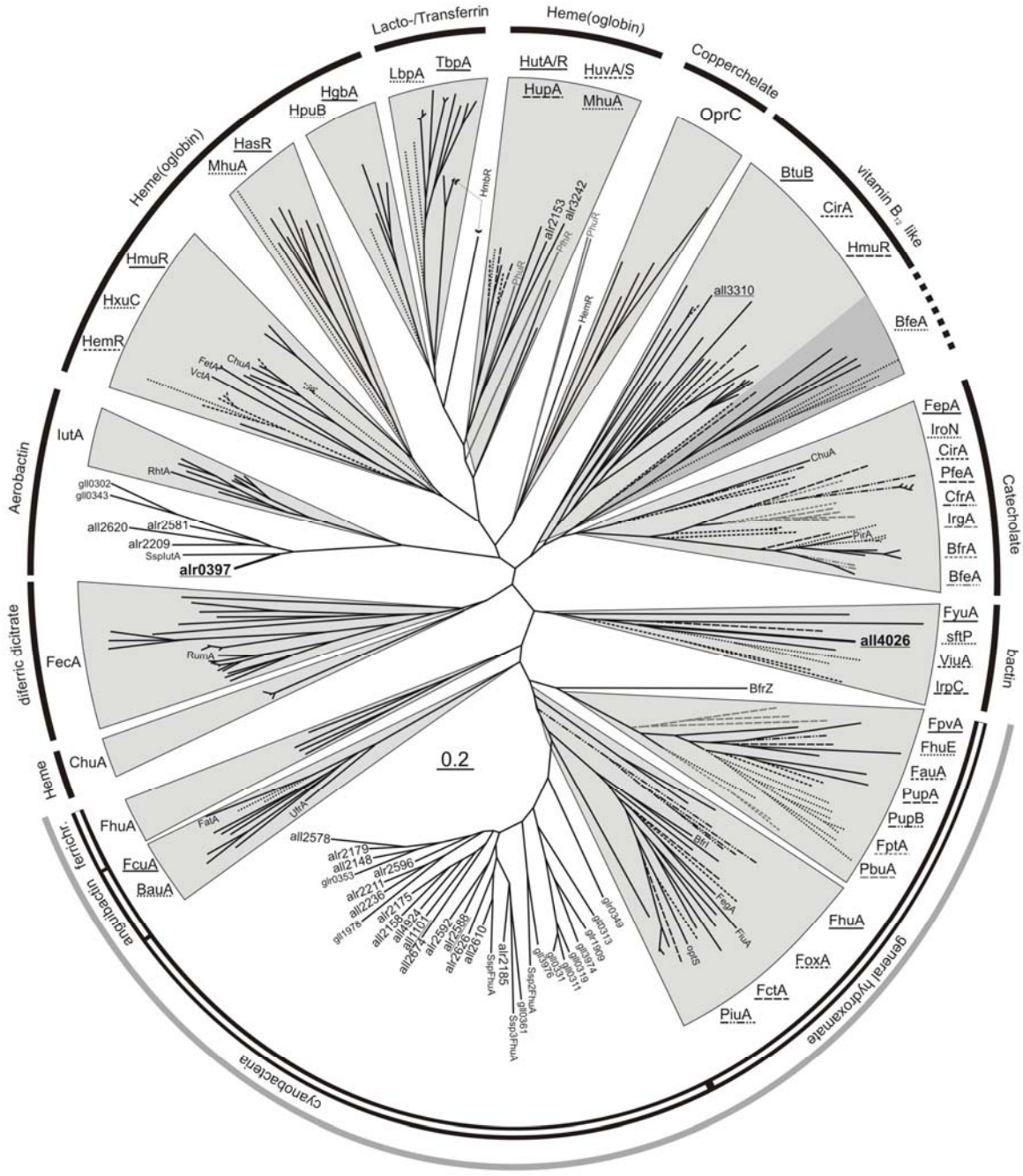

Figure 20. Phylogenetic distribution of the family of 24 predicted iron transporters in *Anabaena* sp. PCC 7120. The phylogenetic tree of 62 annotated classes of bacterial iron transporting TonB-dependent outer membrane proteins is shown. On the outer circle the substrate of the major protein class of each clade is given according to Rakin *et al.* (1994). Separate clades are indicated by a grey background. The names of the protein classes belonging to each clade are indicated on the inner circle and the line under each class name corresponds to the line style of the branches within each clad. If only one sequence of a protein class appears in one clad, the class name is directly indicated on the branch inside of the grey clade area. For *Anabaena* sp. PCC 7120 (all and alr), *Synechocystsis* sp. PCC 6803 (Ssp) and *Gloeobacter violaceus* PCC 7421 (gll and glr) the appearance of each sequence is indicated. Underlined *Anabaena* sp. protein annotation names stand for iron transporters previously identified in the proteomic analysis of the outer membrane of vegetative cells under iron-replete conditions (Tables 5-7).

Even sixteen putative iron transporters of *Anabaena* sp. belong to the second class and are all found within the clade of the hydroxamate-type siderophores which are not citrate-based (e.g. ferrichrome transporter FhuA; Figure 20, the bottom of the tree). The two among five constitutively present transporters detected in the outer membrane proteome belong here (Figure 20, Tables 5-7). The third class has only one putative iron transporter and that is All4026 protein identified in the outer membrane proteome (Tables 5-7). All4026 cluster with the clade of the catecholate-specific transporters similar to yersiniabactin transporter FyuA (Perry *et al*., 1999) and vibriobactin transporter ViuA (Keating *et al*., 2000). Based on this *Anabaena* sp. has, surprisingly, only one putative catecholate transporter among 24 proteins. Also the forth group comprises just one TBDT (All3310) found within the clade of vitamin B_{12} / colicine like transporters (Wandersman and Delepelaire, 2004). This protein was identified as constitutively present while analysing the outer membrane proteome of the vegetative cell too (Tables 5-7). The fifth class contains the two iron transporters of *Anabaena* sp. similar to the heme / hemoglobin specific TBDT (Figure 20; Wandersman and Delepelaire, 2004). According to the phylogeny of the three last sequences from the forth and the fifth class, their substrate specificity toward iron sources is different in comparison to the siderophore transporters.

6.4.2 Alr0397 and All4026 are constitutively expressed iron transporters

The mechanism of iron transport in *Anabaena* sp. is poorly understood. In order to gain the insight into the regulation of *Anabaena* sp. iron homeostasis, two putative iron transporters, All4026 and Alr0397, were investigated closer. The protein modelling of both proteins confirmed a classical three-dimensional structure of TonB-dependent transporters (Oliver Mirus, personal communication; see “Introduction). Both proteins were detected in the proteome of the outer membrane under iron-replete conditions (Tables 5-7). Alr0397 is the only constitutively expressed putative TBDT being at the same time also a candidate for the *Anabaena* sp. schizokinen transporter (Figure 20; Tables 5-7). On the other hand, All4026 protein is the only potential catecholate transporter of *Anabaena* sp. (Figure 20, Tables 5-7).

To confirm the expression of *all4026* and *alr0397* genes under non-iron limiting conditions, 800 bp upstream from the starting codons of *all4026* or *alr0397*, corresponding to the promoter regions of these genes, were cloned in front of the *gfp* gene.

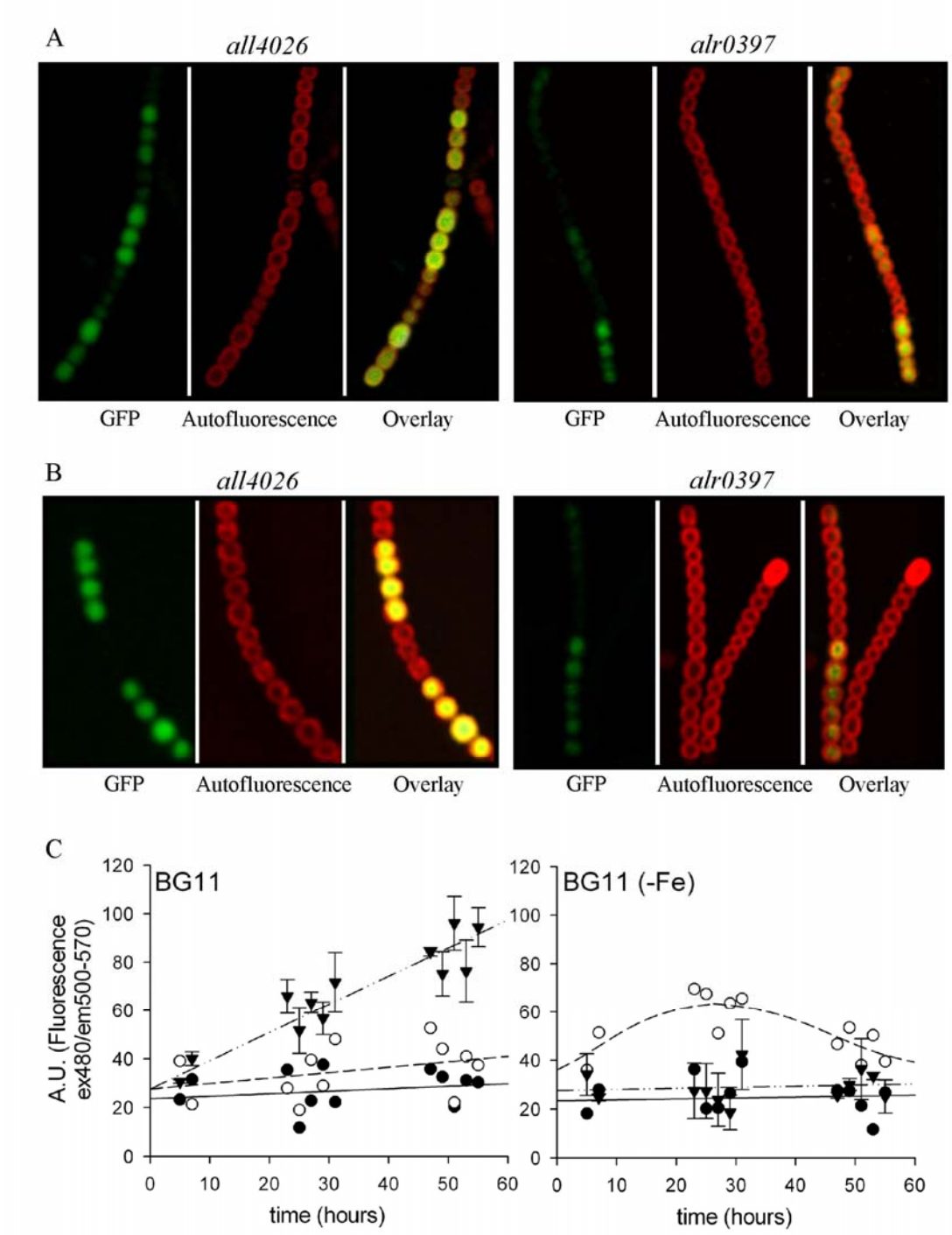

Figure 21. The distribution of *all4026* and *alr0397* expression. Shown are chlorophyll autofluorescence, GFP fluorescence, overlay and GFP signal of NME-*all4026*-GFP (left) and NME-*alr0397*-GFP (right) mutant strains grown under (A) iron replete and (B) iron depleted conditions. (C) The fluorescence of the NME-*all4026*-GFP (triangle), NME-*alr0397*-GFP (open circle) and NME-*alr2887*-GFP strain (closed circle, control strain, see also Figure 12) measured by luminescence spectrometer are presented as the difference to the background of the wild type and for the indicated times before (C) and after (D) the transfer to the iron depleted medium. The errors bars are indicated for *alr4026* gene as example. All GFP strains show basal level of promoter activity.

These constructs were used to generate *Anabaena* sp. promoter-GFP fusion strains NME-*alr0397*-GFP and NME-*all4026*-GFP (see "Methods", section 5.1.3.4.). The obtained GFP mutants were analyzed with Leica confocal microscope. The GFP signal was obtained from both GFP mutants already in the filaments of *Anabaena* sp. grown under normal conditions, where neither iron nor nitrogen source were limited (Figure 21A). It is interesting that the fluorescence was not uniformly distributed along the filaments. Instead the GFP expression from *all4026* and *alr0397* promoters was localized in stretches of about four to eight cells appearing along the filaments (Figure 21A). When exposed to iron limitation, mutant filaments showed again discontinuous pattern similar to the one obtained from the filaments grown in the presence of an iron source (Figure 21B).

Furthermore, under these conditions GFP signal was not obtained in each filament (Figure 21B, Alr0397). When GFP fluorescence was monitored spectroscopically in logarithmic cultures over time period of three days, filaments showed the basal level of expression under normal growth conditions (Figure 21C, left). The expression of *all4026* appears to be slightly enhanced over time period when compared to the *alr2887* expression, whose promoter-GFP fusion strain was used as a control (Figure 21C). The expression from *alr0397* promoter was not affected by time. After the filaments had been shifted to the iron-limited medium, the expression of *alr0397* slightly increased during 30 hours to finally return back to the basal level after two days (Figure 21C, right). In contrast to the observation in normal medium, the expression from *all4026* promoter remained constant (Figure 21C, right). This shows that a significant induction of expression above basal level was not obtained under iron limiting conditions in case of both genes. That parallels constitutive and not by iron limitation induced presence of their protein products (Tables 5-7)**.**

6.4.3 Alr0397 and All4026 are integral outer membrane proteins uniformly distributed in the outer membrane

According to the data obtained by analysing the outer membrane proteome of *Anabaena* sp. and to homology to TonB-dependent iron transporters, All4026 and Alr0397 are in the outer membrane localized proteins. Still the question of their distribution along the filament remained. For this reason the protein localization was further analyzed in *Anabaena* sp. mutant strains NMP-*all4026*-GFP and NMP-*alr0397*-GFP (see "Methods", section 5.1.3.3.) in which GFP was fused to the C-terminus of All4026 and Alr0397

proteins, respectively. After 48 hours growth in the medium without combined nitrogen source, GFP fluorescence of both Alr0397-GFP and All4026-GFP protein fusions was detected with Leica confocal microscope in all cells of the filament, vegetative and heterocysts (Figure 22A). The intensity of the GFP signal was the strongest at the very border of each cell, shaping distinctive ring-like structures (Figure 22A, B, enlarged figures), as expected for the membrane localized proteins. Moreover, the fluorescence was uniformly distributed along the membranes of the entire filament and not just in clusters of four to eight cells (Figures 21, 22). The discrepancy in the pattern of the GFP signal in promoter-GFP and protein-GFP fusions demonstrates difference in the protein distribution and the corresponding gene expression along the filament. The GFP signals also indicate different properties of the continuous periplasmic space of *Anabaena* sp. that allow proper folding of at least part of GFP molecules, in comparison to the periplasmic properties of the unicellular Gram-negative bacteria and cyanobacteria (see "Discussion").

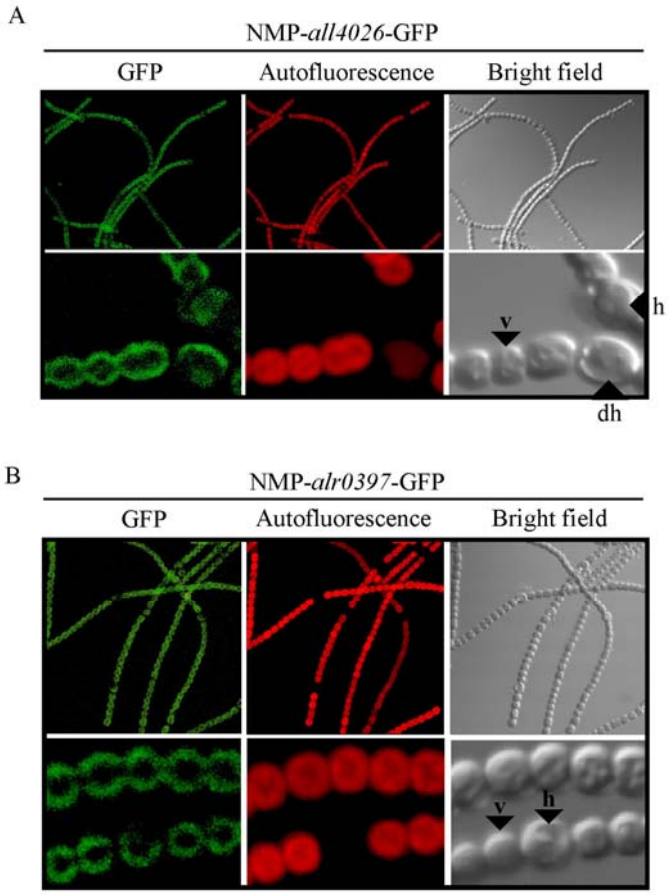

Figure 22. NMP-*all4026*-GFP (A) and NMP-*alr0397*-GFP (B) mutants expressing C-terminal GFP protein fusions were grown 48 hours without combined nitrogen source. The clear ring-like GFP signal allows localization of both proteins to the cell membrane and demonstrated protein presence their presence all through the filament in vegetative cells (v) and in heterocysts (h) and for All4026 also in developing heterocysts (dh).

The fluorescent signals from GFP-protein fusions correspond to the membrane localization of All4026 and Alr0397. To prove the localization of these proteins in the outer membrane, the outer membrane fractions isolated from both GFP-protein fusion mutants were treated with urea (Figure 23, lanes 2, 6), sodium carbonate (Figure 23, lanes 3, 7) or sodium chloride (Figure 23, lanes 4, 8) and immunodecorated with GFP antibody. The ramining protein after the urea/salt treatments show the presence of the GFP-protein fusion in the outer membrane and confirm that both, All4026 and Alr0397, are indeed integral outer membrane proteins, as proposed from their homology to TonB-dependent transporters. The GFP antibody did not cross-react with the wild type outer membranes (not shown).

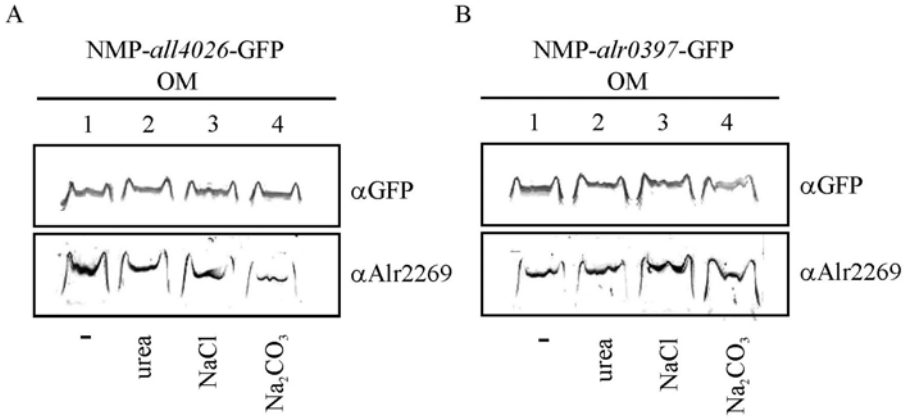

Figure 23. Isolated outer membrane fractions from vegetative cells of NMP-*all4026*-GFP (A) and NMP-*alr0397*-GFP (B) were treated with 8 M urea (lane 2), 1 M sodium chloride (lane 4) or 0.1 M sodium carbonate (lane 3). Lane 1 shows an untreated control. The pelleted membrane fraction (P) and the supernatant (not shown) were probed with antibodies against GFP (αGFP) or integral outer membrane protein Alr2269 (αAlr2269) as a control. No bands were detected after the wild type outer membrane was incubated with the GFP antibody (not shown).

6.4.4 All4026 and Alr0397 protein functions are nonessential

After the expression and the protein localization analyses had been completed (Figures 22, 23) investigations of the functional properties of All4026 and Alr0397 putative iron transporters followed (Figure 24). *alr0379* is a single-standing gene not included in any operon structures. On the other hand, downstream from *all4026* three genes are present whose expression might be controlled by the same promoter as *all4026*. However, repeated attempts to analyse the possible operon structure of this region by RT-PCR analysis failed. The reason was the resistance of this chromosomal region to repeated DNase I treatments during RNA isolation. This resulted in contaminations of RNA isolates with genomic DNA containing this region. *all4025* gene encodes an inner membrane

localized AmpG signal transducer, involved in the regulation of β-lactamase expression (e.g. Lindquist *et al*., 1993; Park, 1995; Dietz *et al*., 1997). The other two genes, *all4024* and *all4023*, encode subunits of the cytochrome D ubiquinol oxidase, a complex unessential for the growth under aerobic conditions (Rice and Hempfling, 1978; Cotter *et al*., 1997) and expressed under oxygen limitation (Cotter *et al.*, 1997). Homologues of not even one of these three genes appear in the operon structure with iron transporter genes in other cyanobacteria such as *Thermosynechococcus elongatus* BP-1 (*tlr0738*, *tll1602* and *tll1601*), *Gloeobacter violaceus* PCC 7421 (*gll1668, gll1196* and *gll1197*) or *Synechocystis* sp. PCC 6803 (*sll1154, slr1379* and *slr1380*). According to this no operon organization would be expected in *Anabaena* sp. as well. Since *all4024* and *all4023* should be up-regulated when cells are exposed to oxygen limitation, GFP signal in GFP-promoter fusions was monitored over time period of 24 hours in the non-shaken cultures (see "Methods", section 5.4.13.). If *all4026* and these two genes are co-expressed from the same promoter, effect of the lack of oxygen should be noticed on the *all4026* promoter activity and GFP fluorescence should increase. However, such effect was not detectable, indicating that these genes are probably not in the operon with *all4026*. Further tests are necessary to confirm this observation.

Two approaches were applied to analyze the function of the All4026 and Alr0397 iron transporters. First, the pCSV3 plasmid was inserted by single homologues recombination into *Anabaena* sp. chromosome at the center of *all4026* or *alr0397* coding sequences (see "Methods", section 5.1.3.1.) and the deletion strains NMΔ-*alr0397* and NMΔ-*all4026* were generated (Figure 24C, D). The Southern blotting confirmed full chromosomal segregation in the case of both deletion mutants showing that the functions of these genes are not essential for *Anabaena* sp. survival (Figure 24A). Both deletion strains grew normally on the medium without combined nitrogen (Figure 24B), indicating that the absence of the All4026 and Alr0397 iron transporters does not effect heterocyst development and function. When grown on the plates (Figure 24E) and in liquid medium (both BG11 and $BG11_0$) and analyzed under the microscope, mutant filaments showed no difference from the wild type filaments (not shown). This result is understandable considering that in each of the deletion mutants 23 more iron transporters exist next to the deleted transporter. Anyhow, since All4026 and Alr0397 are constitutively present in the outer membrane even when the filaments are not exposed to iron limitation, their possible influence on the phenotype undoubtedly had to be tested.

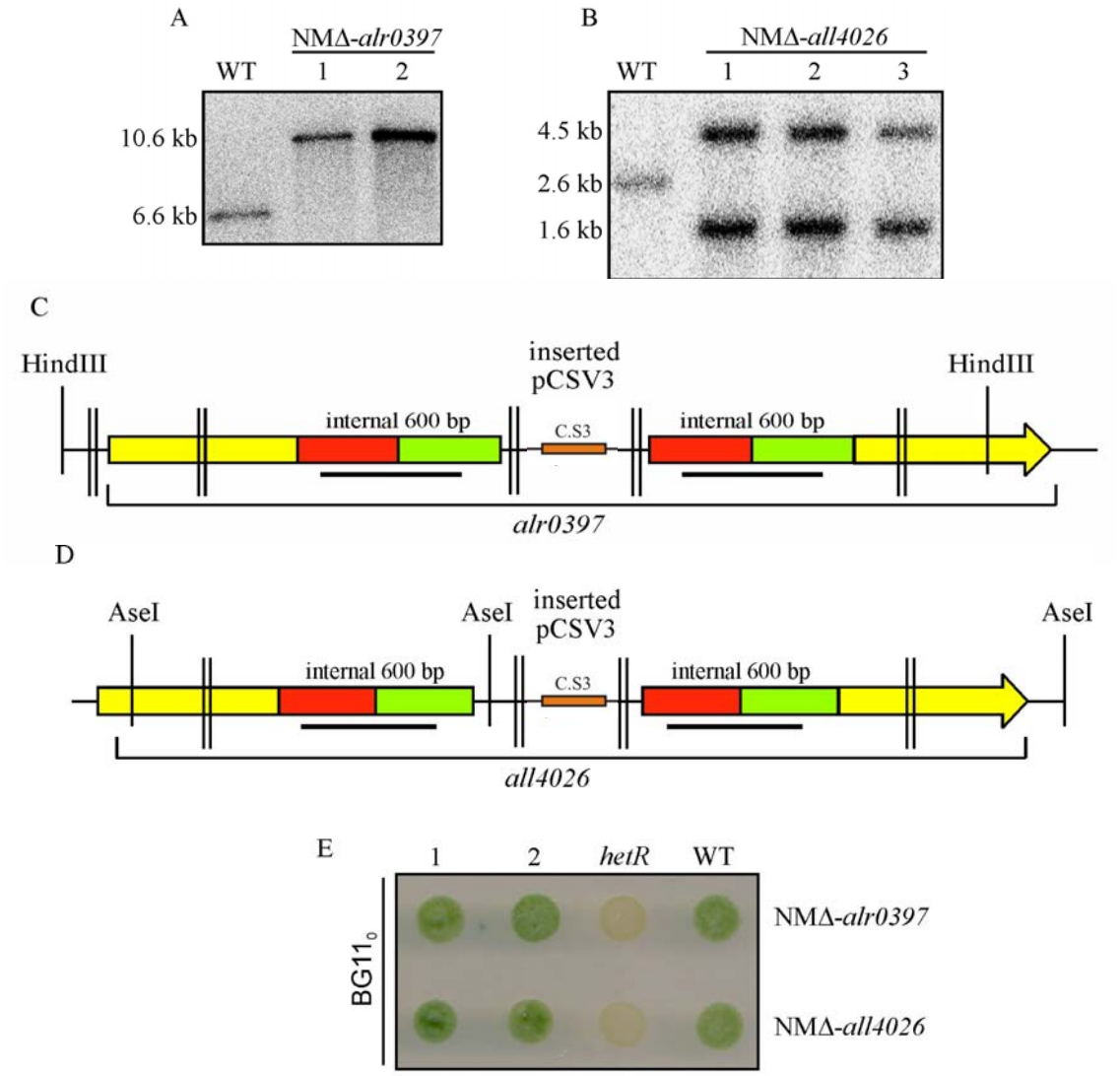

Figure 24. Southern blotting analysis of (A) two independent NMΔ-*alr0397* deletion mutants and (B) three independent NMΔ-*all4026* deletion mutants reveals absence of the wild type band in all mutants and full chromosomal segregation. Chromosomal structure of (C) NMΔ-*alr0397* and (D) NMΔ-*all4026* mutants is interrupted by insertion of the pCSV3 plasmid in the middle of the coding sequence. Single vertical lines show restriction sites and enzymes used to cut the genomic DNA, and fat horizontal bars under gene coding sequences correspond to the places of hybridization of the ^{35}P-labeled probes. (E) NMΔ-*alr0397* and NMΔ-*all4026* deletion mutants (1 and 2 as in figure (A)) show normal growth when placed on BG11$_0$ medium without bound nitrogen source. Wild type filaments and *hetR* (*fox*$^-$) mutant filaments of *Anabaena* sp. are used as controls.

Furthermore, similar as for Alr2887, since All4026 and Alr0397 are outer membrane β-barrels, amino acid uptake assays (see "Methods", section 5.4.12.; Picossi *et al.*, 2005) were performed to show that the deletion of *all4026* or *alr0397* genes had no significant effect on the outer membrane assembly and integrity. Affected membrane assembly could affect general cell uptake capacity, possibly reflecting in influence on the membrane amino acid transporters. However, the amino acid uptake capability of NMΔ-

alr0397 and NMΔ-*all4026* for tested amino acids did not show any alterations in respect to wild type (Table 12). It can be concluded that the deletions of the *all4026* and *alr0397* genes do not alter general biogenesis and functioning of the outer membrane (Table 12).

Table 12. Transport activity of 10 μM of L-[U-^{14}C]-labeled amino acids of the deletion mutants NMΔ-*alr0397* and NMΔ-*all4026* in comparison to the WT, expressed in nmol/mg Chla in 10 min. Shown are results of two independent experiments (lower part of the cell) and middle value for both experiments (upper part of the cell).

Strain	Transport activity (nmol/mg Chla in 10 min)				
	L-Arg 10 μM	L-Asp 10 μM	L-Gln 10 μM	L-Glu 10 μM	L-Phe 10 μM
WT	79.91	30.01	108.73	18.21	133.84
	90.39/69.42	29.40/30.61	72.74/114.71	9.74/26,68	85.85/118.82
NMΔ-*all4026*	130.19	75.77	125.27	25.71	147.21
	145.31/115.07	63.45/88.08	125.42/125.02	20.33/31.09	153.74/140.68
NMΔ-*alr0397*	103.91	52.59	121.41	20.60	147.92
	114.75/93.06	51.48/53.69	109.15/133.67	17.26/23.94	113.54/164.29

As deletion mutants did not show any evident phenotype, the single recombination mutants NMOX-*alr0397* and NMOX-*all4026* over-expressing *all4026* and *alr0397* genes strains were generated and confirmed by PCR (see "Methods", section 5.1.3.2.). In these mutants coding region of the gene, either *all4026* or *alr0397*, was placed under control of the strong *trc* promoter (Figure 25A). The ability of the mutant strains NMOX-*alr0397* and NMOX-*all4026* to grow on the medium with and without the source of combined nitrogen was investigated first. In contrast to the deletion strains enhanced expression of *all4026* resulted in *fox*$^-$ phenotype and the NMOX-*all4026* filaments turned yellow soon after spotting on BG11$_0$ (Figure 25B). On the other hand, filaments over-expressing *alr0397* gene were unaffected when grown without combined nitrogen (Figure 25B).

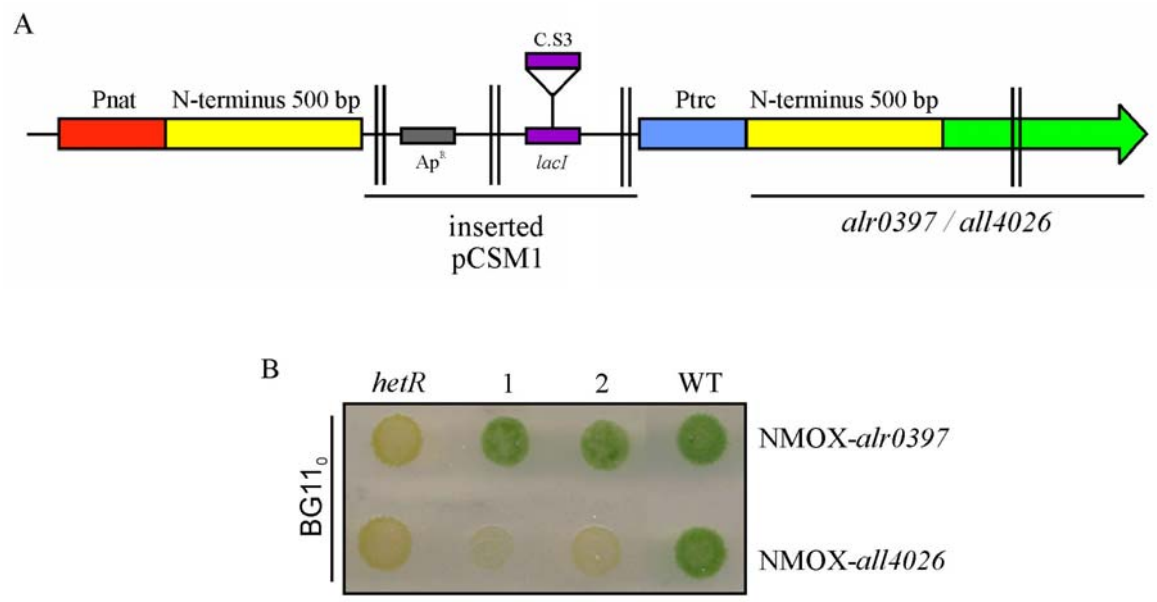

Figure 25. (A) Chromosomal structure of NMOX-*alr0397* or NMOX-*all4026* over-expression mutants with pSCM1 plasmid inserted in the chromosome, resulting in replacement of the native promoter (P_{nat}) with the strong artificial *trc* promoter (P_{trc}) in front of the coding sequence of *alr0397* or *all4026* gene. (B) Grown on the $BG11_0$ medium without bound nitrogen NMOX-*all4026* mutant shows *fox*$^-$ phenotype and deficient growth, while NMOX-*alr0397* mutant grows as wild type.

In addition, analyses of the lipid composition of both over-expression strains in comparison to wild type, in attempt to test the general status of the cells, revealed changes in the lipid pattern of NMOX-*all4026* when grown in the presence and absence of combined nitrogen source (Figure 26, arrows). NMOX-*alr0397* mutant had normal lipid pattern, although reduction in the heterocyst specific glycolipid (HGL1) was visible (Figure 26, green arrow). However, the filaments of both over-expression mutants had normal heterocysts of mature appearance whose polysaccharide layer was stained with Alcian Blue (not shown). Electron microscopy of both mutants further confirmed existence of the heterocysts glycolipid layer and the wild type morphology of the both cell types, vegetative cells and heterocysts (not shown). For this reason altered lipid pattern and *fox*$^-$ phenotype of the NMOX-*all4026* strain can be ascribed not to the heterocysts dysfunction, but to the general stressed condition of this mutant due to the changes in its metal content (see further).

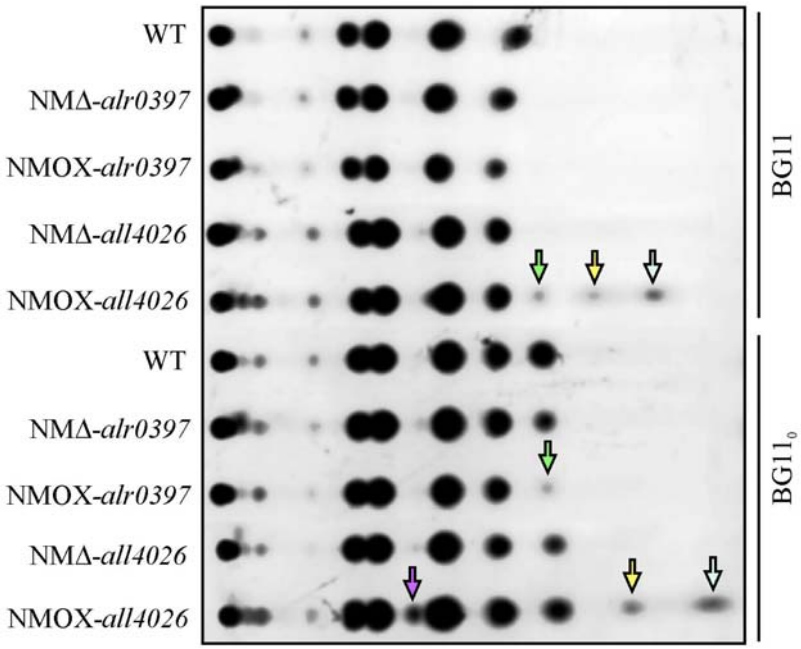

Figure 26. Shown is the lipid analysis of wild type (WT), the deletion and over-expression strains of *all4026* and *alr0397* NMOX-*alr0397* and NMOX-*all4026* grown in BG11 nitrogen-replete medium, and 48 hours in $BG11_0$ medium without combined nitrogen source. Alterations in intensity or pattern of lipid spots are denoted with arrows. Major changes in lipid spot pattern are visible in over-expression strains of *all4026* grown in both media. Without bound nitrogen in the growth medium *alr0397* over-expression strain shows reduction in intensity of the heterocysts specific glycolipid HGL1 spot (green arrow) in comparison to the wild type.

6.4.5 The deletion *all4026* mutant is resistant to intoxication with iron and copper

To confirm the function of All4026 and Alr0397 in iron transport across the outer membrane of *Anabaena* sp., growth of the deletion and the over-expression lines NMΔ-*alr0397*, NMΔ-*all4026*, NMOX-*alr0397* and NMOX-*all4026* was explored under variable iron conditions. If All4026 and Alr0397 are part of an iron transport pathway, alterations of their level in the outer membrane could affect metal sensitivity of the corresponding mutants. The wild type and the mutant filaments were spotted on BG11 plates with increasing iron concentrations in the absence or presence of the copper source in the medium. Copper forms complexes with siderophores (Clarke *et al.*, 1987). Under iron limitation endogenous *Anabaena* sp. siderophore schizokinen is secreted into the medium in big excess, binding not just iron but also other metals like copper. Since copper-schizokinen complexes are not imported into the cells, they accumulate in the medium (Ferreira and Straus, 1994). In this way siderophore secretion moderates copper toxicity, so iron starved cells usually can tolerate higher, already toxic levels of copper (Clarke *et al.*,

1987). However, it is not clear whether copper can enter *Anabaena* sp. cells when bound in complex with some other exogenous or endogenous siderophore. For this reason, copper effect was tested as well.

After two weeks of growth on standard BG11 medium, no significant difference between wild type and any of the four mutants was obtained (Figure 27, lanes 1, 2). On the medium with increasing iron concentrations, however, NMΔ-*all4026* deletion mutant was still growing on iron contraction of 0.1 μM $FeCl_3$ which was lethal for all other strains including the wild type strain (Figure 27, lanes 3-10). The deletion of *all4026* eliminates constitutively present pathway of iron entrance into the cell and thereby enables the cell to tolerate the level of iron normally toxic for wild type (Figure 27, lanes 5-6). The over-expression of *all4026* makes the filaments more sensitive to high iron level than the wild type, possibly by increasing the iron uptake and poisoning the cell (Figure 27, lanes 7-8). The same is the case for the *alr0397* over-expression. The fact that the deletion of *alr0397* gene does not produce the same "resistance" effect can result from different siderophore specificity and affinity toward substrates of these two iron transporters. This is in line with their phylogenetic clustering ascribing Alr0397 to the iron transporters specific for hydroxamate type citrate-based siderophores and All4026 to the catecholate specific siderophores.

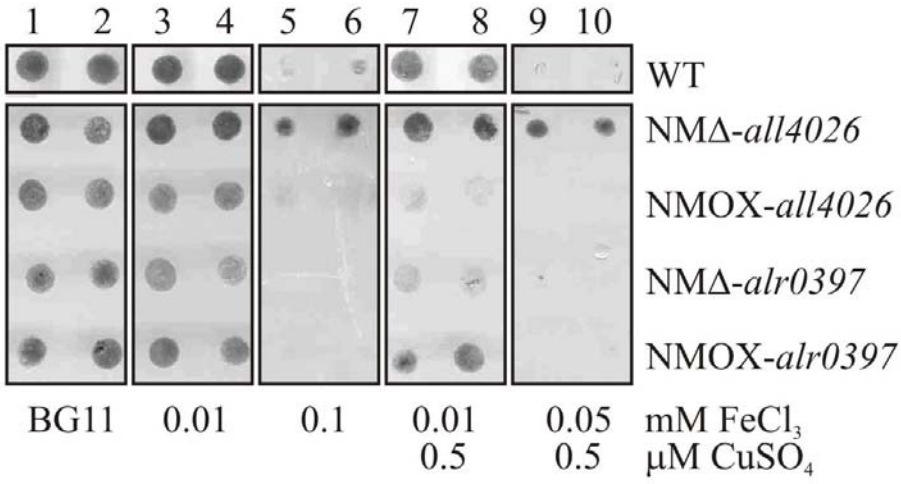

Figure 27. Change in intracellular Alr0397 or All4026 protein level alters the sensitivity of *Anabaena* sp. to intoxication by high metal content. Wild type (WT) and four mutant lines were spotted on BG11 agar plates (lanes 1, 2) or $BG11_{-Fe-Cu}$ agar plates supplemented with 0.01 mM $FeCl_3$ (lanes 3, 4), 0.1 mM $FeCl_3$ (lane 5, 6), 0.01 mM $FeCl_3$ and 0.5 μM $CuSO_4$ (lanes 7, 8), or 0.05 mM $FeCl_3$ and 0.5 μM $CuSO_4$ (lanes 9, 10). Plates were incubated for two weeks under standard conditions. NMΔ-*all4026* strain shows higher tolerance to high iron and iron/copper level than other strains (lane 5-10), while NMOX-*all4026* and NMΔ-*alr0397* are more sensitive in the presence of iron/copper in the medium than wild type (lane 7, 8). NMOX-alr0397 is more resistant than deletion mutant of the same gene (lanes 7, 8). Copper presence increases sensitivity of all mutants and WT except of the NMΔ-*all4026* mutant strain (lanes 7-10).

Moreover, copper presence in the medium increases the metal sensitivity of all mutant filaments and wild type but not of NMΔ-*all4026* (Figure 27, lanes 7-10). In the presence of copper *all4026* and *alr0397* mutants behave opposite: while NMΔ-*all4026* and NMOX-*alr0397* grow better, NMOX-*all4026* and NMΔ-*alr0397* exhibit weaker growth (Figure 27, lanes 7, 8). This can mean that All4026 is a less specific transporter than Alr0397 and that, in contrast to Alr0397, it also mediates copper transport. Therefore, its deletion results in resistance of the mutant on the overload with metals when grown on high metal concentrations.

6.4.6 The deletion of *all4026* or *alr0397* gene results in intracellular iron starvation under iron-replete conditions

To investigate whether the altered protein level of All4026 and Alr0397 causes alterations in iron uptake of the *Anabaena* sp. filaments, the expression of *isiA* gene was analyzed (see "Methods", section 5.1.4.). *isiA* gene encodes a chlorophyll a binding protein that is synthesised when cells are exposed to iron depletion. It serves as a chlorophyll storage protein or an excitation energy quencher, which protects photosystem I and II (PSI and PSII) under unfavourable environmental conditions (Liu *et al.,* 2005; Ivanov *et al.*, 2006). For this reason *isiA* expression is used as an indicator for iron starvation in cyanobacteria (Laudenbach and Straus, 1988; Falk *et al*., 1995; Michel and Pistorius, 2004; Latifi *et al.*, 2005). The expression of *rnpB* gene, encoding an RNA portion of ribonuclease P (Latifi *et al.*, 2005), was used as the RNA quality control.

As expected, in the wild type *Anabaena* sp. *isiA* expression was induced after four days of growth in iron depleted medium (Figure 28, lanes 1, 2, middle and lower panel). That proves that the applied growth conditions are indeed sufficient to induce an iron starvation in the *Anabaena* sp. filaments. On the other hand, *isiA* expression was not observed in the wild type cultures grown under standard iron/copper conditions (Figure 28, lanes 1, 2, upper panel). In the normal medium, however, a weak *isiA* expression was detected in both deletion strains, indicating that the absence of All4026 or Alr0397 iron transporters causes signs of iron starvation. Obviously these proteins are part of functional constitutive iron uptake pathway in *Anabaena* sp. For this reason their deletion is enough to influence the cell iron status even when external iron source is present in the medium (Figure 28). When both iron and copper sources were limited in the growth medium, *isiA* gene was expressed in all strains (Figure 28, lower panel), as expected. In the medium

without iron but with copper source, the *isiA* mRNA level was best visible in the over-expression strain NMOX-*alr0397* among the mutants tested (Figure 28, lines 9, 10, middle panel). Interesting, the *isiA* expression was also clearer in iron and copper depleted cultures, than in just iron depleted cultures.

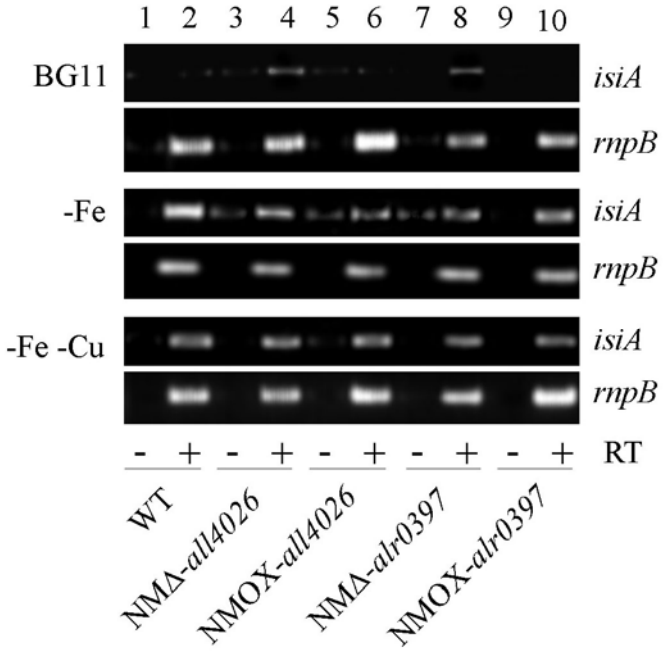

Figure 28. RT-PCR analyses of expression of *isiA* gene in the wild type (lanes 1, 2), NMΔ-*all4026* (lanes 3, 4), NMOX-*all4026* (lanes 5, 6), NMΔ-*alr0397* (lanes 7, 8) or NMOX-*alr0397* (lanes 9, 10) strains grown four days in BG11 without addition of iron source (no $FeCl_3$, -Fe) or without addition of iron and copper source (as $FeCl_3$ and $CuSO_4$;-Fe-Cu). Each reaction was performed in the absence (-RT) or presence (+RT) of reverse transcriptase (RT). Difference in intensity of bands obtained in +RT and –RT reaction means positive result. *rnpB* gene expression was used as RNA quality control. The low level of *isiA* expression is present in both deletion strains under normal growth conditions, the strong expression in all strains is obtained in –Fe-Cu medium, while the level of expression in –Fe medium is the highest in WT and NMOX-*alr0397* strains and lower in others.

The observed signs of iron starvation in two deletion strains were further confirmed by the measurements of the chlorophyll a fluorescence (Figure 29) of the wild type, the deletion and the over-expression strains, utilizing pulse amplitude technique (PAM; see "Methods", section 5.4.14.). As previously described for *Synechococcus* sp. (Ivanov *et al.*, 2006), the quenching of the PSII releases upon activation with actinic white light. That is why the maximum PSII fluorescence in the light adapted state (Fm') increases compared to the maximum PSII fluorescence in the dark adapted state (Fm) (Figure 29, black circle; Falk *et al.*, 1995; Ivanov *et al.*, 2006). On the contrary, cells exposed to iron starvation exhibit only minor state transition changes of Fm' relative to Fm. When the chlorophyll a

fluorescence of the two over-expression strains NMOX-*all4026* and NMOX-*alr0397* grown in normal medium was measured, the wild type behaviour for both strains was obtained (Figure 29, black square and diamond). On the other hand, the deletion mutant NMΔ-*alr0397* in the normal medium showed the same behaviour of the chlorophyll fluorescence as an iron starved wild type grown without an iron source (Figure 29, open diamond). The Fm' to Fm ratio of the chlorophyll fluorescence in the deletion NMΔ-*all4026* strain under iron-replete conditions was only reduced compared to wild type (Figure 29, white square).

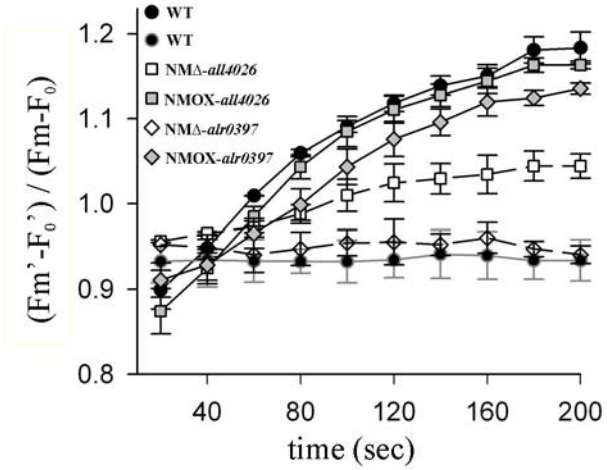

Figure 29. Average values of three independent measurements of the chlorophyll fluorescence of the wild type (black circle), the deletion NMΔ-*all4026* and NMΔ-*alr0397* strains (white square and diamond) and the over-expression NMOX-*all4026* and NMOX-*alr0397* strains (gray square and diamond) grown under normal iron conditions. For comparison the fluorescence of wild type *Anabaena* sp. (black circle with gray frame), grown four days under iron-depletion in the medium without iron/copper source, was determined as described (Ivanov *et al*., 2006). The ratio between maximum PSII fluorescence in the light adapted state (Fm'-F_0') and maximum PSII fluorescence in the dark adapted state (Fm-F_0) is expressed in dependence of the light pulse duration (measured by PAM instrument). NMΔ-*alr0397* deletion shows almost the same very low difference of fluorescence in the light and the dark adapted state, as an iron-stressed wild type. NMΔ-*all4026* shows decreased values of the (Fm'-F_0') / (Fm-F_0) ratio.

It is known that the chlorophyll a properties in cyanobacteria depend on the iron level available in the growth medium (Guikema and Sherman, 1983). Under iron limitation characteristic blue shift of the chlorophyll a absorption peak by 5 nm appears in cyanobacterial cells (Guikema and Sherman, 1983). When the absorption spectra of *Anabaena* sp. wild type grown under normal conditions were compared to the spectra measured under iron depletion, the same shift was observed (Table 13). Next, the chlorophyll spectra of the mutants NMΔ-*all4026*, NMΔ-*alr0397*, NMOX-*all4026* and

NMOX-*alr0397* were analysed in comparison to the wild type *Anabaena* sp. in different media. The results summarized in Table 13. show characteristic blue shift of chlorophyll absorption in both deletion mutants grown under iron-replete conditions. It is interesting that, when grown without iron, but with copper source, the blue shift is not measured in the over-expression mutant of *all4026* (Table 13). It seems that the mutant with increased number of All4026 transporters is able to use the minute iron amounts existing in the medium and satisfy its iron needs. It is also possible that this mutant replaces missing iron with copper uptake and in that way delays an appearance of the metal depletion signals. In the medium without iron/copper source this over-expression *all4026* mutant shows characteristic blue shift, supporting the idea about its involvement in the copper homeostasis as well. This parallels the increased sensitivity of NMOX-*all4026* strain to metals in comparison to wild type and the deletion *all4026* mutant when grown on the metal over-loaded medium (Figure 27, lanes 7, 8). It is also in line with almost imperceptible *isiA* expression in the medium with no iron and with copper source (Figure 28). Altogether confirms once again the influence of the *all4026* and *alr0397* mutations on iron homeostasis in *Anabaena* sp.

Table 13. The peak positioning of the chlorophyll a absorption measured for *Anabaena* sp. wild type (WT) and NMΔ-*all4026*, NMΔ-*alr0397*, NMOX-*all4026* and NMOX-*alr0397* mutant strains grown in the standard BG11 medium, after four days in the medium without iron source (-Fe) and in the medium without iron and copper source (-Fe/-Cu). Characteristic 5 nm blue shift is present in both deletion mutants already when grown under the standard BG11 metal conditions. The absorption peak of chlorophyll a is not shifted in NMOX-*all4026* strain in –Fe medium.

Strain	BG11	-Fe	-Fe/-Cu
WT	678 nm	673 nm	673 nm
NMΔ-*all4026*	**673 nm**	673 nm	673 nm
NMOX-*all4026*	678 nm	**678 nm**	673 nm
NMΔ-*alr0397*	**673 nm**	673 nm	673 nm
NMOX-*alr0397*	678 nm	673 nm	673 nm

In order to analyse general effect of the mutations in *all4026* and *alr0397* genes on *Anabaena* sp. filaments, the growth rate in the standard medium, iron depleted medium and iron and copper depleted medium was measured (see “Methods”, section 5.4.3.). The

growth rate of the wild type strain turned out to be reduced by 40% when the source of iron or the source of iron and copper were removed from the growth medium (Figure 30A). Subsequently the growth rate of the mutant strains was compared to the growth rate of wild type *Anabaena* sp. and expressed in relation to the wild type values under the same growth conditions (Figure 30B). Although the small differences in growth were detected, the overall effect on the growth rate of the deletion and the over-expression mutants in comparison to the wild type was still not significant (Figure 30A, B).

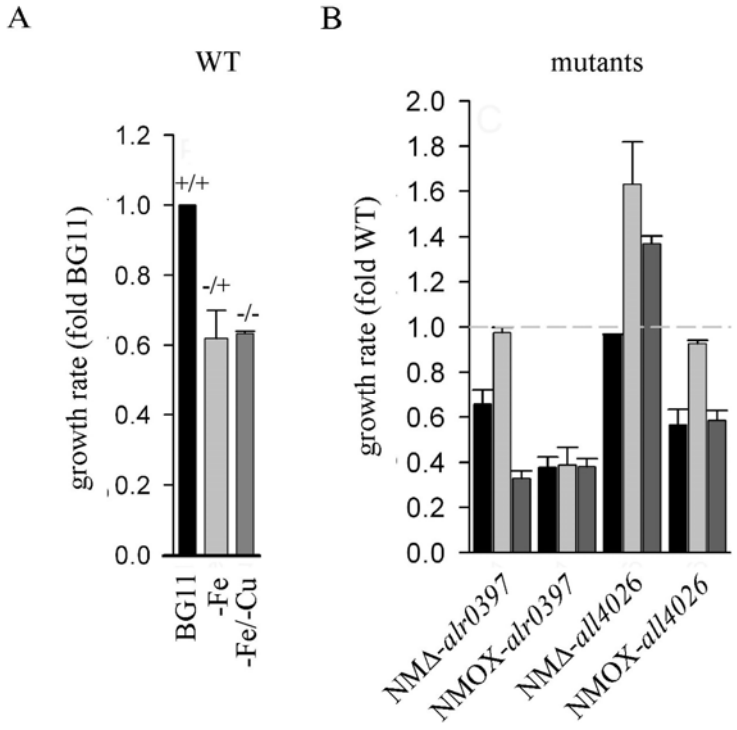

Figure 30. Wild type and mutants NMΔ-*all4026*, NMΔ-*alr0397* (deletion) and NMOX-*all4026* and NMOX-*alr0397* (over-expression) were grown in the standard BG11 medium (black bar), in the medium without addition of an iron source (light grey bar, -Fe) and in the medium without addition of an iron and copper source (dark grey bar, -Fe/ -Cu). Starting chlorophyll a concentration in all measurements was 0.4 µg/ml. The growth was analyzed by measuring the protein concentration each 12 hours for five days. Shown in (A) is the growth rate for wild type, normalized in all three media according to the wild type growth values in BG11 (value 1). Growth of the wild type is somewhat weaker in -Fe and -Fe/-Cu medium. (B) For the mutant lines growth rate was normalized to the growth rate of the wild type strain under indicated medium conditions (value 1).

The strain NMOX-*alr0397* showed 0.5-fold growth reduction even under normal iron/copper conditions. Interestingly, the growth of the strain NMΔ-*all4026* did not show a significant difference from the wild type. The other two strains NMΔ-*alr0397* and NMOX-*alr0397* were slightly reduced in their growth rate in comparison to the wild type in BG11 medium. When the growth of the lines in iron-depleted medium was compared to wild

type, the *alr0397* over-expression line again showed the strongest reduction. The strain NMΔ-*all4026* showed 0.5-fold higher growth rate when compared to the wild type under the same conditions (Figure 30B). In turn, the growth of the deletion strain did not reveal any significant difference when compared with its growth under normal conditions. In the medium depleted of iron and copper sources, all strains were reduced in their growth in comparison to wild type, with the exception of the strain NMΔ-*all4026*. However, these are all small differences in growth rates and they demonstrate that the affect on the general phenotype is low, although consequences of the mutations are detectable on finer intracellular and molecular levels (Figures 28, 39, 31, 32). The mutants adapt to the unfavourable situation probably by regulating iron homeostasis with a help of other 23 putative iron-uptake pathways present in *Anabaena* sp. (Figure 20).

6.4.7 All4026 and Alr0397 proteins are involved in metal uptake

Recently it has been reported that the iron starvation leads to a certain degree of oxidative stress in *Anabaena* sp. which causes the peroxidation of lipids (Latifi *et al.*, 2005). Some compounds produced during lipid peroxidation are chemoluminescent species. This luminescence is of very low level and it can be significantly enhanced by slowly heating the sample to the temperatures above 100°C. Measuring this so called thermoluminescence after exposure of filaments to iron depletion is a way to detect and quantify lipid peroxidation and oxidative stress in plants and cyanobacteria (Havaux, 2003; Havaux *et al*., 2006). As described in Latifi *et al.* (2005), an increase of the luminescence appears for the temperatures above 55°C when wild type *Anabaena* sp. filaments are grown in the medium without iron supply (Figure 31A). The maximal peak is expected at about 110°C; however, with the laboratory equipment available this was impossible to achieve (see "Methods", section 5.4.10.). For this reason, the difference in thermoluminescence obtained between 40°C to 70°C was used for data analyses (Figure 31B). Even in this limited temperature range, six-fold increase of the wild type luminescence in the absence of iron or iron and copper was detectable, ensuring that the method can be applied (Figure 31A, B). The thermoluminescence was further measured for the *all4026* and *alr0397* deletion and over-expression lines. As a result the deletion mutants, NMΔ-*all4026* and NMΔ-*alr0397*, showed enhancement of luminescence by factor 3 to 4 in comparison to the wild type when grown in the standard BG11 medium (Figure 31C).

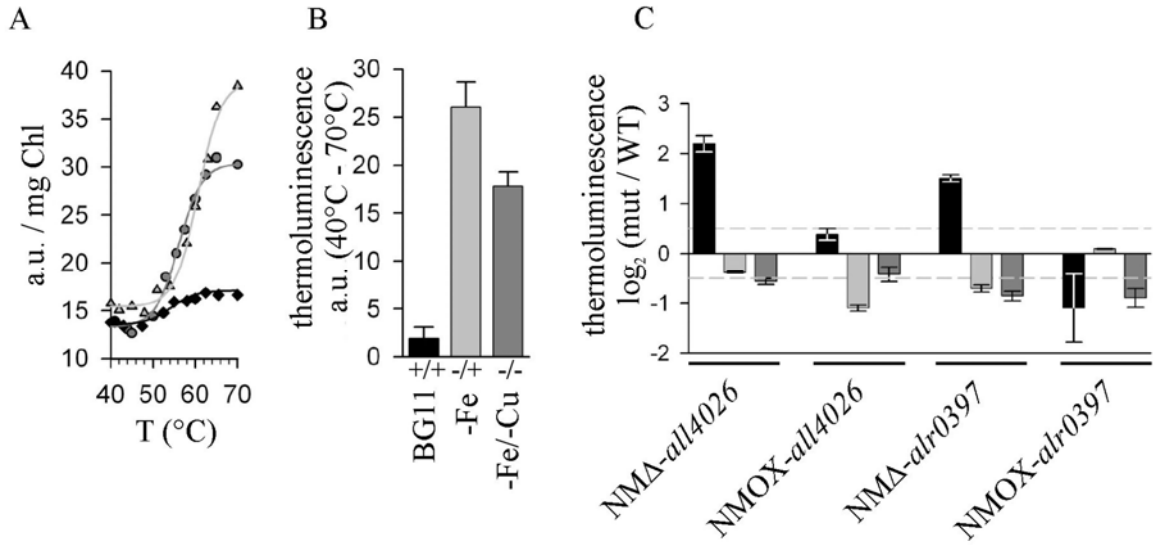

Figure 31. Alterations in Alr0397 or All4026 protein levels cause peroxidation of lipids and thermoluminescence already under iron repletion. (A) The temperature dependent luminescence (in arbitrary units) of wild type *Anabaena* sp. Wild type filaments were grown in standard BG11 medium (black diamond), in BG11 without iron source (grey triangle) or BG11 without iron and copper source (dark grey circle). The thermoluminescence was analyzed at increasing temperatures and normalized to the chlorophyll a content of the cultures. One representative result is shown. (B) An average of three independent measurements of the thermoluminescence between 40°C and 70°C for wild type *Anabaena* sp. grown in BG11 (black bar), BG11 without iron source (-Fe, light grey bar) or BG11 without iron and copper source (-Fe/-Cu, dark grey bar) is shown**.** (C) The $\log_2$ value of the ratio between thermoluminescence of each mutant (NMOX-*all4026*, NMOX-*alr0397*, NMΔ-*all4026* and NMΔ-*alr0397*) and thermoluminescence of wild type *Anabaena* sp. grown in BG11 (black bar), BG11 without iron source (light grey bar) or BG11 without iron and copper source (dark grey bar) is presented.

This was not the case in the BG11 grown over-expression mutants, since they are expectedly iron-transport proficient. However, when growing under iron or iron/copper limiting conditions all strains exhibited no significant change of a thermoluminescence signal over the wild type level. It appears that the luminescence was rather slightly decreased in the iron starved mutants in relation to the iron starved wild type (Figure 31C). Since iron or iron/copper depleted conditions should induce at least some of the other putative iron uptake pathways in *Anabaena* sp., it is understandable that this can be a way to moderate the effect of a single *all4026* or *alr0397* mutation in the corresponding mutant lines to the level measured in wild type. Even more, the over-expression of these genes, especially of *all4026*, could even somewhat decrease thermoluminescence of the filaments under metal depletion conditions in relation to wild type (Figure 31C). This again parallels the earlier findings (Table 13, Figures 27, 28).

All4026 and Alr0397 transporters seem to be part of constitutive pathways for iron and, in the case of All4026, copper uptake. Therefore, the affect of the corresponding mutations in NMOX-*all4026*, NMOX-*alr0397*, NMΔ-*all4026* and NMΔ-*alr0397* *Anabaena* sp. strains on the intracellular level of three metals: copper, iron and magnesium, was investigated by flame spectrometry of the lyophilized cultures (see "Methods", section 5.4.11.). Magnesium was used as a control metal (Figure 32).

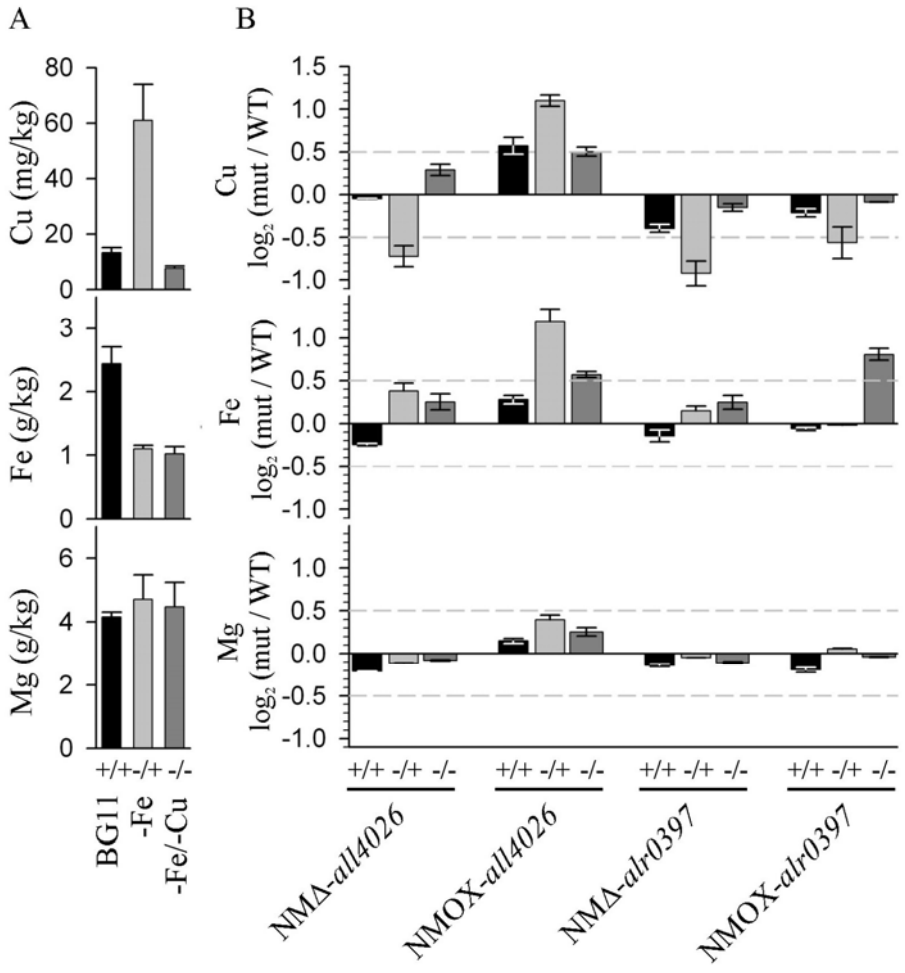

Figure 32. Influence of the deletion or over-expression of *alr0397* or *all4026* genes on the metal content of *Anabaena* sp. filaments in NMΔ-*all4026,* NMOX-*all4026*, NMΔ-*alr0397* and NMOX-*alr0397* strains. (A) The amount of copper (top), iron (middle) and magnesium (bottom) found in wild type grown in standard BG11 medium (black bar), in BG11 without iron source (-Fe, light grey bar) or BG11 without iron and copper source (-Fe/-Cu, dark grey bar) was quantified with flame spectrometry and expressed in relation to a dry cell weight. (B) The $\log_2$ value of the ratio between copper (top), iron (middle) or magnesium (bottom) content of each of the indicated mutants and wild type grown in BG11 (black bar), BG11 without iron source (light grey bar) or BG11 without iron and copper source (dark grey bar) is presented. Error bars are result of three independent analyses. Everything above the zero line indicates $\log_2$ increase and everything below the line indicates $\log_2$ decrease in the metal content of a dry cell weight.

For the wild type cultures grown in BG11 medium under applied laboratory conditions (see "Methods", section 5.4.1.) around 13 mg/kg of copper, 2.5 g/kg of iron and 4.1 g/kg of magnesium in the dry cells weight was measured (Figure 32A). These values agree well with the earlier published observations (Sandmann *et al.*, 1990; Fiore and Tervors, 1994). When wild type *Anabaena* sp. was grown in iron-depleted medium with and without copper source, the amount of magnesium was unaffected (Figure 32A). On the other hand, the iron mass content decreased by a factor of 1-1.5 in both media. This confirms good adaptability of wild type *Anabaena* sp. to the unfavorable conditions of iron depletion and its capacity to preserve metal homeostasis. Surprisingly, the copper concentration was found to be even three to four-fold enhanced in the wild type when grown in the medium without iron but supplied with copper source (Figure 32A). This suggests that in iron limited environment uptake of copper by *Anabaena* sp. filaments increases significantly. Even more, when both iron and copper supply were depleted in the medium, the intracellular copper level decreased even bellow its level in the BG11 grown filaments for about 50% (Figure 32A). This kind of behavior implies mutual dependence of iron and copper homeostasis in *Anabaena* sp.

The iron content of the mutant strains grown under the same conditions was analyzed further and expressed in relation to the wild type values (Figure 32B). Magnesium level showed no noteworthy changes in any mutants and under any conditions. Additionally, under all three tested growth conditions the content of iron in the two deletion strains NMΔ-*all4026* and NMΔ-*alr0397* was comparable to that of the wild type filaments (Figure 32B). That shows that these single deletion mutants, as expected, are still able to regulate iron homeostasis to the level of wild type, despite the absence of one the constitutive iron transporter. The same was the case for the over-expression strain NMOX-*alr0397*, except that this strain accumulated iron to the level of wild type in BG11 medium when grown under iron/copper limitation. On the other hand, under both iron limited and iron/copper limited conditions, the over-expressing strain NMOX-*all4026* also showed an increase of the intracellular iron level to the level of the BG11 grown wild type.

The alterations in the copper amount of the filaments showed two-fold and one-fold decrease in the deletion and the over-expression *alr0397* strains in comparison to the wild type (Figure 32B) in iron depleted and copper supplied medium. Copper level was not affected in the same strains in iron/copper depleted medium (Figure 32B). In contrast, the deletion NMΔ-*all4026* strain in iron depleted, copper supplied medium showed 1.5-fold decrease in copper accumulation when compared to the wild type in the same medium. No

such change was detected when no iron and no copper source were available. Interesting, over-expression strain NMOX-*all4026* in the same medium accumulated two times more copper that the wild type under the same conditions. In other words, the copper amount in this mutant reached value of about 120-150 mg/kg when exposed to iron depletion. On the other side copper level in the same mutant in iron/copper limited conditions did not exceed 20 mg/kg, being the amount of copper in BG11 grown wild type.

In conclusion, *Anabaena* sp. filaments, even though bearing mutations in *alr0397* and *all4026* and/or being iron starved, still succeed to regulate iron level and survive. The result is understandable in the light of a huge family of putative iron transporters found in this cyanobacterium (Figure 20). On the other hand, iron and copper uptake are mutually dependent in the wild type (Figure 32A). The effect on the intracellular copper amount obtained by mutating *alr0397* gene does not indicate involvement of Alr0397 TonB-dependent transporter on copper transport. On the contrast, the data on the deletion and the over-expression of *all4024* gene demonstrate that TonB-dependent transporter mediates not only iron uptake also participates in regulation of the intracellular copper level.

7. Discussion

7.1. The outer membrane continuum of *Anabaena* sp. PCC 7120

On the basis of electron micrographs the existence of microplasmodesmata as cytoplasmic bridges (Lang and Fay, 1971) or even proteinaceous pore forming connections (Guglielmi and Cohen-Bazire, 1982) between neighboring cells in the filament was suggested. However, since then no experimental proof of such structures and of their role in intercellular compound exchange has been offered. Recently it has been proposed that the outer membrane and the periplasmic space of Gram-negative cyanobacterium *Anabaena* sp. PCC 7120 are continuous along the entire filament. This means that the outer membrane and the periplasmic space are common for all cells, vegetative and heterocysts, while the inner membrane is separate for each cell (Flores *et al*., 2006). On the basis of this, it was suggested that the transport of metabolites and signal molecules between the cells of filamentous cyanobacterium *Anabaena* sp. passes rather through the continuous periplasm than through the cytoplasm of each cell in the filament (Figure 33; Flores *et al*., 2006).

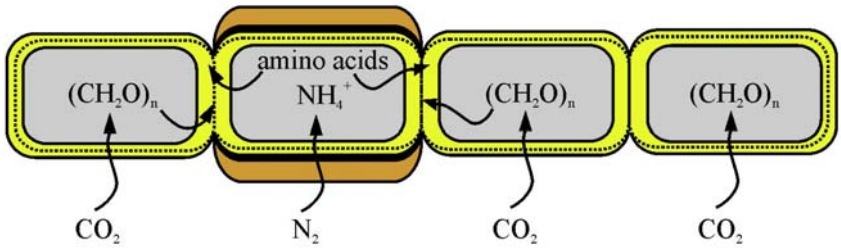

Figure 33. Continuum of the outer membrane and the periplasm in *Anabaena* sp. PCC 7120 filament (according to Flores *et al*., 2006). The yellow area represents the periplasmic continuum surrounded by the continuous outer membrane and the inner membrane which is separate for every cell. The dotted line represents the peptidoglycan layer, the grey area is the cytoplasm. The arrows indicate metabolite exchange between vegetative cells and heterocysts through the continuous periplasm. Vegetative cells supply heterocysts with sugars (sucrose) as products of photosynthesis, while heterocysts supply vegetative cells with products of nitrogen fixation (amino acids).

Furthermore, each heterocyst originates from an ordinary vegetative cell and transforms drastically in the process of differentiation (see "Introduction"). In line with this, alterations in the outer membrane proteome of heterocysts during differentiation could be expected. However, in the light of the continuum of the outer membrane (Figure 33) it is also possible that no such major proteome changes are necessary. The performed

analyses of the outer membrane proteomes in both cell types of *Anabaena* sp. and subsequent detailed comparison of their composition support the later notion (Tables 5-10).

In the outer membrane fraction of vegetative cells 55 proteins were identified; 22 of them as putative β-barrel outer membrane proteins (Tables 5-7). The rest of detected sequences contained cytoplasmic and periplasmic protein contaminations and proteins possibly associated with the outer membrane. No thylakoid proteins were detected. Even more, 10 among 55 identified proteins could not be assigned to the known proteins of *Synechocystis* sp. PCC 6803, justifying over again separate investigation of *Anabaena* sp. proteome.

While analyzing the vegetative cell proteome, certain findings appeared as rather unexpected. For example, two proteins with S-layer homology domain and predicted either outer membrane or extracytoplasmic localization were identified in the vegetative cell fraction (Tables 5-7). S-layer is a monomolecular surface layer of identical proteins or glycoproteins present in many bacteria that encompasses the whole cell. When existing, S-layer comprises up to 15% of the total protein content of a bacterial cell (Sleytr and Beveridge, 1999). Although it appears in some cyanobacterial groups, it was never noticed in *Nostocales* including *Anabaena* sp. (Smarda *et al*., 2002).

In the heterocyst outer membrane fraction 18 proteins were detected and only five among them were not found in the outer membrane of vegetative cells. Subsequent structural and functional analyses showed that these proteins had mostly been soluble heterocysts contaminations and that only Alr5055 protein had a putative outer membrane localization (Tables 10 and 11). It still cannot be excluded that some proteome alternations have escaped the analysis, since large scale mass spectrometry approaches favor the detection of abundant and non-hydrophobic proteins. Furthermore, the periplasmic protein involved in the heterocyst polysaccharide layer deposition All4388 (Maldener *et al*., 2003) was found in vegetative cells and in heterocysts. This could be a consequence of the low level heterocyst differentiation appearing when *Anabaena* sp. filaments grow in a dense culture in the presence of nitrate as nitrogen source. However, even though All4388 is involved in heterocysts function, its presence and function in vegetative cells also cannot be excluded, as discussed for Alr2887 (see below).

On the basis of comparison of the two proteomes, where no significant alterations were detected, it can be suggested that the continuous outer membrane has on its disposal the same protein collection to carry out the functions in vegetative cells and in heterocysts. It is possible that the same protein machineries take over new responsibilities or simply

add them to already existing ones in order to support differentiation process and heterocyst-specific functions. In line with the proteomic results and a proposed metabolite transport through the continuous periplasm (Figure 33), more significant proteomic difference between vegetative cells and heterocyst might be expected in their inner membrane proteomes.

The second line of evidence for the continuity of the *Anabaena* sp. outer membrane (Figure 33) was obtained through investigations of the intracellular protein localization and the corresponding gene expression of iron transporters All4026 and Alr0397 (Figure 21, 22). The GFP fusions with the C-terminus of these outer membrane localized proteins resulted in a strong ring-like fluorescence on the cell periphery consistent with a proposed membrane localization. The signal was uniformly distributed along the periphery of the whole filament (Figure 22A, B). The similar was obtained in the case of the GFP fusion of *Anabaena* sp. Omp85 homologue, Alr2269 (Figure 8). This finding is interesting, as All4026, Alr0397 and Alr2269 proteins are translocated across the inner membrane via Sec translocon, which exports mainly unfolded proteins (Rusch and Kendall, 2006). In non-filamentous bacteria and cyanobacteria once it reaches the periplasm, GFP (Feilmeier *et al*., 2000; Thomas *et al*., 2001) does not gain its activity, probably due to the disulfide bond formation and improper folding. However, if the transport of metabolites (e.g. products of photosynthesis and nitrogen fixation; Herrero *et al*., 2004) and signal molecules (e.g. PatS inhibitor of heterocyst differentiation; Yoon and Golden, 2001) occurs through the continuous periplasm, a higher metabolic activity, a different reducing capacity and/or a higher chaperone activity could be proposed for the *Anabaena* sp. periplasm than for the periplasm of the non-filamentous bacteria. This could, on the other hand, assist proper GFP folding (Jackson et al., 2006) of at last one part of the GFP molecules.

However, the GFP-promoter fusions, used to monitor the gene expression pattern, demonstrate that *all4026* and *alr0397* genes are not uniformly expressed along the filament, but their expression is localized to the non-continuous stretches of cells (Figure 21A, B). On the contrary, according to the fluorescent signal of the protein-GFP fusions, Alr0397 and All4026 proteins are uniformly distributed all the way through the continuous outer membrane (Figure 22A, B). This discrepancy suggests that these proteins either migrate through the periplasm prior to insertion in the outer membrane or they even migrate in the membrane after already being inserted. That once again supports the proposed continuity of the outer membrane and the periplasm and an idea of the intercellular transport through the periplasmic continuum (Flores *et al*., 2006). Besides,

these proteins might have long half life; once they are synthesized and inserted into the outer membrane their presence can be long detected, while their gene expression level in separate cells or cell groups changes.

7.2. TolC protein and the heterocyst glycolipid layer deposition

The complex analysis of the outer membranes of vegetative cells has resulted in identification of the two protein complexes (Figure 7). In the first complex Alr2269 protein was found (Ertel *et al*., 2005; Bredemeier *et al*., 2006). Alr2269 belongs to an Omp85 family of β-barrel proteins conserved among Gram-negative bacteria (Voulhoux and Tommassen, 2004). The complex is a tetramer of identical subunits, being in line with an earlier proposed structure of the pore-forming Omp85 complexes (Schleiff *et al.*, 2003; Voulhoux *et al.*, 2003). Omp85 proteins are essential for the cell survival as they are responsible for the outer membrane biogenesis, most probably by protein assembly into the outer membrane (Voulhoux and Tommassen, 2004). Involvement of this protein family in the outer membrane lipid assembly has also been proposed (Genevrois *et al*., 2003).

The second complex identified is composed of the three identical Alr2887 subunits. Alr2887 protein is homologous to the TolC efflux protein family (Maldener *et al*., 2003) conserved among Gram-negative bacteria (Andersen *et al*., 2000). However, based on its influence on lipid assembly into the glycolipid layer, it could be speculated that Alr2887 is a functional homologue of Imp/OstA (Braun and Silhavy, 2002), which is thought to facilitate the lipid transport in proteobacteria (Bos *et al.*, 2004). However, secondary structure predictions reveal that Imp/OstA contains mainly β-strands, whereas Alr2887 has a very high content of α-helices. According to the PHYRE server Alr2887 is a TolC-like protein, in which each of the three subunits contributes four transmembrane β-strands and four α-helices to a single channel-tunnel structure. That parallels the proposed trimeric structure of Alr2887 complex, as shown by the complex analyses of the outer membrane of *Anabaena* sp. vegetative cells (Figure 7). Following this prediction a model of Alr2887 / TolC was created (Figure 34A, protein modeling by Oliver Mirus) and further supported by experimental data (see below).

Phylogenetic analysis of the TolC family (Oliver Mirus, personal communication; Figure 34) shows sub-grouping of the TolC channel-tunnels to the protein secretion group, the drug efflux group and the cation efflux group (Koronakis *et al*., 2004; Posadas *et al*.,

2007). Alr2887 clusters with the TolC family members involved primary in protein secretion (Figure 34B). This is in line with experimental data (Figure 19) and confirms Alr2887 involvement in the transport of the proteins / enzymes connected with the glycolipid layer deposition, rather than in the transport of lipids or lipid moieties.

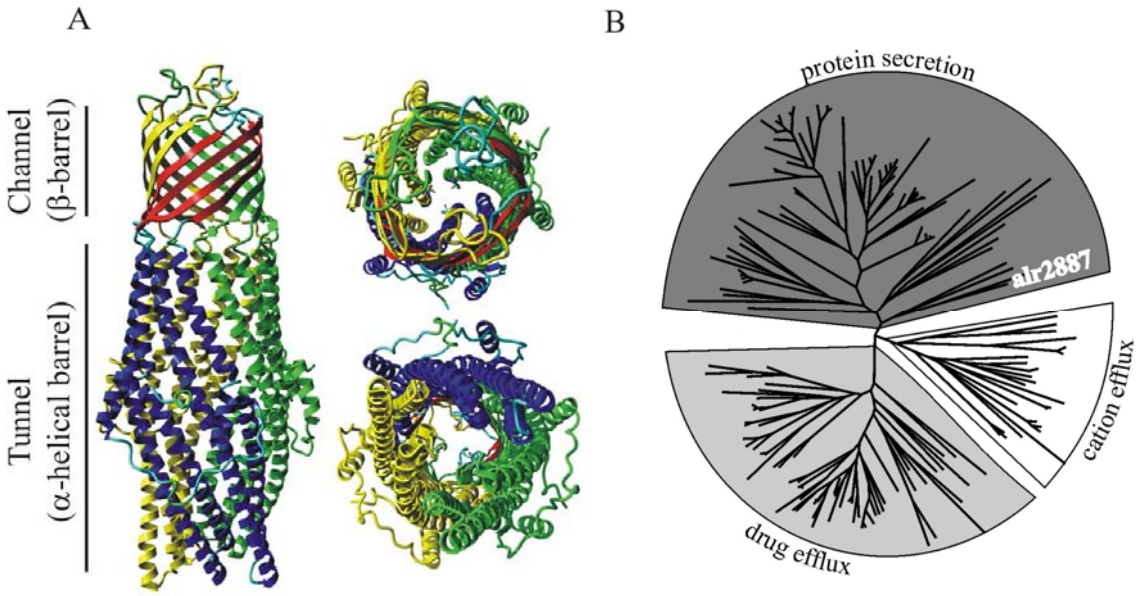

Figure 34. (A) Three-dimensional structural model of Alr2887 based on the homology with *E. coli* TolC channel-tunnel. Shown are the side, top, and the bottom view on the structure. (B) In the phylogenetic analysis of the TolC protein family Alr2887, as *Anabaena* sp. PCC 7120 TolC homologue, clusters with the TolC proteins involved primary in protein secretion (phylogenetics and modeling performed by Oliver Mirus).

The deletion *alr2887* mutant shows full segregation and normal growth when grown on nitrate as bound nitrogen source (Figure 15). This parallels the findings that the TolC-like proteins are not essential for the cell survival under conditions when their function is not required (Wandersman and Delepelaire, 1990) since they are mostly involved in secretion of big bacterial protein toxins, like hemolysin (Glaser *et al*., 1988; Koronakis and Hughes, 1993; Paulsen *et al*., 1997), or small toxic compounds, like antibiotics, out of the cell (Zgurskaya and Nikaido, 2000). After being transferred on dinitrogen, the deletion mutant shows incapability of nitrogen fixation in the presence of oxygen (*fox*$^-$ phenotype, Figure 16; Ramirez *et al*., 2005), its filaments strongly fragmentize, turn yellow and lose growth competence (Figure 16). This indicates the defect in connection to the heterocyst function. However, the mutant differentiates heterocysts

with mature polysaccharide layer (Figure 16) and active nitrogenase when filaments are grown anaerobically. This kind of phenotype has been described for the mutants with aberrant heterocysts specific layers (Ernst *et al*., 1992) or *cox* mutants with defective heterocyst specific cytochrome oxydase affected in respiration (Schmetterer *et al*., 2001). In other words, heterocysts of the deletion *alr2887* mutant are not able to provide microoxic environment crucial for the nitrogenase activity. The reason for this behavior is that this mutant does not deposit glycolipid layer between the outer membrane and the polysaccharide layer (Figure 17) even though the heterocyst specific glycolipids (HGLs) are synthesized in the cell (Figure 18). Therefore, the glycolipid barrier that prevents oxygen from "leaking" into the cell is missing in the absence of Alr2887 / TolC function.

Although further experiments are necessary to support these notions, two proteins appeared in the course of the studies as possible candidates for Alr2887 substrate: All2736 and Alr0267. All2736 is a small protein co-isolated with Alr2887 complex (Figure 7, Table 8, section 6.3.9.). It was not detected in the outer membrane proteome (Tables 5-7), but as part of the Alr2887 complex. Alr2887 structure is a long tunnel able to accommodate secondary structure elements and even small unfolded proteins (Sharf *et al*., 2001). Hence, All2736 could be a possible substrate that "got stuck" in the tunnel. All2736 protein is similar to plant lipid transfer proteins (Charvolin *et al*., 1999). These are small extracellular proteins for which different functions were proposed, such as involvement in formation of cutin layers extracellular to plant cell by transport of cutin monomers (Sterk *et al*., 2003), plant cell wall extension (Nieuwland *et al*., 2005), etc. It is possible that a protein similar to plant lipid transfer proteins is necessary for the glycolipid layer deposition and that it utilizes TolC as an exit duct to reach its extracellular place of action. The second possible substrate, Alr0267 protein, was identified in the pool of proteins secreted by *Anabaena* sp. filaments in the medium. Alr0267 was detected as a protein secreted by wild type, but not by the deletion *alr2887* mutant (Figure 19). The predicted structure of Alr0267 corresponds to the 7-bladed β-propeller domain found as N-terminal domain of α-integrins (Hynes, 2002) and in some enzymes like lipases (Raikwar *et al*., 2005). A lipase-like enzyme could participate in the formation of the heterocyst glycolipid layer. Since TolC is a promiscuous protein, co-operating with different substrate-specific inner membrane components, it is not excluded that both these proteins are potential Alr2887 / TolC substrates.

The TolC family members depend on the action of the inner membrane ABC transporters and their adaptor proteins, which create contact between the inner and the

outer membrane components (Thanabalu *et al.*, 1998). The only potential plasma membrane protein identified in the outer membrane fraction of vegetative cells is All3144, an *Anabaena* sp. HlyD homologue (Tables 5-7, protein 49). HylD protein is an adaptor protein of the HlyA (hemolysin) secretion system from *E. coli* (see "Introduction", Figure 2; Oropeza-Wekerle *et al*., 1990) where it connects the outer membrane TolC with the inner membrane ABC transporter HylB (Koronakis and Hughes, 1993). The adaptor proteins are periplasmic proteins anchored with a single transmembrane segment to the inner membrane (Figure 2; Thanabalu *et al*., 1998). Therefore, All3144 could be an inner membrane component of the TolC transport system in vegetative cells of *Anabaena* sp. If associated with TolC in the moment of membrane preparation, it might find its way to the outer membrane fraction.

Fiedler *et al.* (1998a,b) have demonstrated that the *Anabaena* sp. *devBCA* operon encodes components of the inner membrane ABC transporter. *devBCA* mutants fail to deposit the heterocyst specific glycolipid layer and result in a strikingly similar phenotype to the phenotype of the *alr2887* deletion mutant (Fiedler *et al*., 1998). This suggests that the DevBCA exporter co-operates with the outer membrane Alr2887 / TolC channel-tunnel in *Anabaena* sp. (Figure 35).

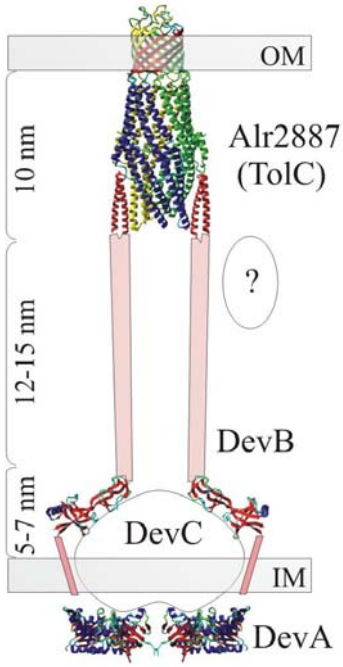

Figure 35. The protein model of Alr2887 / TolC channel-tunnel in interaction with DevBCA complex. DevBCA complex is composed of the inner membrane DevA / DevC ABC transporter and DevB adaptor protein (Fiedler *et al*., 1998a). Coiled coil prolongation of DevB protein is indicated in pink. The question mark stands for still unknown way of stabilization of this elongated structure (protein models prepared by Oliver Mirus).

DevA protein (Maldener *et al*., 1994) corresponds to the cytoplasmic ATP-binding domain of HlyB ABC transporter from *E. coli*, whereas DevC corresponds to the inner membrane domain of the same protein (Fiedler *et al*., 1998). Accordingly, 1-1

stoichiometry between DevA and DevC is expected. DevB is similar to the adaptor protein HlyD of *E. coli*. Unlike HlyD, DevB shows remarkable extension in the form of coiled coil domain with periodicity of 18 (predicted by the REPPER server; Gruber *et al*., 2005). The estimated length of this extension is 12-15 nm assuming diametric anti-parallel coiled coil domain (Figure 35). The dimensions of DevB with its coiled coil prolongation summed up with the estimated dimensions of Alr2887 / TolC are exactly enough to bridge the 30 - 40 nm wide periplasmic space of *Anabaena* sp. (Figure 35, TolC protein modelling by Oliver Mirus). Therefore, DevBCA exporter is a good candidate for the ATP-binding cassette transporter with the adaptor protein that creates a complex with Alr2887/TolC in heterocysts in order to bridge the periplasm and export the proteins participating in the formation of the heterocyst glycolipid layer.

Although Alr2887 / TolC protein is present in vegetative cells, its gene expression increases after nitrogen step-down to fall back again to the basic level after 24 hours (Figure 12A, B). This elevated expression of *alr2887* gene probably supports increased transport needs enabling the fast glycolipid layer formation and heterocysts maturation in just about 20 hours (Fay, 1992; Wolk *et al.*, 1994; Adams and Duggan, 1999). The *devBCA* operon expression is NtcA dependent and appears only after nitrogen step down in developing heterocysts (Fiedler *et al*., 2001). While TolC is present in the continuous outer membrane of the entire filament under any nitrogen conditions, the DevBCA exporter is present only in heterocysts where it determines the substrate specificity of the whole complex.

7.3. TonB-dependent transporters of *Anabaena* sp. PCC 7120

Microorganisms have usually few different TonB dependent transporters / receptors (TBDT) specific for different siderophores, endogenous ones as well as siderophores produced by other bacteria or fungi (Braun *et al*., 2003; Andrews *et al*., 2003). Detection of five putative TBDT in the outer membrane proteome of vegetative cells of *Anabaena* sp. grown under iron repletion proves this to be the case in this cyanobacterium as well (Tables 5-8). Nevertheless, this result was unexpected for two reasons. First, expression of the genes encoding TBDT is up-regulated when cultures are exposed to iron starvation (Katoh *et al*., 2001a; Braun *et al*., 2003 and 2006; Andrews *et al*., 2003). Some TBDT, however, are weakly detectable even under normal iron conditions, as shown for *Synechocysts* sp. PCC 6803 (Katoh *et al*., 2001a; Singh *et al.*, 2003). Second, up till now

only four TBDT have been described in *Synechocystis* sp. PCC 6803 and six have been described in *E. coli* (Katoh *et al*., 2001; Buchanan, 2005). Since cyanobacteria are photosynthetic microorganisms they have normally higher iron needs than nonphotosynthetic microorganisms in order to maintain the functionality of their photosynthetic apparatus (Keren *et al.*, 2002, 2004). However, from comparison with the unicellular *Synechocysts* sp., the presnce of the five putative TBDT in the *Anabaena* sp. outer membrane under iron repletion is a surprisingly high number.

When the whole *Anabaena* sp. genome was probed for the TBDT coding sequences, 24 sequences were detected in total (see "Results", Figure 20). Compared to the number of TBDT members in other Gram-negative bacteria and unicellular cyanobacteria, this is an extremely abundant protein family. These results, therefore, indicate exceptional sensitivity of *Anabaena* sp. in respect to iron regulation and/or higher iron requirements than in unicellular photosynthetic *Synechocystis* sp. Since different TBDT are specific for different siderophore substrates (Clarke *et al.*, 2001; Ferguson and Deisenhofer, 2002) existing redundancy of TBDT in *Anabaena* sp. might serve to this cyanobacterium to exploit wide spectrum of in the medium available siderophores.

The following features of *Anabaena* sp. support these notions. First, except performing photosynthesis and nitrogen fixation, *Anabaena* sp. is a multicellular bacterium. This can be a reason for increased metabolic activity and thereby higher cellular iron needs. Second, *Anabaena* sp. differentiates heterocysts when starved for nitrogen compounds (Herrero *et al*., 2004) which increases metabolic activity and again iron demands in the filaments. Further, one of the main ways of heterocysts to eliminate oxygen in order to create and preserve microoxic environment is increased respiration (Murry and Wolk, 1989; Valadares *et al*., 2003). Hence, five constitutively present TBDT can enable *Anabaena* sp. to satisfy higher intracellular iron demands from the iron-replete medium. Microarray data from Ehira *et al.* (2003) on the general gene expression in *Anabaena* sp. after nitrogen step-down show that *all4026* gene is up-regulated during 24 hour of nitrogen depletion. This indicates, on one hand, high iron demands of a differentiating filament and, on the other hand, the role of Alr4026 transporters in satisfying those demands.

Alternatively, when grown in a dense culture on nitrate as combined nitrogen source, *Anabaena* sp. can starve itself for the nitrogen compounds and differentiate a certain number of heterocysts. If iron starvation can be caused in a similar way by growth in dense cultures, used normally for membrane preparation, this could result in the presence of five TBDT detected in the outer membrane of vegetative cells. Still, that could

not explain the existence of 24 TBDT coding sequences in *Anabaena* sp. genome. Furthermore, in laboratory growth medium siderophores secreted by other microorganisms are not present and *Anabaena* sp. filaments depend there primary on the ability to utilize available iron source (ferric ammonium citrate, see "Methods"). Inability to achieve that may result in appearance of the constitutive iron transporters.

The phylogenetic analysis of the TBDT family reveals the distribution of 24 TBDT through different phylogenetic clades. Accordingly, in *Anabaena* sp. catecholate-like and hydroxamate-like transporters are found, with a strong prevalence of hydroxamate transporters (Neilands, 1995; Winkelman, 2002). This can mean that in the natural *Anabaena* sp. habitat hydroxamate type siderophores are more available than catecholate type. It is interesting that *Anabaena* sp. has no receptors for the simple siderophore ferric-citrate (Braun *et al*., 2003; Mahren *et al*., 2005). On the other hand, it does have four aerobactin-like transporters specific for the citrate-based hydroxamate siderophore aerobactin structularry similar to endogenous siderophore of *Anabaena* sp. schizokinen (de Lorenzo *et al.*, 1986). The discovery of a transporter similar to colicin / vitamin B_{12} specific transporters and two transporters similar to heme / hemoglobin specific transporters also draws attention. The heme / hemoglobin type of transporters appears often in parasitic microorganisms (Wandersman and Stojiljkovic, 2000; Cornelissen, 2003; Wandersman and Delepelaire, 2004). In *Anabaena* sp. they can possibly transport heme-iron originating from the photosynthetic machineries of other cyanobacteria.

The five transporters that are constitutively expressed belong to catecholate type (All4026 similar to vibriobactin or yersiniabactin transporters), hydroxamate type of transporters (All1101 and Alr2588 as ferrichrome-like, Alr0397 as aerobactin-like transporter) and to colicin / vitamin B_{12}-like transporters (All3310) (Figure 20). According to this, almost every class of iron transporters identified in *Anabaena* sp. has one or two constitutively expressed representatives. The two constitutively present iron transporters, All4026 and Alr0397, were analyzed closer. All4026 is the only iron receptor in *Anabaena* sp. clustering with catecholate-specific transporters (Figure 20, right part). On the other hand, Alr0397 is the only constitutive TBDT found in the phylogenetic clade of aerobactin-specific receptors (Figure 20, left part). Thus, Alr0397 is a candidate for the *Anabaena* sp. schizokinen transporter. *all4026* and *alr0397* genes are, beside being expressed under normal iron conditions, expectedly expressed under iron starvation as well (Figure 21). In the case of *alr0397* basal expression is slightly enhanced upon iron depletion, but it decreases back to the basal level with time as iron depletion continues.

Similar expression behavior shows *Synechocystis* sp. ferrichrome like receptor Sll1409 (Singh *et al*., 2003). On the other hand, aerobactin-like receptor Sll1206 of *Synechocystis* sp. is not expressed under iron-replete conditions (Katoh *et al.*, 2001).

As shown, the deletion of one out of 24 TonB-dependent iron transporters, even if it is a constitutively expressed one, does not cause a drastic effect on the corresponding mutant (Figures 24, 30). In line with this, All4026 and Alr0397 functions are not essential, similar as reported for the deletion mutants of iron transport genes in *Synechocystis* sp. (Figure 24, Katoh *et al*., 2001). This also explains why in the corresponding mutants no obvious morphological phenotype change or growth defect is noticeable (section 6.4.4., Figures 24, 30). However, influence of the mutations affecting *all4026* and *alr0397* genes is detectable on the molecular and cell level. Particularly compelling is the finding that the absence of All4026 or Alr0397 iron transporter results in the signs of intracellular iron starvation of the mutant filaments even when they grow in the presence of an iron source. This is confirmed by four different experiments. First, in both deletion mutants *isiA* gene expression is detectable (Figure 28). IsiA is a chlorophyll binding protein which protects photosystems under iron stress and its gene expression is a marker for an iron starvation (Laudenbach and Straus, 1988; Falk *et al*., 1995, Michel and Pistorius, 2004; Latifi *et al.*, 2005). Second, both *all4026* and *alr0397* deletion mutants show significant increase of thermoluminescence induced normally by iron starvation. In this case thermoluminescence of the deletion mutants appears when the deletion mutants grow on iron source (Figure 31; Latifi *et al.*, 2005). Third, in both deletion mutants 5 nm blue shift of a chlorophyll a absorption peak characteristic for iron-starved cells is measurable under iron repletion (Table 13; Guikema and Sherman, 1983). And fourth, the deletion mutants exhibit weaker state transition PSII fluorescence between the light and of the dark adapted state as characteristic for iron-starved cells (Figure 29; Falk *et al*., 1995; Ivanov *et al.*, 2006). This proves that All4026 and Alr0397 functions are indeed important, although not essential, for *Anabaena* sp. filaments under conditions where cells do not suffer from iron starvation. This parallels the suggested higher iron requirements of this multicellular cyanobacterium.

The same effect, on the other hand, was not achieved in the two over-expression mutants. The over-expression strains do not suffer from iron starvation, as one of their iron transport facilities, either All406 or All0397, is enhanced. It is interesting that, in regard to the signs of iron starvation, behaviour of the mutants (in the first place deletion ones) approaches to the values of the wild type, when experiments are performed under iron or iron/copper depletion (Figures 28, 31, 32). In these conditions iron starvations signals

appear but their values do not differ from the signals appearing in the wild type. These conditions induce expression of at least some of the numerous iron transporting systems of *Anabaena* sp. that could enable the filaments to moderate the iron starvation signals.

The phylogeny of bacterial TonB-dependent transporters has already predicted different substrate specificity of All4028 and Alr0397 outer membrane transporters (Figure 20). The different sensitivity of the deletion and the over-expression mutants on intoxication with iron or iron/copper confirms the phylogenetic predictions. The deletion of *all4026* gene makes *Anabaena* sp. cells resistant to the iron and iron/copper levels that are lethal for other three mutant strains and wild type. Whereas copper presence in the medium increases sensitivity of the wild type and the mutants to growing iron concentration, it almost does not influence the resistance of *all4026* deletion mutant. Furthermore, in the medium overloaded with iron, expression of the TBDT systems should not be enhanced. The achieved effect should, therefore, be a consequence of the substrate specificities and affinities of All4026 and Alr0397 transporters. Thus, All4026 and Alr0397 are specific for different siderophore substrates (All4026 for the catecholates and Alr0397 for the citrate-based hydroxamates) and All4026 might be a less specific transporter than Alr0397 which transports different iron sources, and possibly even copper.

The general knowledge on the copper transport systems in Gram-negative bacteria is poor. While simple diffusion is suggested to be a way in which copper crosses the inner membrane, it is proposed that the outer membrane β-barrels play a role in the copper uptake across the outer membrane (Rensing and Grass, 2003; Yamamoto and Ishihama, 2005). Under iron limitation copper binds to siderophores that are secreted usually in significant excess and available for reactions with iron, but also with some other metals (Clarke *et al*., 1987). It was shown that copper-schizokinen complexes are not transported into *Anabaena* sp. filaments. However, from the literature available today it is not clear if this is also the case for the copper complexed to some other siderophores. It is possible that some copper-siderophore complexes can enter the cell through some of the available TonB-dependent systems. For this reason an idea that one of the two transporters is influencing not only iron but also intracellular copper level was tested by measuring the metal content of the *Anabaena* sp. wild type and mutant filaments in different iron and iron/copper containing media (Figure 32). Interestingly, it was noticed that wild type *Anabaena* sp. grown in iron limited / copper containing medium accumulates intracellular copper significantly (Figure 32A). The copper content increases from about 16 mg/kg measurable in the standard medium to 60 to70 mg/kg of the dry cell mass in iron starvation

and falls back to about 10 mg/kg when both copper and iron source are limited in the medium (Figure 32A). This clearly demonstrates the strong mutual interference of iron and copper homeostasis in photosynthetic *Anabaena* sp. where iron and copper are both essential for photosynthesis. Detected effect could be a consequence of the replacement of iron containing proteins with copper containing proteins in attempt of the cells to fight agains iron depletion (Ferreira and Straus, 1994).

Among tested mutants the copper level was clearly influenced in the *all4026* mutant (Figure 32 B). The *all4026* deletion mutant shows almost two-fold decrease of the copper content in the iron limited / copper containing medium in relation to the wild type in the same medium. On the other hand, in the absence of an iron source but the presence of a copper source the over-expression *all4026* mutant further increased copper content in comparison to the wild type, reaching the value of even 120-150 mg/kg. This confirms that All4026 TonB-dependent transporter influences indeed copper uptake and its intracellular accumulation, although by still unknown mechanism (Figure 32B).

Iron content, however, was not affected drastically in any of the mutants except possibly in the *all4026* over-expression, which seems to increase the iron uptake to the level of the wild type grown in the normal medium. That again proves the potential of the *Anabaena* sp. filaments to survive the iron stress and regulate iron level with assistance of other available iron transporting systems. The adaptability to metal depletion is possible even when *Anabaena* sp. is affected by mutations eliminating one of iron transporter systems and in the medium depleted of an iron or iron/copper source.

In conclusion, All4026 and Alr0397 are two constitutively expressed iron transporters of *Anabaena* sp. PCC 7120 and a part of a large family of TonB-dependent transporters in that cyanobaceterium. Their function is required for maintaining the iron homeostasis of the filaments under iron-replete conditions and for that reason their expression and protein presence are constant and not enhanced upon iron limitation. All4026 and Alr0397 have different specificity for siderophore substrates and in addition to iron transport, All4026 protein is also capable of copper uptake, thereby influencing *Anabaena* sp. copper homeostasis as well.

7.4. Future directions

Many new questions that should be addressed in the future are raised by this work. First, comparison of the inner membrane proteome of vegetative cells and heterocysts could help understanding changes accompanying differentiation and bring insight into the functions of periplasmic continuum. Second, experimental identification of Alr2887 / TolC substrates and substrate-specific inner membrane transporters in both cell types could unveil specificities of the TolC functions in *Anabaena* sp. This, on the other hand, could provide more general picture on adjustments of the outer membrane proteome in the course of differentiation. An experimental confirmation of All3144 (HlyD homologue) as the adaptor protein of the TolC system in vegetative cells and of All2736 and Alr0267 proteins as potential TolC substrates should still be given. Third, the discovery of a large family of TonB-dependent transporters suggests sensitive and complex regulation of iron homeostasis in *Anabaena* sp. The basis for this abundance in *Anabaena* sp. and the expression features and functions of separate transporters should be additionally addressed. The possibility that some putative iron transporters are also mediating copper uptake and the mechanism involved should become a subject of future experiments.

8. References

Adams D.G., Duggan P.S. (1999) Heterocyst and akinete differentiation in cyanobacteria. *New Phytol.* 144: 3-33.

Adams D.G. (2000) Heterocyst formation in cyanobacteria. *Curr. Opin. Microbiol*. 3: 618-624.

Allen M.B., Arnon D.I. (1955) Studies on nitrogen-fixing blue-green algae. I. Growth and Nitrogen Fixation by *Anabaena Cylindrica* Lemm. *Plant Physiol*. 30: 366-372.

Almiron M., Link A.J., Furlong D., Kolter R. (1992) A novel DNA-binding protein with regulatory and protective roles in starved *Escherichia coli*. *Genes Dev*. 12B: 2646-2654.

Andersen C., Hughes C., Koronakis V. (2000) Chunnel vision. Export and efflux through bacterial channel-tunnels. *EMBO Rep*. 1: 313-318.

Andrews S.C., Robinson A.K., Rodriguez-Quinones F. (2003) Bacterial iron homeostasis. *FEMS Microbiol. Rev.* 27: 215-37.

Anraku Y., Gennis R.B. (1987) The aerobic respiratory chain of *Escherichia coli*. *Trends in Biol. Sci.* 12: 262-266.

Arora A., Abildgaard F., Bushweller J.H., Tamm L.K. (2001) Structure of outer membrane protein A transmembrane domain by NMR spectroscopy. *Nat. Struct. Biol*. 8(4): 334-338.

Arroyo C.M., Kirby S.D., Werrlein R.J., McCarthy R.L., Moran T.S., Keeler J.R. (1994) Reactive oxygen species produced in metal-catalyzed oxidation of bis(trifluoromethyl)disulfide and protection by ZE. *J. Toxicol. Environ. Health*. 41(3): 329-344.

Awai K., Wolk C.P. (2007) Identification of the glycosyl transferase required for synthesis of the principal glycolipid characteristic of heterocysts of *Anabaena* sp. strain PCC 7120. *FEMS Microbiol. Lett.* 266(1): 98-102.

Bagg A., Neilands J.B. (1987) Ferric uptake regulation protein acts as a repressor, employing iron (II) as a cofactor to bind the operator of an iron transport operon in Escherichia coli. *Biochemistry*. 26: 5471–5477.

Bagos, P. G., Liakopoulos, T. D., Spyropoulos, I. C., Hamodrakas, S. J. (2004a) A Hidden Markov Model method, capable of predicting and discriminating beta-barrel outer membrane proteins. *BMC Bioinformatics*. 5: 29.

Bagos P. G., Liakopoulos T. D., Spyropoulos I. C., Hamodrakas S. J. (2004b) PRED-TMBB: a web server for predicting the topology of beta-barrel outer membrane proteins. *Nucleic Acids Res.* 32: 400-404.

Baier K., Lehmann H., Stephan D.P., Lockau W. (2004). NblA is essential for phycobilisome degradation in *Anabaena* sp. strain PCC 7120 but not for development of functional heterocysts. *Microbiol.* 150: 2739-2749.

Bateman A., Coin L., Durbin R., Finn R.D., Hollich V., Griffiths-Jones S., Khanna A., Marshall M., Moxon S., Sonnhammer E.L., Studholme D.J., Yeats C., Eddy S.R. (2004) The Pfam protein families database. *Nucleic Acids Res*. 32(Database issue): D138-141.

Bauer C.C., Ramaswamy K.S., Endley S., Scappino L.A., Golden J.W., Haselkorn R. (1997) Suppression of heterocyst differentiation in *Anabaena* PCC 7120 by a cosmid carrying wild-type genes encoding enzymes for fatty acid synthesis. *FEMS Microbiol. Lett.* 151: 23-30.

Baumler A.J., Hantke K. (1992) A lipoprotein of *Yersinia enterocolitica* facilitates ferrioxamine uptake in Escherichia coli. *J. Bacteriol*. 174: 1029-1035.

Bendtsen J.D., Nielsen H., von Heijne G., Brunak S. (2004). Improved prediction of signal peptides: SignalP 3.0. *J. Mol. Biol.* 340: 783-795.

Bindereif A., Braun V., Hantke K. (1982) The cloacin receptor of ColV-bearing *Escherichia coli* is part of the Fe3+-aerobactin transport system. *J. Bacteriol.* 150: 1472-1475.

Black T.A., Cai Y., Wolk C.P. (1993) Spatial expression and autoregulation of *hetR*, a gene involved in the control of heterocyst development in *Anabaena*. *Mol. Microbiol*. 9: 77-84.

Black K., Buikema W.J., Haselkorn R. (1995) The *hglK* gene is required for localization of heterocyst-specific glycolipids in the cyanobacterium *Anabaena* sp. strain PCC 7120. *J. Bacteriol*. 177: 6440-6448.

Bölter B., Soll J., Schulz A., Hinnah S., Wagner R. (1998) Origin of a chloroplast protein importer. *Proc. Natl. Acad. Sci. USA.* 95: 15831-15836.

Bos M.P., Tefsen B., Geurtsen J., Tommassen J. (2004) Identification of an outer membrane protein required for the transport of lipopolysaccharide to the bacterial cell surface. *Proc. Natl. Acad. Sci. USA.* 101(25): 9417-9422.

Borthakur P.B., Orozco C.C., Young-Robbins S.S., Haselkorn R., Callahan S.M. (2005) Inactivation of *patS* and *hetN* causes lethal levels of heterocyst differentiation in the filamentous cyanobacterium *Anabaena* sp. PCC 7120. *Mol. Microbiol*. 57(1): 111-123.

Braun V. (1997) Surface signaling: novel transcription initiation mechanism starting from the cell surface. *Arch. Microbiol*. 167: 325–331.

Braun M., Silhavy T.J. (2002) Imp/OstA is required for cell envelope biogenesis in *Escherichia coli*. Mol Microbiol. 45(5):1289-1302.

Braun V., Mahren S., Ogierman M. (2003) Regulation of the FecI-type ECF sigma factor by transmembrane signalling. *Curr. Opin. Microbiol*. 6(2): 173-180.

Braun V., Mahren S., Sauter A. (2005) Gene regulation by transmembrane signaling. *Biometals.* 18(5): 507-517.

Bredemeier R., Schlegel T., Ertel F., Vojta A., Borissenko L., Bohnsack M.T., Groll M., von Haeseler A., Schleiff E. (2006). Functional and phylogenetic properties of the pore forming beta-barrel transporters of the Omp85 family. *J. Biol. Chem*. 282: 1882-1890.

Buchanan S.K., Smith B.S., Venkatramani L., Xia D., Esser L., Palnitkar M., Chakraborty R., van der Helm D., Deisenhofer J. (1999) Crystal structure of the outer membrane active transporter FepA from *Escherichia coli*. *Nat. Struct. Biol.* 6(1): 56-63.

Buchanan S.K. (2001) Type I secretion and multidrug efflux: transport through the TolC channel-tunnel. *Trends Biochem. Sci*. 26(1): 3-6.

Buchanan S.K. (2005) Bacterial metal detectors. *Mol. Microbiol.* 58(5): 1205-1209.

Buikema W. J., Haselkorn R. (1991) Characterization of a gene controlling heterocyst differentiation in the cyanobacterium *Anabaena* 7120. *Genes Dev*. 5: 321-330.

Cai Y.P., Wolk C.P. (1990) Use of a conditionally lethal gene in *Anabaena* sp. strain PCC 7120 to select for double recombinants and to entrap insertion sequences. *J. Bacteriol*. 172: 3138-3145.

Callahan S.M., Buikema W.J. (2001) The role of HetN in maintenance of the heterocyst pattern in *Anabaena* sp. PCC 7120. *Mol. Microbiol*. 40(4): 941-950.

Campbell E.L., Cohen M.F., Meeks J.C. (1997) A polyketide-synthase-like gene is involved in the synthesis of heterocyst glycolipids in *Nostoc punctiforme* strain ATCC 29133. *Arch. Microbiol*. 167: 251-258.

Cardemil L., Wolk C.P. (1976) The polysaccharides from heterocyst and spore envelopes of a blue-green alga. Methylation analysis and structure of the backbones. *J. Biol. Chem.* 251: 2967-2975.

Carvalho Ade O., Gomes V.M. (2007) Role of plant lipid transfer proteins in plant cell physiology-a concise review. *Peptides*. 28(5): 1144-1153.

Charvolin D., Douliez J.P., Marion D., Cohen-Addad C., Pebay-Peyroula E. (1999) The crystal structure of a wheat nonspecific lipid transfer protein (ns-LTP1) complexed with two molecules of phospholipid at 2.1 A resolution. *Eur. J. Biochem*. 264(2): 562-568.

Chimento D.P., Mohanty A.K., Kadner R.J., Wiener M.C. (2003) Substrate-induced transmembrane signaling in the cobalamin transporter BtuB. *Nat. Struct. Biol.* 10(5): 394-401.

Clarke S.E., Stuart J., Sanders-Loehr J. (1987) Induction of siderophore activity in *Anabaena* spp. and its moderation of copper toxicity. *Appl. Environ. Microbiol.* 53: 917-922.

Clarke T.E., Ku S.Y., Dougan D.R., Vogel H.J., Tari L.W. (2000) The structure of the ferric siderophore binding protein FhuD complexed with gallichrome. *Nat. Struct. Biol.* 7(4): 287-291.

Clarke T.E., Tari L.W., Vogel H.J. (2001) Structural biology of bacterial iron uptake systems. *Curr. Top. Med. Chem.* 1: 7-30.

Cobessi D., Celia H., Folschweiller N., Schalk I.J., Abdallah M.A., Pattus F. (2005a) The crystal structure of the pyoverdine outer membrane receptor FpvA from *Pseudomonas aeruginosa* at 3.6 angstroms resolution. *J. Mol. Biol.* 347(1): 121-134.

Cobessi D., Celia H., Pattus F. (2005b) Crystal structure at high resolution of ferric-pyochelin and its membrane receptor FptA from *Pseudomonas aeruginosa. J. Mol. Biol.* 352(4): 893-904.

Cope L.D., Yogev R., Muller-Eberhard U., Hansen E.J. (1995) A gene cluster involved in the utilization of both free heme and heme:hemopexin by *Haemophilus influenzae* type b. *J. Bacteriol.* 177: 2644-2653.

Cornelis P., Matthijs S. (2002) Diversity of siderophore-mediated iron uptake systems in fluorescent pseudomonads: not only pyoverdines. *Environ. Microbiol*. 4: 787-798.

Cornelissen C.N., Sparling P.F. (1994) Iron piracy: acquisition of transferrin-bound iron by bacterial pathogens. *Mol. Microbiol*. 14(5): 843-850.

Cornelissen C.N. (2003) Transferrin-iron uptake by Gram-negative bacteria. *Front. Biosci.* 8: d836-847.

Cotter P.A., Melville S.B., Albrecht J.A., Gunsalus R.P. (1997) Aerobic regulation of cytochrome d oxidase (cydAB) operon expression in *Escherichia coli:* roles of Fnr and ArcA in repression and activation. *Mol. Microbiol*. 25: 605-615.

Coulanges V., Andre P., Ziegler O., Buchheit L., Vidon D.J. (1997) Utilization of iron-catecholamine complexes involving ferric reductase activity in *Listeria monocytogenes*. *Infect Immun*. 65(7): 2778-85.

Cowan S.W., Schirmer T., Rummel G., Steiert M., Ghosh R., Pauptit R.A., Jansonius J.N., Rosenbusch J.P. (1992) Crystal structures explain functional properties of two *E. coli* porins. *Nature*. 358(6389): 727-733.

Crosa J.H., Walsh C.T. (2002) Genetics and assembly line enzymology of siderophore biosynthesis in bacteria. *Microbiol. Mol. Biol. Rev*. 66(2): 223-249.

Curatti L., Flores E., Salerno G. (2002) Sucrose is involved in the diazotrophic metabolism of the heterocyst-forming cyanobacterium *Anabaena* sp. *FEBS Lett.* 513(2-3): 175-178.

de Lorenzo V., Bindereif A., Paw B.H., Neilands J.B. (1986) Aerobactin biosynthesis and transport genes of plasmid ColV-K30 in *Escherichia coli* K-12. *J. Bacteriol.* 165: 570-578.

Delepelaire P. (2004) Type I secretion in Gram-negative bacteria. *Biochim. Biophys. Acta*. 1694(1-3): 149-161.

Dietz H., Pfeifle D., Wiedemann B. (1997) The signal molecule for beta-lactamase induction in *Enterobacter cloacae* is the anhydromuramyl-pentapeptide. *Antimicrob. Agents. Chemother.* 41: 2113-2120.

Doerrler W.T. (2006) Lipid trafficking to the outer membrane of Gram-negative bacteria. *Mol. Microbiol*. 60: 542-552.

Dong C., Beis K., Nesper J., Brunkan-Lamontagne A.L., Clarke B.R., Whitfield C., Naismith J.H. (2006) Wza the translocon for *E. coli* capsular polysaccharides defines a new class of membrane protein. *Nature*. 444(7116): 226-229.

Drechsel H., Jung G. (1998) Peptide siderophores. *J. Pept. Sci.* 4(3): 147-181.

Dyer D.W., West E.P., Sparling P.F. (1987) Effects of serum carrier proteins on the growth of pathogenic neisseriae with heme-bound iron. *Infect. Immun.* 55(9): 2171-2175.

Ehira S., Ohmori M., Sato N. (2003) Genome-wide expression analysis of the responses to nitrogen deprivation in the heterocyst-forming cyanobacterium *Anabaena* sp. strain PCC 7120. *DNA Res.* 10(3): 97-113.

Ehira S., Ohmori M. (2006). NrrA, a nitrogen-responsive response regulator facilitates heterocyst development in the cyanobacterium *Anabaena* sp. strain PCC 7120. *Mol. Microbiol.* 59: 1692-1703.

Elhai J., Wolk C.P. (1988a) A versatile class of positive-selection vectors based on the nonviability of palindrome-containing plasmids that allows cloning into long polylinkers. *Gene* 68: 119-138.

Elhai J., Wolk C.P. (1988b) Conjugal transfer of DNA to cyanobacteria. *Methods Enzymol.* 167: 747-754.

Elhai J., Wolk, C.P. (1990). Developmental regulation and spatial pattern of expression of the structural genes for nitrogenase in the cyanobacterium *Anabaena*. *EMBO J.* 9: 3379–3388.

Enz S., Mahren S., Stroeher U.H., Braun V. (2000) Surface signaling in ferric citrate transport gene induction: interaction of the FecA, FecR, and FecI regulatory proteins. *J. Bacteriol.* 182: 637–646.

Enz S., Brand H., Orellana C., Mahren S., Braun V. (2003) Sites of interaction between the FecA and FecR signal transduction proteins of ferric citrate transport in *Escherichia coli* K-12. *J. Bacteriol.* 185: 3745–3752.

Ernst A., Kirschenlohr H., Diez J., Böger P.. (1984) Glycogen content and nitrogenase activity in *Anabaena variabilis*. *Arch. Microbiol*. 140: 120-125.

Ernst A., Black T., Cai Y.,. Panoff J.M, Tiwari D.N., Wolk C.P.. (1992) Synthesis of nitrogenase in mutants of the cyanobacterium *Anabaena* sp. strain PCC 7120 affected in heterocyst development or metabolism. *J. Bacteriol.* 174: 6025-6032.

Ertel F., Mirus O., Bredemeier R., Moslavac S., Becker T., Schleiff E. (2005) The evolutionarily related beta-barrel polypeptide transporters from *Pisum sativum* and *Nostoc* PCC 7120 contain two distinct functional domains. *J. Biol. Chem.* 280: 28281-28289.

Escolar L., Pérez-Martín J., de Lorenzo V. (1998) Binding of the fur (ferric uptake regulator) repressor of *Escherichia coli* to arrays of the GATAAT sequence. *J. Mol. Biol*. 283(3): 537-547.

Escolar L., Perez-Martin J., de Lorenzo V. (1999) Opening the iron box: transcriptional metalloregulation by the Fur protein. *J. Bacteriol* 181: 6223–6229.

Escolar L., Pérez-Martín J., de Lorenzo V. (2000) Evidence of an unusually long operator for the fur repressor in the aerobactin promoter of *Escherichia coli. J. Biol. Chem*. 275(32): 24709-24714.

Fadeev E.A., Luo M., Groves J.T. (2005) Synthesis and structural modeling of the amphiphilic siderophore rhizobactin-1021 and its analogs. *Bioorg. Med. Chem. Lett*. 15(16): 3771-3774.

Falk S., Samson G., Bruce D., Hunner N.P., Laudenbach A. (1995) Functional analysis of the iron-stress induced CP 43′ polypeptide of PS II in the cyanobacterium *Synechococcus* sp. PCC 7942. *Photosynth. Res*. 45: 51-60.

Fan Q., Huang G., Lechno-Yossef S., Wolk C.P., Kaneko T., Tabata S. (2005) Clustered genes required for synthesis and deposition of envelope glycolipids in *Anabaena* sp. strain PCC 7120. *Mol. Microbiol*. 58: 227-243.

Faraldo-Gomez J.D, Sansom M.S. (2003) Acquisition of siderophores in Gram-negative bacteria. *Nat. Rev. Mol. Cell Biol.* 4: 105-116.

Fay P., Stewart W.D., Walsby A.E., Fogg G.E. (1968) Is the heterocyst the site of nitrogen fixation in blue-green algae? *Nature*. 220 (5169): 810-812.

Fay P. (1992) Oxygen relations of nitrogen fixation in cyanobacteria. *Microbiol. Rev.* 56: 340-373.

Feilmeier B.J., Iseminger G., Schroeder D., Webber H., Phillips G.J. (2000). Green fluorescent protein functions as a reporter for protein localization in *Escherichia coli*. *J. Bacteriol.* 182: 4068-4076.

Ferguson A.D., Chakraborty R., Smith B.S., Esser L., van der Helm D., Deisenhofer J. (2002) Structural basis of gating by the outer membrane transporter FecA. *Science*. 295(5560): 1715-1719.

Ferguson A.D., Hofmann E., Coulton J.W., Diederichs K., Welte W. (1998) Siderophore-mediated iron transport: crystal structure of FhuA with bound lipopolysaccharide. *Science*. 282(5397): 2215-2220.

Ferguson A.D., Deisenhofer J. (2002a) TonB-dependent receptors - structural perspectives. *Biochim. Biophys. Acta*. 1565: 318-332.

Ferguson A.D., Chakraborty R., Smith B.S., Esser L., van der Helm D., Deisenhofer J. (2002b) Structural basis of gating by the outer membrane transporter FecA. *Science.* 295: 1715–1719.

Ferguson A.D., Deisenhofer J. (2004) Metal import through microbial membranes. *Cell*. 116: 15–24.

Ferreira F., Straus N.A. (1994) Iron deprivation in cyanobacteria. *J. Appl. Phyc*. 6: 199-210.

Fiedler G., Arnold M., Hannus S., Maldener I. (1998a) The DevBCA exporter is essential for envelope formation in heterocysts of the cyanobacterium *Anabaena* sp. strain PCC 7120. *Mol. Microbiol*. 27: 1193-1202.

Fiedler G., Arnold M., Maldener I. (1998b). Sequence and mutational analysis of the *devBCA* gene cluster encoding a putative ABC transporter in the cyanobacterium *Anabaena variabilis* ATCC 29413. *Biochim. Biophys. Acta*. 1375: 140-143.

Fiedler G., Muro-Pastor A.M., Flores E., Maldener I. (2001) NtcA-dependent expression of the *devBCA* operon, encoding a heterocyst-specific ATP-binding cassette transporter in *Anabaena* spp. *J. Bacteriol.* 183(12): 3795-3799.

Fiore M.F., Trevors J.T. (1994) Cell composition and metal tolerance in cyanobacteria. *BioMetals.* 7: 83-103.

Flores E., Herrero A., Wolk C.P., Maldener I. (2006) Is the periplasm continuous in filamentous multicellular cyanobacteria? *Trends Microbiol*. 14: 439-443.

Forst D., Welte W., Wacker T., Diederichs K. (1998) Structure of the sucrose-specific porin ScrY from *Salmonella typhimurium* and its complex with sucrose. *Nat. Struct. Biol.* 5(1): 37-46.

Frías J.E., Flores E., Herrero A. (1994) Requirement of the regulatory protein NtcA for the expression of nitrogen assimilation and heterocyst development genes in the cyanobacterium *Anabaena* sp. PCC 7120. *Mol. Microbiol*. 14: 823-832.

Fulda S., Huang F., Nilsson F., Hagemann M., Norling B. (2000) Proteomics of *Synechocystis* sp. Strain PCC 6803. Identification of periplasmic proteins in cells grown at low and high salt concentrations. *Eur. J. Biochem*. 267: 5900-5907.

Furano K., Luke N.R., Howlett A.J., Campagnari A.A. (2005) Identification of a conserved *Moraxella catarrhalis* haemoglobin-utilization protein, MhuA. *Microbiology*. 151: 1151-1158.

Furrer J.L., Sanders D.N., Hook-Barnard I.G., McIntosh M.A. (2002) Export of the siderophore enterobactin in *Escherichia coli:* involvement of a 43 kDa membrane exporter. Mol. *Microbiol.* 44(5): 1225-1234.

Gallon J. R. (1992) Tansley Review No. 44. Reconciling the Incompatible: N2 Fixation and O2 New Phytologist, Vol. 122, No. 4 pp. 571-609.

Gambacorta A., Romano I., Sodano G., Trincone A. (1998) Heterocyst glycolipids from nitrogen fixing cyanobacteria other then *Nostocaceae*. *Phytochem*. 48: 801-805.

Gantt E. (1994) in The Molecular Biology of Cyanobacteria (Bryant, D. A., ed) pp. 119-138, Kluwer, Dordrecht, The Netherlands.

Gardy J.L., Laird M.R., Chen F., Rey S., Walsh C.J., Ester M., Brinkman F.S. (2005). PSORTb v.2.0: expanded prediction of bacterial protein subcellular localization and insights gained from comparative proteome analysis. *Bioinformatics*. 21: 617-623.

Genco C.A., Desai P.J. (1996) Iron acquisition in the pathogenic *Neisseria*. *Trends. Microbiol*. 4: 179-184.

Genevrois S., Steeghs L., Roholl P., Letesson J.J., van der Ley P. (2003) The Omp85 protein of *Neisseria meningitidis* is required for lipid export to the outer membrane. *EMBO J.* 22(8): 1780-1789.

Giddings T.H. Jr., Staehelin L.A. (1979) Changes in thylakoid structure associated with the differentiation of heterocysts in the cyanobacterium, *Anabaena cylindrica*. *Biochim. Biophys. Acta* 546: 373-382.

Glaser P., Sakamoto H., Bellalou J., Ullmann A., Danchin A. (1988) Secretion of cyclolysin, the calmodulin-sensitive adenylate cyclase-haemolysin bifunctional protein of *Bordetella pertussis*. *EMBO J*. 7: 3997-4004.

Golden J.W., Whorff L.L., Wiest D.R. (1991). Independent regulation of *nifHDK* operon transcription and DNA rearrangement during heterocyst differentiation in the cyanobacterium *Anabaena* sp. strain PCC 7120. *J. Bacteriol*. 173: 7098-7105.

Golden J.W., Yoon H.S. (2003) Heterocyst development in *Anabaena*. *Curr. Opin. Microbiol.* 6(6): 557-563.

Goldman S.J., Lammers P.J., Berman M.S., Sanders-Loehr J. (1983) Siderophore-mediated iron uptake in different strains of *Anabaena* sp. *J. Bacteriol*. 156: 1144-1150.

Gray-Owen S.D., Schryvers A.B. (1996) Bacterial transferrin and lactoferrin receptors. *Trends Microbiol*. 4(5): 185-191.

Gruber M., Soding J., Lupas A.N. (2005) REPPER--repeats and their periodicities in fibrous proteins. *Nucleic Acids Res*. 33: W239-243.

Guglielmi G., Cohen-Bazire G. (1982) Structure et distribution des pores et des perforations de l'enveloppe de peptydoglycane chez quelques cyanobacteries. *Parisitologica* 18: 152-165.

Guikema J.A., Sherman L.A. (1983) Organization and Function of Chlorophyll in Membranes of Cyanobacteria during Iron Starvation. *Plant Physiol*. 73(2): 250-256.

Hanahan D. (2005) Techniques for transformation of *E. coli*. In DNA cloning I, a practical approach, Glover, D.M.; ed., IRL PressLtd, Oxford, 109-135.

Haury J.F., Wolk C.P. (1978) Classes of *Anabaena variabilis* mutants with oxygen-sensitive nitrogenase activity. *J. Bacteriol.* 136: 688-692.

Havaux M. (2003) Spontaneous and thermoinduced photon emission: new methods to detect and quantify oxidative stress in plants. *Trends Plant Sci*. 8: 409-413.

Havaux M., Triantaphylides C., Genty B. (2006) Autoluminescence imaging: a non-invasive tool for mapping oxidative stress. *Trends Plant Sci.* 11, 480-484.

Heins L., Soll J. (1998) Chloroplast biogenesis: mixing the prokaryotic and the eukaryotic? *Curr. Biol.* 8(6): R215-217.

Herrero A., Muro-Pastor A.M., Flores E. (2001) Nitrogen control in cyanobacteria. *J. Bacteriol.* 183: 411-425.

Herrero A., Muro-Pastor A.M., Valladares A., Flores E. (2004) Cellular differentiation and the NtcA transcription factor in filamentous cyanobacteria. *FEMS Microbiol. Rev*. 28(4): 469-487.

Higgs P.I., Myers P.S., Postle K. (1998) Interactions in the TonB-dependent energy transduction complex: ExbB and ExbD form homomultimers. *J. Bacteriol.* 180(22): 6031-6038.

Higgs P.I., Larsen R.A., Postle K. (2002) Quantification of known components of the *Escherichia coli* TonB energy transduction system: TonB, ExbB, ExbD and FepA. *Mol. Microbiol*. 44(1): 271-281.

Hopwood D.A., D.H. Sherman. (1990) Molecular genetics of polyketides and its comparison to fatty acid biosynthesis. *Annu. Rev. Genet.* 24: 37-66.

Huang F., Hedman E., Funk C., Kieselbach T., Schroder W.P., Norling B. (2004) Isolation of outer membrane of *Synechocystis* sp. PCC 6803 and its proteomic characterization. *Mol. Cell Proteomics*. 3: 586-595.

Huang G., Fan Q., Lechno-Yossef S., Wojciuch E., Wolk C.P., Kaneko T., Tabata S.. (2005) Clustered genes required for the synthesis of heterocyst envelope polysaccharide in *Anabaena* sp. strain PCC 7120. *J. Bacteriol.* 187: 1114-1123.

Hutber G.N., Hutson K.G., Rogers L.J. (1977) Effect of iron deficiency on levels of two ferredoxins and flavodoxin in a cyanobacterium. *FEMS Microbiol. Lett.* 1: 193–196.

Hynes R.O. (2002) A reevaluation of integrins as regulators of angiogenesis. *Nat. Med.* 8(9): 918-921.

Ignoul S., Eggermont J. (2005) CBS domains: structure, function, and pathology in human proteins. *Am. J. Physiol. Cell Physiol.* 289: C1369-1378.

Ikeda T.P., Shauger A.E., Kustu S. (1996) *Salmonella typhimurium* apparently perceives external nitrogen limitation as internal glutamine limitation. *J. Mol. Biol.* 259(4): 589-607.

Ishida K. (2005) Protein targeting into plastids: a key to understanding the symbiogenetic acquisitions of plastids. *J. Plant Res.* 118(4): 237-245.

Ivanov A.G., Krol M., Sveshnikov D., Selstam E., Sandstrom S., Koochek M., Park Y.I., Vasil'ev S., Bruce D., Oquist G., Huner N.P. (2006) Iron deficiency in cyanobacteria causes monomerization of photosystem I trimers and reduces the capacity for state

transitions and the effective absorption cross section of photosystem I in vivo. *Plant Physiol.* 141: 1436-1445.

Jubelin G., Vianney A., Beloin C., Ghigo J.M., Lazzaroni J.C., Lejeune P., Dorel C. (2005) CpxR/OmpR interplay regulates curli gene expression in response to osmolarity in *Escherichia coli*. *J. Bacteriol*. 187(6): 2038-2049.

Jackson S.E., Craggs T.D., Huang J.R. (2006) Understanding the folding of GFP using biophysical techniques. *Expert. Rev. Proteomics*. 3: 545-559.

Johnson J.M., Church G.M. (1999) Alignment and structure prediction of divergent protein families: periplasmic and outer membrane proteins of bacterial efflux pumps. *J. Mol. Biol.* 287(3): 695-715.

Jordan P., Fromme P., Witt H.T., Klukas O., Saenger W., Krauss N. (2001) Three-dimensional structure of cyanobacterial photosystem I at 2.5 A resolution. *Nature.* 411: 909–917.

Juncker A.S., Willenbrock H., von Heijne G., Nielsen H., Brunak S., Krogh A. (2003) Prediction of lipoprotein signal peptides in Gram-negative bacteria. *Protein Sci*. 12: 1652-1662.

Kader J.C. (1997). Lipid-transfer proteins: A puzzling family of plant proteins. *Trends. Plant Sci.* 2: 66–70.

Kadner R. J. (1990).Vitamin B12 transport in *Escherichia coli:* energy coupling between membranes. *Mol. Microbiol*. 4: 2027-2033

Kamio Y., Nikaido H. (1976) Outer membrane of *Salmonella typhimurium*: accessibility of phospholipid head groups to phospholipase c and cyanogen bromide activated dextran in the external medium. *Biochemistry*. 15(12): 2561-1570.

Kamiya N., Shen J.R. (2003) Crystal structure of oxygen-evolving photosystem II from *Thermosynechococcus vulcanus* at 3.7-A resolution. *Proc. Natl. Acad. Sci. USA* 100: 98–103.

Kammler M., Schön C., Hantke K. (1993) Characterization of the ferrous iron uptake system of *Escherichia coli*. *J. Bacteriol.* 175(19): 6212-6219.

Kaneko T., Nakamura Y., Wolk C.P., *et al*. (2001) Complete genomic sequence of the filamentous nitrogen-fixing cyanobacterium *Anabaena* sp. strain PCC 7120. *DNA Res.* 8: 205-213.

Kanemasa Y., Akamatsu Y., Nojima S. (1967) Composition and turnover of the phospholipids in *Escherichia coli.* Biochim. Biophys. Acta. 144(2): 382-390.

Katoh H., Hagino N., Grossman A.R., Ogawa T. (2001) Genes essential to iron transport in the cyanobacterium *Synechocystis* sp. strain PCC 6803. *J. Bacteriol*. 183: 2779-2784.

Keating T.A., Miller D.A., Walsh C.T. (2000) Expression, purification, and characterization of HMWP2, a 229 kDa, six domain protein subunit of *Yersiniabactin synthetase*. *Biochemistry*. 39(16):4729-4739.

Keegstra K., Werner-Washburne M., Cline K., Andrews J. (1984) The chloroplast envelope: is it homologous with the double membranes of mitochondria and Gram-negative bacteria? *J. Cell. Biochem*. 24: 55-68.

Keren N., Aurora R., Pakrasi H.B. (2004) Critical roles of bacterioferritins in iron storage and proliferation of cyanobacteria. *Plant Physiol.* 135: 1666-1673.

Kim I., Stiefel A., Plantor S., Angerer A., Braun V. (1997) Transcription induction of the ferric citrate transport genes via the N-terminus of the FecA outer membrane protein, the Ton system and the electrochemical potential of the cytoplasmic membrane. *Mol. Microbiol*. 23: 333–344.

Klebba P.E., Newton S.M. (1998) Mechanisms of solute transport through outer membrane porins: burning down the house. *Curr. Opin. Microbiol*. 1(2): 238-247.

Koebnik R., Hantke K., Braun V. (1993) The TonB-dependent ferrichrome receptor FcuA of *Yersinia enterocolitica*: evidence against a strict co-evolution of receptor structure and substrate specificity. *Mol. Microbiol.* 7: 383-393.

Koebnik R., Locher K.P., Van Gelder P. (2000) Structure and function of bacterial outer membrane proteins: barrels in a nutshell. *Mol. Microbiol*. 37: 239-253.

Koebnik R. (2005) TonB-dependent trans-envelope signalling: the exception or the rule? *Trends Microbiol.* 13: 343–347.

Koronakis V., Hughes C. (1993) Bacterial signal peptide-independent protein export: HlyB-directed secretion of hemolysin. *Semin. Cell Biol*. 4(1): 7-15.

Koronakis V., Sharff A., Koronakis E., Luisi B., Hughes C. (2000) Crystal structure of the bacterial membrane protein TolC central to multidrug efflux and protein export. *Nature.* 405: 914-919.

Koronakis V., Eswaran J., Hughes C. (2004) Structure and function of TolC: the bacterial exit duct for proteins and drugs. *Annu. Rev. Biochem*. 73: 467-489.

Krogh A., Larsson B., von Heijne G., Sonnhammer E.L.L. (2001) Predicting transmembrane protein topology with a hidden Markov model: Application to complete genomes. *J. Mol. Biol*. 305: 567-580.

Lammers P. J., Sanders-Loehr J. (1982) Active transport of ferric schizokinen in *Anabaena* sp. *J. Bacteriol.* 151: 288-294.

Lang N.J., Fay P.Y. (1971) The heterocysts of bluegreen algae. II. Details of ultrastructure. *Proc. R. Soc. Lond. B. Biol. Sci.* 178: 193-203.

Latifi A., Jeanjean R., Lemeille S., Havaux M., Zhang C.C. (2005) Iron starvation leads to oxidative stress in *Anabaena* sp. strain PCC 7120. *J. Bacteriol.* 187: 6596-6598.

Laudenbach D.E., Straus N.A. (1988) Characterization of a cyanobacterial iron stress-induced gene similar to *psbC*. *J. Bacteriol.* 170: 5018-5026.

Laurent S., Chen H., Bédu S., Ziarelli F., Peng L., Zhang C.C. (2005) Nonmetabolizable analogue of 2-oxoglutarate elicits heterocyst differentiation under repressive conditions in *Anabaena* sp. PCC 7120. *Proc. Natl. Acad. Sci. USA*. 102(28): 9907-9912.

Le Cam E., Frechon D., Barray M., Fourcade A., Delain E. (1994) Observation of binding and polymerization of Fur repressor onto operator-containing DNA with electron and atomic force microscopes. *Proc. Natl. Acad. Sci. USA*. 91(25): 11816-11820.

Lee B.C. (1995) Quelling the red menace: haem capture by bacteria. *Mol. Microbiol*. 18(3): 383-390.

LeVier K.; Guerinot M.L. (1996) The *Bradyrhizobium japonicum fegA* gene encodes an iron-regulated outer membrane protein with similarity to hydroxamate-type siderophore receptors. *J. Bacteriol*. 178: 7265-7275.

Levy S.B. (1992) Active Efflux Mechanisms for Antimicrobial Resistance. *Antimicrob-Agents Chemother*. 36: 695-703.

Lindquist S., Weston-Hafer K., Schmidt H., Pul C., Korfmann G., Erickson J., Sanders C., Martin H.H., Normark S. (1993) AmpG, a signal transducer in chromosomal beta-lactamase induction. *Mol. Microbiol.* 9: 703-715.

Locher K.P., Rees B., Koebnik R., Mitschler A., Moulinier L., Rosenbusch J.P., Moras D. (1998) Transmembrane signaling across the ligand-gated FhuA receptor: crystal structures of free and ferrichrome-bound states reveal allosteric changes. *Cell*. 95(6): 771-778.

Lonetto M.A., Brown K.L., Rudd K.E., Buttner M.J. (1994) Analysis of the *Streptomyces coelicolor sigE* gene reveals the existence of a subfamily of eubacterial RNA polymerase sigma factors involved in the regulation of extracytoplasmic functions. *Proc. Natl. Acad. Sci. USA.* 91(16): 7573-7577.

Luck S.N., Turner S.A., Rajakumar K., Sakellaris H., Adler B. (2001) Ferric dicitrate transport system (Fec) of *Shigella flexneri* 2a YSH6000 is encoded on a novel pathogenicity island carrying multiple antibiotic resistance genes. *Infect. Immun*. 69(10): 6012-6021.

Luirink J., Samuelsson T., de Gier J.W. (2001) YidC/Oxa1p/Alb3: evolutionarily conserved mediators of membrane protein assembly. *FEBS Lett.* 501(1): 1-5.

Lundrigan M.D., Kadner R.J. (1986) Nucleotide sequence of the gene for the ferrienterochelin receptor FepA in *Escherichia coli*. Homology among outer membrane receptors that interact with TonB. *J. Biol. Chem.* 261(23): 10797-10801.

Mahren S., Schnell H., Braun V. (2005) Occurrence and regulation of the ferric citrate transport system in *Escherichia coli B, Klebsiella pneumoniae, Enterobacter aerogenes, and Photorhabdus luminescens*. *Arch. Microbiol.* 184(3): 175-186.

Maldener I., Fiedler G., Ernst A., Fernandez-Pinas F., Wolk C.P. (1994) Characterization of *devA*, a gene required for the maturation of proheterocysts in the cyanobacterium *Anabaena* sp. strain PCC 7120. *J. Bacteriol*. 176: 7543-7549.

Maldener I., Hannus S., Kammerer M. (2003) Description of five mutants of the cyanobacterium *Anabaena* sp strain PCC 7120 affected in heterocyst differentiation and identification of the transposon-tagged genes. *FEMS Microbiol. Lett*. 224: 205-213.

Martin W., Stoebe B., Goremykin V., Hapsmann S., Hasegawa M., Kowallik K.V. (1998a) Gene transfer to the nucleus and the evolution of chloroplasts. *Nature*. 393(6681): 162-165.

Martin W., Rujan T., Richly E., Hansen A., Cornelsen S., Lins T., Leister D., Stoebe B., Hasegawa M., and Penny D. (2002) Evolutionary analysis of *Arabidopsis*, cyanobacterial, and chloroplast genomes reveals plastid phylogeny and thousands of cyanobacterial genes in the nucleus. *Proc. Natl. Acad. Sci. USA.* 99: 12246-12251.

Martínez J.L., Herrero M., de Lorenzo V. (1994) The organization of intercistronic regions of the aerobactin operon of pColV-K30 may account for the differential expression of the *iucABCD iutA* genes. *J. Mol. Biol.* 238(2): 288-293.

Mazoy R., Osorio C.R., Toranzo A.E., Lemos M.L. (2003) Isolation of mutants of *Vibrio anguillarum* defective in haeme utilisation and cloning of *huvA*, a gene coding for an outer membrane protein involved in the use of haeme as iron source. *Arch. Microbiol.* 179: 329-338.

Meeks J.C., Elhai J. (2002) Regulation of cellular differentiation in filamentous cyanobacteria in free-living and plant-associated symbiotic growth states. *Microbiol. Mol. Biol. Rev*. 66(1): 94-121

Mey A.R., Payne S.M. (2001) Haem utilization in *Vibrio cholerae* involves multiple TonB-dependent haem receptors. *Mol. Microbiol*. 42: 835-849.

Mey A.R., Wyckoff E.E., Oglesby A.G., Rab E., Taylor R.K., Payne S.M. (2002) Identification of the *Vibrio cholerae* enterobactin receptors VctA and IrgA: IrgA is not required for virulence. *Infect. Immun*. 70: 3419-3426.

Michel K.P., Pistorius E.K. (2004) Adaptation of the photosynthetic electron transport chain in cyanobacteria to iron deficiency: The function of IdiA and IsiA. *Physiol. Plant*. 120(1): 36-50.

Minh B.Q., Vinh L.S., von Haeseler A., Schmidt H.A. (2005) pIQPNNI: Parallel reconstruction of large maximum likelihood phylogenies. *Bioinformatics*. 21: 3794-3796.

Mirus O., Schleiff E. (2005). Prediction of beta-barrel membrane proteins by searching for restricted domains. *BMC Bioinformatics.* 6: 254.

Mourino S., Rodriguez-Ares I., Osorio C.R., Lemos M.L. (2005) Genetic variability of the heme uptake system among different strains of the fish pathogen *Vibrio anguillarum*: identification of a new heme receptor. *Appl. Environ. Microbiol*. 71: 8434-8441.

Murata N., Omata T. (1988) Isolation of cyanobacterial plasma membranes. *Methods Enzymol*. 167: 245-251.

Muro-Pastor A.M., Olmedo-Verd E., Flores E. (2006). All4312, an NtcA-regulated two-component response regulator in *Anabaena* sp. strain PCC 7120. *FEMS Microbiol. Lett*. 256: 171-177.

Murry M.A., Wolk C.P. (1989) Evidence that the barrier to the penetration of oxygen into heterocysts depends upon two layers of the cell envelope. *Arch. Microbiol.* 151: 469-474.

Neilands J.B. (1995) Siderophores: structure and function of microbial iron transport compounds. *J. Biol. Chem*. 270(45): 26723-26726.

Nieuwland J., Feron R., Huisman B.A., Fasolino A., Hilbers C.W., Derksen J., Mariani C. (2005) Lipid transfer proteins enhance cell wall extension in tobacco. *Plant Cell*. 17(7): 2009-2019.

Nikaido H. (2003) Molecular basis of bacterial outer membrane permeability revisited. *Microbiol. Mol. Biol. Rev.* 67(4): 593-656.

Norling B., Zak E., Andersson B., Pakrasi H. (1998) 2D-isolation of pure plasma and thylakoid membranes from the cyanobacterium Synechocystis PCC680. *FEBS Lett.* 436: 189-192.

Ochsner U.A., Johnson Z., Vasil M.L. (2000) Genetics and regulation of two distinct haem-uptake systems, *phu* and *has*, in *Pseudomonas aeruginosa*. *Microbiology*. 146: 185-198.

Olmedo-Verd E., Flores E., Herrero A., Muro-Pastor A.M. (2005). HetR-dependent and -independent expression of heterocyst-related genes in an *Anabaena* strain overproducing the NtcA transcription factor. *J. Bacteriol*. 187: 1985-1991.

Olmedo-Verd E., Muro-Pastor A.M., Flores E., Herrero A. (2006) Localized Induction of the *ntcA* Regulatory Gene in Developing Heterocysts of *Anabaena* sp. Strain PCC 7120. *J. Bacteriol.* 188: 6694-6699.

Omata T., Murata N. (1984). Isolation and characterization of three types of membranes from the cyanobacterium (blue green alga) *Synechocystis* sp. PCC 6714. *Arch. Microbiol*. 139: 113-116.

Omata T. (1995) Structure, function and regulation of the nitrate transport system of the cyanobacterium *Synechococcus* sp. PCC7942. *Plant Cell Physiol.* 36(2): 207-213.

Park J.T. (1995) Why does *Escherichia coli* recycle its cell wall peptides? *Mol. Microbiol.* 17: 421-426.

Paschen S.A., Neupert W., Rapaport D. (2005) Biogenesis of beta-barrel membrane proteins of mitochondria. *Trends Biochem. Sci*. 30(10): 575-582.

Paulsen I.T., Park J.H., Choi P.S., Saier M.H. (1997) A family of Gram-negative bacterial outer membrane factors that function in the export of proteins, carbohydrates, drugs and heavy metals from Gram-negative bacteria. *FEMS Microbiol. Lett.* 156(1): 1-8.

Pelludat C., Rakin A., Jacobi C.A., Schubert S., Heesemann J. (1998) The yersiniabactin biosynthetic gene cluster of *Yersinia enterocolitica*: organization and siderophore-dependent regulation. *J. Bacteriol*. 180: 538-546.

Perkins-Balding D., Ratliff-Griffin M., Stojiljkovic I. (2004) Iron transport systems in *Neisseria meningitidis*. *Microbiol. Mol. Biol. Rev*. 68: 154-171.

Perry R.D., Balbo P.B., Jones H.A., Fetherston J.D., DeMoll E. (1999) Yersiniabactin from *Yersinia pestis*: biochemical characterization of the siderophore and its role in iron transport and regulation. *Microbiology*. 145(Pt 5): 1181-1190.

Pfanner N., Wiedemann N. (2002) Mitochondrial protein import: two membranes, three translocases. *Curr. Opin. Cell. Biol*. 4(4): 400-411.

Picossi S., Montesinos M.L.,. Pernil R., Lichtle C., Herrero A., Flores E. (2005) ABC-type neutral amino acid permease N-I is required for optimal diazotrophic growth and is repressed in the heterocysts of *Anabaena* sp. strain PCC 7120. *Mol. Microbiol*. 57: 1582-1592.

Poole K. (2001) Multidrug resistance in Gram-negative bacteria. *Curr. Opin. Microbiol.* 4: 500-508.

Posadas D.M., Martín F.A., Sabio y García J.V., Spera J.M., Delpino M.V., Baldi P., Campos E., Cravero S.L., Zorreguieta A. (2006) The TolC homologue of *Brucella suis* is involved in resistance to antimicrobial compounds and virulence. *Infect Immun.* 75(1): 379-389.

Postle K., Kadner R.J. (2003) Touch and go: tying TonB to transport. *Mol. Microbiol.* 49: 869–882.

Postle K. (1990) TonB and the Gram-negative dilemma. *Mol. Microbiol.* 4: 2019-2025.

Pradel E., Locht C. (2001) Expression of the putative siderophore receptor gene *bfrZ* is controlled by the extracytoplasmic-function sigma factor BupI in *Bordetella bronchiseptica*. *J. Bacteriol.* 183: 2910-2917.

Raikwar N.S., Bowen R.F., Deeg M.A. (2005) Mutating His29, His125, His133 or His158 abolishes glycosylphosphatidylinositol-specific phospholipase D catalytic activity. *Biochem. J.* 391(Pt 2): 285-289.

Rakin A., Saken E., Harmsen D., Heesemann J. (1994) The pesticin receptor of *Yersinia enterocolitica*: a novel virulence factor with dual function. *Mol. Microbiol.* 13: 253-263.

Ramírez M.E., Hebbar P.B., Zhou R., Wolk C.P., Curtis S.E. (2005) *Anabaena* sp. strain PCC 7120 gene *devH* is required for synthesis of the heterocyst glycolipid layer. *J. Bacteriol*. 187(7): 2326-2331.

Rensing C., Grass G. (2003) *Escherichia coli* mechanisms of copper homeostasis in a changing environment. *FEMS Microbiol Rev.* 27(2-3): 197-213.

Rice C.W., Hempfling W.P. (1978) Oxygen-limited continuous culture and respiratory energy conservation in *Escherichia coli*. *J. Bacteriol*. 134(1): 115-124.

Rippka R., Dereules J., Waterbury J.B, Herdman M., Stanier R.Y. (1979) Generic assignments, strain stories and properties of pure cultures of cyanobacteria. *J. Gen. Microbiol.* 111: 1-61.

Robinson C., Thompson S.J., Woolhead C. (2001) Multiple pathways used for the targeting of thylakoid proteins in chloroplasts. *Traffic*. 2: 245-51.

Ruiz N., Kahne D., Silhavy T.J. (2006) Advances in understanding bacterial outer-membrane biogenesis. *Nat. Rev. Microbiol*. 4(1): 57-66.

Rusch S.L., Kendall D.A. (2007) Oligomeric states of the SecA and SecYEG core components of the bacterial Sec translocon. *Biochim. Biophys. Acta.* 1768(1):5-12.

Saiki R.K, Gelfand D.H., Stoffel S., Scharf S.J., Higuchi R., Horn G.T., Mullis K.B., Erlich H.A. (1988) Primer-directed enzymatic amplification of DNA with a thermostable DNA polymerase. *Science*. 239(4839): 487-491.

Sali A., Blundell T.L. (1993) Comparative protein modelling by satisfaction of spatial restraints. *J. Mol. Biol.* 234: 779-815.

Sambrook J.F., Fritsch E.F., Maniatis T. (1989) Molecular Cloning: A Laboratory Manual New York. *Cold Spring Harbor Laboratory Press*, New York.

Sandmann G., Peleato M.L., Fillat M.F., Lazaro M.C., Gomez-Moreno C. (1990) Consequences of the iron-dependent formation of ferredoxin and flavodoxin on photosynthesis and nitrogen fixation on *Anabaena* strains. *Photosynthesis Research*. 26: 119-125.

Schalk I.J., Yue W.W., Buchanan S.K. (2004) Recognition of iron-free siderophores by TonB-dependent iron transporters. *Mol. Microbiol*. 54: 14–22.

Schirmer T., Keller T.A., Wang Y.F., Rosenbusch J.P. (1995) Structural basis for sugar translocation through maltoporin channels at 3.1 A resolution. *Science*. 267(5197): 512-514.

Schleiff E., Soll J., Küchler M., Kühlbrandt W., Harrer R. (2003a) Characterization of the translocon of the outer envelope of chloroplasts. *J. Cell Biol.* 160(4): 541-551.

Schleiff E., Eichacker L.A., Eckart K., Becker T., Mirus O., Stahl T., Soll, J. (2003b) Prediction of the plant beta-barrel proteome: a case study of the chloroplast outer envelope. *Protein Sci.* 12: 748-759.

Schleiff E., Soll J. (2005) Membrane protein insertion: mixing eukaryotic and prokaryotic concepts. *EMBO Rep.* 6(11):1023-1027.

Schmetterer G., Valladares A., Pils D., Steinbach S., Pacher M., Muro-Pastor A.M., Flores E., Herrero A. (2001) The *coxBAC* operon encodes a cytochrome c oxidase required for heterotrophic growth in the cyanobacterium *Anabaena variabilis* strain ATCC 29413. *J. Bacteriol.* 183(21): 6429-6434.

Schramm E., Mende J., Braun V., Kamp R.M. (1987) Nucleotide sequence of the colicin B activity gene *cba*: consensus pentapeptide among TonB-dependent colicins and receptors. *J. Bacteriol*. 169(7): 3350-3357.

Sharff A., Fanutti C., Shi J., Calladine C., Luisi B. (2001) The role of the TolC family in protein transport and multidrug efflux. From stereochemical certainty to mechanistic hypothesis. *Eur. J. Biochem.* 268: 5011-5026.

Singh A.K., McIntyre L.M., Sherman L.A. (2003) Microarray analysis of the genome-wide response to iron deficiency and iron reconstitution in the cyanobacterium *Synechocystis sp.* PCC 6803. *Plant Physiol.* 132: 1825-1839.

Sleytr U. B., Beveridge T. J. (1999) Bacterial S-layers. *Trends. Microbiol*. 7: 253-260.

Slynn G.M., Sammons R.L., Smith D.A., Moir A., Corfe, B.M. (1994). Molecular genetical and phenotypical analysis of the gerM spore germination gene of *Bacillus subtilis* 168. *FEMS Microbiol. Lett.* 121: 315-320.

Smarda J., Smajs D., Komrska J., Krzyzanek, V. (2001) S-layers on cell walls of cyanobacteria. *Micron.* 33: 57-77.

Smit J., Kamio Y., Nikaido H. (1975) Outer membrane of *Salmonella typhimurium:* chemical analysis and freeze-fracture studies with lipopolysaccharide mutants. *J. Bacteriol.* 124(2): 942-958.

Smith B.S., Kobe B., Kurumbail R., Buchanan S.K., Venkatramani L., Van Der Helm D., Deisenhofer J. (1998) Crystallization and preliminary X-ray analysis of ferric enterobactin receptor FepA, an integral membrane protein from *Escherichia coli*. *Acta. Crystallogr. D. Biol. Crystallogr.* 54(Pt 4): 697-699.

So A.K., Espie G.S., Williams E.B., Shively J.M., Heinhorst S., Cannon G.C. (2004) A novel evolutionary lineage of carbonic anhydrase (epsilon class) is a component of the carboxysome shell. *J. Bacteriol.* 186: 3-30.

Soll J., Schleiff E. (2004) Protein import into chloroplasts. *Nat. Rev. Mol. Cell Biol.* 5: 198-208.

Srikumar R., Mikael L.G., Pawelek P.D., Khamessan A., Gibbs B.F., Jacques M., Coulton J.W. (2004) Molecular cloning of haemoglobin-binding protein HgbA in the outer membrane of *Actinobacillus pleuropneumoniae. Microbiology.* 150: 1723-1734.

Sterk P., Booij H., Schellekens G.A., Van Kammen A., De Vries S.C. (1991) Cell-specific expression of the carrot EP2 lipid transfer protein gene. *Plant Cell*. 3: 907 921.

Stroebel D., Choquet Y., Popot J.L., Picot D. **(**2003) An atypical haem in the cytochrome b_6f complex. *Nature.* 426**:** 413–418.

Tamm L.K., Hong H., Liang B. (2004) Folding and assembly of beta-barrel membrane proteins. *Biochim. Biophys. Acta.* 1666(1-2): 250-263.

Thanabalu T., Koronakis E., Hughes C., Koronakis V. (1998) Substrate-induced assembly of a contiguous channel for protein export from *E. coli*: Reversible bridging of an inner-membrane translocase to an outer membrane exit pore. *EMBO J.* 17: 6487–6496.

Thanassi D.G., Hultgren S.J. (2000) Multiple pathways allow protein secretion across the bacterial outer membrane. *Curr. Opin. Cell Biol.* 12: 420-430.

Thomas J., Meeks J.C., Wolk C.P., Shaffer P.W., Austin S.M. (1977) Formation of glutamine from [13n]ammonia, [13n]dinitrogen, and [14C]glutamate by heterocysts isolated from *Anabaena cylindrica*. *J. Bacteriol.* 129(3): 1545-1555.

Thomas J.D., Daniel R.A., Errington J., Robinson C. (2001). Export of active green fluorescent protein to the periplasm by the twin-arginine translocase (Tat) pathway in *Escherichia coli*. *Mol. Microbiol.* 39: 47-53.

Timmis J.N., Ayliffe M.A., Huang C.Y., Martin W. (2004) Endosymbiotic gene transfer: organelle genomes forge eukaryotic chromosomes. *Nat. Rev. Genet.* 5(2): 123-135.

Ting C.S, Rocap G., King J., Chisholm S.W. (2002) Cyanobacterial photosynthesis in the oceans: the origins and significance of divergent light-harvesting strategies. *Trends. Microbiol.* 10(3): 134-142.

Tokuda H., Matsuyama S. (2004) Sorting of lipoproteins to the outer membrane in *E. coli*. *Biochim. Biophys. Acta*. 1694(1-3): IN1-9.

Valladares A., Muro-Pastor A.M., Fillat M.F., Herrero A., Flores E. (1999) Constitutive and nitrogen-regulated promoters of the *petH* gene encoding ferredoxin:NADP+ reductase in the heterocyst-forming cyanobacterium *Anabaena* sp. *FEBS Lett.* 449: 159-164.

Valladares A., Herrero A., Pils D. Schmetterer G., Flores E. (2003) Cytochrome c oxidase genes required for nitrogenase activity and diazotrophic growth in *Anabaena* sp. PCC 7120. *Mol. Microbiol*. 47: 1239-1249.

Vinh L.S., von Haeseler A. (2004) IQPNNI: Moving fast through tree space and stopping in time. *Mol. Biol. Evol.* 21: 1565-1571.

Voulhoux R., Bos M.P., Geurtsen J., Mols M., Tommassen J. (2003) Role of a highly conserved bacterial protein in outer membrane protein assembly. *Science*. 299 (5604): 262-265.

Voulhoux R., Tommassen J. (2004) Omp85, an evolutionarily conserved bacterial protein involved in outer-membrane-protein assembly. *Res. Microbiol*. 155(3): 1291-1235.

Waldron K.J, Tottey S., Yanagisawa S., Dennison C., Robinson N.J. (2007) A periplasmic iron-binding protein contributes toward inward copper supply. *J. Biol. Chem.* 282(6): 3837-3846.

Wandersman C., Delepelaire P. (1990) TolC, an *Escherichia coli* outer membrane protein required for hemolysin secretion. *Proc. Natl. Acad. Sci. USA.* 87(12): 4776-4780.

Wandersman C., Delepelaire P. (2004) Bacterial iron sources: from siderophores to hemophores. *Annu. Rev. Microbiol.* 58: 611-647.

Wandersman C., Stojiljkovic, I. (2000) Bacterial heme sources: the role of heme, hemoprotein receptors and hemophores. *Curr. Opin. Microbiol.* 3: 215–220.

Weiss M.S., Abele U., Weckesser J., Welte W., Schiltz E., Schulz G.E. (1991) Molecular architecture and electrostatic properties of a bacterial porin. *Science*. 254(5038): 1627-30.

Wiener M. (2005) TonB-dependent outer membrane transport: going for Baroque? *Curr. Opin. Struc. Biol*. 15: 394–400.

Wimley W.C. (2003) The versatile beta-barrel membrane protein. *Curr. Opin. Struct. Biol.* 13(4): 404-411.

Wimley W.C. (2002) Toward genomic identification of beta-barrel membrane proteins: composition and architecture of known structures. *Protein Sci.* 11, 301-312.

Winkelmann G. (2002) Microbial siderophore-mediated transport. *Biochem. Soc. Trans.* 30(4): 691-696.

Winkenbach F., Wolk C.P., Jost M. (1972) Lipids of membranes and if the cell envelope in heterocysts of a blue-green alga. *Planta.* 107: 69-80.

Wolk C.P., Thomas J., Shaffer P.W., Austin S.M., Galonsky A. (1976) Pathway of nitrogen metabolism after fixation of ^{13}N-labeled nitrogen gas by the cyanobacterium, *Anabaena cylindrica*. *J. Biol. Chem*. 251(16): 5027-5034.

Wolk C.P. (1996) Heterocyst formation. *Annu. Rev. Genet.* 30: 59-78.

Wolk C.P., Ernst A., Elhai J. 1994. Heterocyst metabolism and development, p. 769-823. In D. A. Bryant (ed.), The Molecular biology of cyanobacteria. *Kluwer Academic Publishers*, Dordrecht, The Netherlands.

Wolk C.P. (2000) Heterocyst formation in *Anabaena*. Washington D.C.: ASM Press.

Yamamoto K., Ishihama A. (2005) Transcriptional response of *Escherichia coli* to external copper. *Mol. Microbiol.* 56(1): 215-227.

Yoon H.S., Golden J.W. (1998) Heterocyst pattern formation controlled by a diffusible peptide. *Science*. 282(5390): 935-938.

Yoon H.S., Golden J.W. (2001) PatS and products of nitrogen fixation control heterocyst pattern. *J. Bacteriol.* 183(8): 2605-2613.

Yue W.W., Grizot S., Buchanan S.K. (2003) Structural evidence for iron-free citrate and ferric citrate binding to the TonB-dependent outer membrane transporter FecA. *J. Mol. Biol.* 332(2): 353-368.

Zgurskaya H.I., Nikaido H. (2002) Mechanistic parallels in bacterial and human multidrug efflux transporters. *Curr. Protein Pept. Sci*. 3(5): 531-540.

Publications

Moslavac S., Reisinger V., Berg M., Vojska O., Plöscher M., Flores E., Eichacker A.L., Schleiff E. (2007) The proteome of the heterocyst cell wall in *Anabanea* sp. PCC 7120. *Biol. Chem.* 388(8): 823-829.

Ertel F., Mirus O., Bredemeier R., **Moslavac S.**, Becker T., Schleiff E. (2005) The evolutionary related beta-barrel polypeptide transporters from *Pisum sativum* and *Nostoc* PCC 7120 contain two distinct functional domains. *J. Biol. Chem.* 280(31): 28281-28289.

Moslavac S., Bredemeier R., Mirus O., Granvogl B., Eichacker A. L., Schleiff E. (2005) Proteomic analysis of the outer membrane of *Anabaena* sp. strain PCC 7120. *J. Proteome Res.* 4(4): 1330-1338.

Moslavac S., Mirus O., Bredemeier R., Soll J., von Haeseler A., Schleiff E. (2005) Conserved pore-forming regions in polypeptide-transporting proteins. *FEBS J.* 272(6): 1367-1378.

Ivančić-Bače I., Peharec P., **Moslavac S.**, Škrobot N., Salaj-Šmic E., Brčić-Kostić K. (2003) RecFOR function is required for DNA repair and recombination in a RecA loading-deficient *recB* mutant of *Escherichia coli*. *Genetics*. 163(2): 485-494.

Curriculum Vitae

First Name / Surname	Sunčana Moslavac
Date of Birth	15. March 1978
Place of Birth	Zagreb, Croatia
Nationality	Croatian

Education

1992-1996	High School Education Gymnasium "Petar Preradović", Virovitica, Croatia
1997-2002	Study of Molecular Biology (Dipl.-Ing.) Faculty of Sciences, University of Zagreb, Croatia
2001-2002	Diploma Thesis Division of Molecular Biology Ruđer Bošković Institute, Zagreb, Croatia,
2003-2007	PhD Thesis Department Biology II Ludwig-Maximilians-Universität München, Germany Supervision and Working Group of PD Dr. Enrico Schleiff
2006 (01-04)	Centro de Investigaciones Cientificas Isla de la Cartuja Universidad de Sevilla, Spain Working Group of Prof. Dr. Enrique Flores

Acknowledgements

I would very much like to thank to my supervisor PD Dr. Enrico Schleiff for a giving me a chance to work on an interesting subject, for being always supportive, ready for discussion and rich source of new and original ideas. Thanks also for his patience, humor and never-ending enthusiasm which keep us all moving through the good times and the bad times.

I would also very much like to thank to Prof. Dr. Jürgen Soll for giving me the opportunity to join his laboratory in the first place.

To Prof. Dr. Enrique Flores, Prof Dr. Antonia Herrero and Dr. Alicia Muro-Pastor I am deeply grateful for the scientific supervision and for the friendship during my time in their laboratory in Seville - it made me feel like home. To PD Dr. Iris Maldener I want to thank not only for her scientific support and a great time in Seville and Regensburg, but above all for being such a good friend.

Many, many thanks to Oliver Mirus whose bioinformatical skills were irreplaceable help and for exciting scientific discussions. A lot of thanks to Ms. Anke Toltz for her patience with my numerous EM samples and for her hospitality in Bremen. To Serena Steinhübl many thanks for her eternal innovative spirit and help with GFP constructs and to Mislav for being a “walking encyclopedia” of every knowledge- it saved me some days of my life.

To Serena, Kerstin, Petra and Anastazia and all the memberes of AG Schleiff I am truly grateful for having them as the best possible everyday company. I am grateful to Mislav, Tihana, Rolf, Ewa, Johanna, Nico, Marcel, Torsten, Rita, Claudia, Soumya, Monica and many others for a lot of nice moments.

My warm thankfulness goes to all the members of the Lab 9-10 from CSIC Sevilla (Elvira, Rafa, Rocio, Ana, Ignatio, Barbara, Vir, Javi and J. Enrique) for giving me the most wonderful three months and for helping me patiently with my experiments.

My special gratitude belongs to my very dear friends Lena, Thomas, and Fatima who are my best legacy from the last four years. To Lena my big thank you for hours spent over my manuscript.

Endless thank you to Heide and Brigitte for their acceptance and for being my most wonderful new family. My biggest and warmest thank you belongs to my whole family and my most precious: my Grandparents, my Tomo, my Alex, my Mum, and my Dad - because you are always on my side and because you love me for who I am.